Technische Universität München

Fakultät für Medizin

The molecular function of MLL/AF4 for patient derived acute leukemias growing in mice

Birgitta Christine Heckl

Vollständiger Abdruck der von der Fakultät für Medizin der Technischen Universität München zur Erlangung des akademischen Grades eines

Doktors der Naturwissenschaften (Dr. rer. nat.)

genehmigten Dissertation.

Vorsitzender:	Prof. Dr. Jürgen Ruland
Prüfer der Dissertation:	1. Prof. Dr. Marc Schmidt-Supprian
	2. apl. Prof. Dr. Arnd Kieser

Die Dissertation wurde am 29.03.2018 bei der Technischen Universität München eingereicht und durch die Fakultät für Medizin am 10.10.2018 angenommen.

Für meine Eltern

Life is like riding a bicycle.
To keep your balance,
you must keep moving.

Albert Einstein

Parts of this work have been published in:

Birgitta Christine Heckl*, Michela Carlet*, Binje Vick, Catrin Roolf, Ameera Alsadeq, Michaela Grunert, Wen-Hsin Liu, Andrea Liebl, Wolfgang Hiddemann, Rolf Marschalek, Denis Martin Schewe, Karsten Spiekermann, Christian Junghanss, Irmela Jeremias:

“**Frequent and reliable engraftment of certain adult primary acute lymphoblastic leukemias in mice**”

Leuk Lymphoma 2018 Sept 20:1-4.

Table of contents

1. Summary

Acute leukemia is a frequent disease in children and adults, which remains difficult to treat in a major part of adult patients. Novel treatment options are highly required. The disease is often associated with MLL rearrangements, causing aggressive leukemias. In order to study the molecular biology of acute leukemia more in detail and to find novel druggable targets for successful therapies, suitable animal models representing the heterogeneity and complexity of the disease are urgently needed.

In this study, primary adult ALL samples were successfully engrafted and amplified with an individualized patient derived xenograft (PDX) mouse model. Genetic engineering of PDX cells was achieved by lentiviral vectors and genetically engineered PDX (GEPDX) cells were subsequently applied to perform *in vivo* experiments. We focused on MLL/AF4, the main chromosomal translocation found in ALL patients and investigated its importance for tumor cell growth in cell line cells *in vitro* and in PDX cells *in vivo*. Therefore, we established an inducible competitive knock-down system based on the $CreER^{T2}$ enzyme. A FLIP cassette was designed using differently mutated loxP sites to enable DNA recombination upon tamoxifen treatment and miRNA-embedded shRNAs delivered efficient knock-down of the gene of interest. Furthermore, we were able to monitor different cell populations using five fluorochromes in parallel, in order to analyze competitive *in vitro* and *in vivo* assays. Performing competitive assays allows the direct comparison between control cells and cells expressing the knock-down of the gene of interest within the same experimental setting and the same animal.

A strong growth disadvantage upon MLL/AF4 loss was observed in SEM cell line cells *in vitro* and in three different PDX samples using a constitutive knock-down approach *in vivo*. This clearly demonstrated the importance of the fusion protein MLL/AF4 for tumor cell growth and suggests its application as a therapeutic drug target.

Taken together, we established a novel technique to identify and investigate new promising targets in the individualized xenograft mouse model of acute leukemia, thus providing a valuable tool to find new therapy approaches for patients with aggressive subtypes of the hematologic disease. In this context, MLL/AF4 was successfully validated as a promising candidate for novel therapy development in MLL-rearranged leukemia patients.

Zusammenfassung

Akute Leukämie ist eine häufige Erkrankung bei Kindern und Erwachsenen, die bei einem Großteil der adulten Patienten schwierig zu behandeln ist. Neuartige Behandlungsmöglichkeiten werden dringend benötigt. Die Krankheit ist oftmals mit MLL-Rearrangements assoziiert, die aggressive Leukämien verursachen können. Um die Molekularbiologie der akuten Leukämie näher zu untersuchen und neue Angriffspunkte für erfolgreiche Therapien zu finden, werden geeignete Tiermodelle benötigt, welche die Heterogenität und Komplexität der Erkrankung repräsentieren.

In dieser Studie wurden primäre adulte ALL Proben erfolgreich transplantiert und mittels eines individualisierten von Patienten abgeleiteten Xenograft (PDX) Mausmodells amplifiziert. Gentechnische Veränderungen von PDX Zellen wurde unter Verwendung lentiviraler Vektoren durchgeführt und genetisch veränderte PDX (GEPDX) Zellen wurden anschließend zur Durchführung von *in vivo* Experimenten verwendet. Unser Fokus lag auf MLL/AF4, der wichtigsten chromosomalen Translokation bei ALL Patienten, und wir untersuchten dessen Bedeutung für das Tumorzellwachstum in Zelllinien *in vitro* und in PDX Zellen *in vivo*. Dazu etablierten wir ein induzierbares kompetitives knock-down System, das auf dem Enzym $CreER^{T2}$ basiert. Um eine DNA Rekombination nach Tamoxifen Behandlung zu ermöglichen, wurde eine FLIP Kassette unter Verwendung von unterschiedlich mutierten loxP Sequenzen erstellt. ShRNAs, die in die miRNA eingebettet waren, erzielten einen effizienten knock-down des Zielgens. Des Weiteren konnten wir mithilfe von fünf Fluorochromen verschiedene Zellpopulationen beobachten und somit kompetitive *in vitro* und *in vivo* Assays analysieren. Durch einen kompetitiven Assay können direkt Kontrollzellen und Zellen, die den knock-down des Zielgens exprimieren, innerhalb der gleichen Versuchsanordnung und des gleichen Tieres verglichen werden.

Ein starker Wachstumsnachteil aufgrund des MLL/AF4 Verlustes wurde in SEM Zelllinien *in vitro* und in drei verschiedenen PDX Proben *in vivo* in einem konstitutiven knock-down Ansatz beobachtet. Dies zeigte die hohe Bedeutung des Fusionsproteins MLL/AF4 für den Tumorzellwachstum und legt seine Anwendung als therapeutisches Angriffsziel nahe.

Zusammenfassend haben wir eine neuartige Technik zur Identifizierung und Untersuchung neuer vielversprechender Targets im individualisierten Xenograft-Mausmodell für akute Leukämie etabliert und damit ein wertvolles

Instrument entwickelt, um neue Therapieansätze für Patienten mit aggressiven Subtypen der hämatologischen Erkrankung zu finden. In diesem Zusammenhang wurde MLL/AF4 als vielversprechender Kandidat erfolgreich für eine neuartige Therapieentwicklung bei MLL-rearrangierten Leukämiepatienten validiert.

2. Introduction

2.1 Acute leukemia is a cancer of the hematopoietic system

Acute leukemia is a cancer of the hematopoietic system characterized by an overproduction and accumulation of immature blood cells. Together with chronic leukemia, it is one of the ten most common cancers regarding the percentage of new cancer cases (3.4 %) and cancer deaths (4.1 %) (Siegel et al., 2016). In children, acute leukemia is known to be the most common malignancy and approximately one third of all pediatric cancers are caused by this hematopoietic disorder (Esparza and Sakamoto, 2005).

In healthy people, hematopoietic stem cells differentiate into myeloid and lymphoid stem cells, which then mature into different cell types of the hematopoietic system like erythrocytes, lymphoid, or myeloid cells (**Figure 1**).

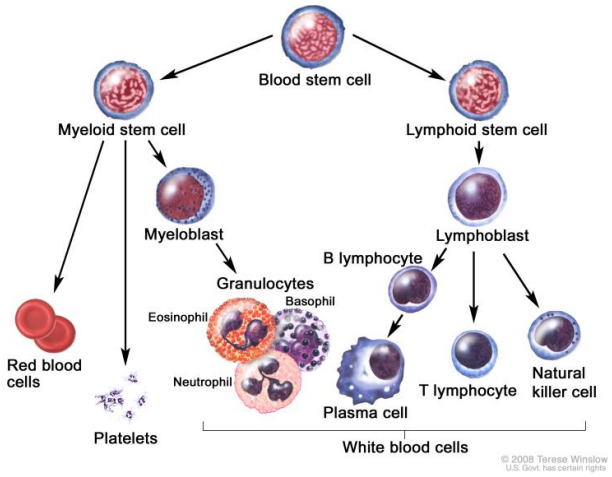

Figure 1: Blood cell development in healthy individuals
Blood stem cells develop into either myeloid stem cells or lymphoid stem cells and finally become red blood cells, platelets or white blood cells. Reprinted with permission (For the National Cancer Institute © 2008 Terese Winslow, U.S. Govt. has certain rights).

In acute leukemia, immature cells cannot fully differentiate into functional lymphoid and myeloid cells and accumulate in the bone marrow and at later stages in the peripheral blood. Depending on the affected cell type, two subtypes of acute leukemia are described: In acute lymphoblastic leukemia, (ALL) lymphoblasts undergo oncogenic alterations, whereas in acute myeloid leukemia (AML) myeloblasts are affected. Both hematologic diseases are very aggressive and patients suffer from symptoms like weakness, fever, frequent infections, shortness of breath, and fatigue. A low number

of functional blood cells, which remains in the hematopoietic system, causes these symptoms (Estey, 2014; Zimmermann et al., 2013). In the following, the two acute leukemia subtypes will be described in more detail.

2.1.1 Acute lymphoblastic leukemia

ALL occurs in both pediatric and adult patients, but the main occurrence is observed in children between two and five years of age. Overall, around 6,600 new cases are reported in the USA each year (Pui and Evans, 2006; Siegel et al., 2016). In Germany, ~ 1,000 people were diagnosed for ALL in the year 2016 according to the Robert-Koch Institute (Haberland and Wolf, 2015; Nennecke et al., 2014). Certain risk factors, for example genetic disorders like Down Syndrome or exposure to radiation, increase the probability to develop ALL (Stewart, 2009). Due to advances in treatment and supportive care, the 5-year overall survival rate of children suffering from ALL almost reaches 90 %. In patients older than 18 years, the 5-year survival rate accounts for only 35 %. One reason for the lower survival rate in elderly patients is the biologic heterogeneity of the disease. This demands highly complex treatments and makes therapies more difficult. Additionally, patients with a relapse respond less to treatment due to chemotherapeutic resistance and hence show poor survival rates (Bassan and Hoelzer, 2011; Inaba et al., 2013; Pui et al., 2012).

The World Health Organization (WHO) classified ALL into three therapeutically distinct subtypes according to their immunophenotypes: T-cell, B-cell precursor (BCP) and mature B-cell ALL. Furthermore, different genotypes can be distinguished through analyzation of karyotypic abnormalities, such as aneuploidy or chromosomal translocations (Arber et al., 2016; Pui et al., 2011; Pui et al., 2008).

2.1.2 Acute myeloid leukemia

Around 20,000 new cases are diagnosed with AML in the USA per year, showing a higher incidence for AML than for ALL (Siegel et al., 2016). In Germany, the Robert-Koch Institute monitored 2,600 males and 3,000 females new diagnoses for AML in the year 2016 showing a slightly higher incidence for women compared to men (Haberland and Wolf, 2015; Nennecke et al., 2014). AML mainly affects adults, where patients disease occurrence and outcome correlates with age. Patients with an age under 60 years are cured in 35 - 40 % of the cases, whereas patients over 60 years

show 5-year survival rates of only 5 - 15 % depending on the AML subtype. In addition, older people suffer from chemotherapeutic side-effects and therefore, patients > 65 years have 1-year survival rates of only 30 % after treatment (Dohner et al., 2015; Krug et al., 2017).

Risk factors for AML are similar as described for ALL, namely blood or genetic disorders, for example idiopathic myelofibrosis or Trisomy 8. Moreover, exposure to chemicals like cigarette smoke, chemical benzene, or radiation increase the risk for AML development (Bjorkholm et al., 2011; Malfuson et al., 2008). AML subtypes are classified in two main systems, the French-American-British (FAB) system and the WHO classification. FAB classification for AML specifies that at least 30 % of accumulated myeloblasts must be detected in the bone marrow (BM) or in peripheral blood (PB) of patients to diagnose the disease (Amin et al., 2005). Eight different subtypes from M0 to M7 characterize the immunophenotypic morphology of the cells. Subcategories according to the WHO are defined by analyzing factors such as genetic abnormalities, myelodysplasia-related changes or immunophenotypic changes (Arber et al., 2016; Yang et al., 2017).

Despite medical progresses concerning the therapies for ALL and AML, survival rates are still poor, especially for patients suffering from relapse. Therefore, understanding the genetic and epigenetic mechanisms behind the hematologic pathogenesis is necessary to develop new successful treatments.

2.2 Epigenetic regulators in acute leukemia

In hematopoietic cells, epigenetic regulators are responsible for controlling and maintaining the equilibrium between gene activation and repression. In acute leukemia, the epigenome is characterized by a global hypermethylation and a local hypomethylation. Especially tumor suppressor genes, which are responsible for cell protection against cancer development, are affected by hypermethylation and thereby inactivated (Baylin and Jones, 2011; Plass et al., 2013).

Recurrent chromosomal structural variations and mutations are found in important target genes of pathways regulating cell cycle, hematopoiesis, signal transduction, or the ribosomal machinery (Van der Meulen et al., 2014). One example is FMS-like tyrosine kinase 3 (*FLT3*), which is mutated in 30 - 35 % of AML patients and causes a constitutive activation of the kinase resulting in increased cell survival and proliferation

(Gilliland and Griffin, 2002). Additionally, more than 80 % of patients diagnosed with acute leukemia carry mutations in epigenetic regulators, which occur as very early events in leukemogenesis and transform healthy hematopoietic stem cells into pre-leukemia cells (Burke and Bhatla, 2014; Metzeler et al., 2016). For instance, *ten-eleven translocation 1* (*TET1*) (14 %), mutated i*socitrate dehydrogenase 2* (*IDH2*), (9 %) or *enhancer of zeste homolog 2* (*EZH2*) (18 %) are frequently involved in the formation of mutations during the early leukemogenesis in patients (Kalender Atak et al., 2012; Peirs et al., 2015; Zhang et al., 2012). However, initiating mutations are not sufficient to induce leukemia. Late events are required to manifest the blood disease (Ley et al., 2013; Li et al., 2016).

In healthy individuals, epigenetic regulators are highly important players to control transcriptional processes and therefore are a sensitive machinery to activate or inactivate gene expression.

2.2.1 Classes of epigenetic regulators

Generally, genes are regulated by alteration of local chromatin structures, which occur as chemical modifications of DNA or histone protein complexes. Epigenetic regulators are categorized into three main classes: writers, readers and erasers (**Figure 2**) (Gallipoli et al., 2015; Hansen, 2012).

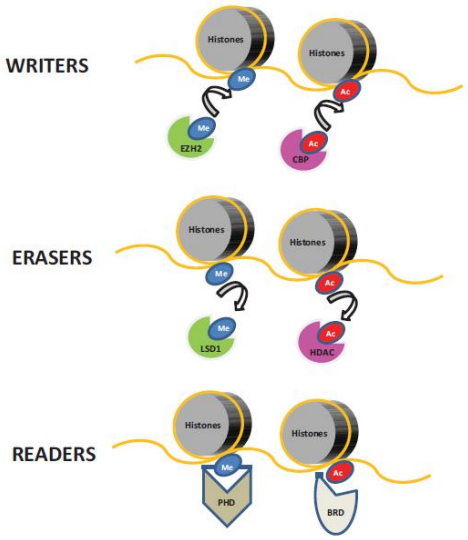

Figure 2: The three main classes of epigenetic regulators
Three main classes are distinguished: epigenetic writers, erasers and readers. Epigenetic modifications, such as methylation and acetylation, are performed by writers, recognized by readers and removed by erasers. Reprinted with permission (Gallipoli et al., 2015).

The first class, epigenetic writers, performs covalent modifications of DNA and histones. For instance, DNA methylation and acetylation takes place at CpG islands, whereas histones are methylated and acetylated at lysine and arginine residues (Rothbart and Strahl, 2014; Zhang et al., 2015b). Among them, DNA methyltransferase 3A (DNMT3A) plays an important role in catalyzing the transfer of methyl groups to cytosine nucleotides at specific CpG sites. Adult patients diagnosed with AML manifest DNMT3A mutations in 22 % of the cases, which correlates with poor prognosis and bad overall survival indicating the importance of correct DNA methylation (Ley et al., 2010; Thol et al., 2011; Van Vlierberghe et al., 2011). Xu and colleagues showed that DNMT3A mutations correlate with enhanced epithelial-mesenchymal transition and thus, form the basis of metastasis in cancer (Xu et al., 2016).

Another important epigenetic writer is the cAMP response element-binding protein (CREB) binding protein (CBP). This enzyme is an acetyltransferase that catalyzes the covalent binding of acetyl groups to lysine residues of all four nucleosomal core histones (Roth et al., 2001; Sterner and Berger, 2000). CBP is a transcriptional coactivator of transcription factors with a CREB motif. CREB plays a critical role in leukemogenesis of AML by promoting abnormal proliferation and aberrant cell cycle progression through upregulation of target gene expression, for example cycline A1 (Matt, 2002; Ogryzko et al., 1996; Shankar et al., 2005).

The second class of epigenetic regulators consists of epigenetic erasers, which remove covalently labelled residues from histones. Lysine specific demethylase 1 (LSD1) specifically removes methyl groups from lysine residues, whereas histone deacetylase (HDAC) catalyzes removal of acetyl groups from lysine residues (Chen et al., 2012; Seto and Yoshida, 2014). LSD1 is involved in demethylating histone H3 lysine 4, which is linked to both active transcription and gene repression (Forneris et al., 2006; Shi et al., 2004). The removal of a negatively charged acetyl group from a positively charged lysine by HDAC increases the interaction between DNA and histones and thus results in reduced transcriptional activity (Zentner and Henikoff, 2013). Deregulated expression of both HDAC and LSD1 leads to various types of tumors involving myeloproliferative disorders in AML caused by transcriptional silencing of tumor suppressor genes (Shahbazian and Grunstein, 2007; Sprussel et al., 2012; Zheng et al., 2015). Schenk and colleagues showed the importance of LSD1 reactivating cell differentiation in AML upon LSD1 inhibition (Schenk et al., 2012).

The third group of epigenetic regulators, epigenetic readers, can recognize and bind specific posttranslational modifications of histones and DNA. For instance, methyl-CpG-binding domain proteins recognize DNA methylation and thus recruit chromatin remodelers like HDAC or LSD1 (Du et al., 2015). Epigenetic readers directly interfere with DNA-related processes like replication or transcription. Plant homeodomain (PHD) or bromodomain (BRD) are examples for selective protein domains that are able to interact with the chromatin and read posttranslational labelling (Dawson et al., 2012).

Taken together, epigenetic regulators play an important role in controlling and modifying the epigenetic code. The whole chromatin is arranged in a highly dynamic manner but changes in its accessibility as well as covalent modifications can only be achieved by the cooperation of epigenetic writers, erasers and readers (Gallipoli et al., 2015).

2.2.2 Mutations in epigenetic regulators

Mutations in epigenetic regulators are very frequent in acute leukemia and the overall occurrence is higher than 80 % leading to transformation of hematopoietic stem cells (Byrne et al., 2014; Redon et al., 2006; Zhang et al., 2015a). Point mutations cause epigenetic site modifications, for example 5-methylcytosine or 5-hydroxymethylcytosine. DNA deletions result in frameshift mutations leading to mutated lysine residues in histone proteins. Moreover, DNA sections are duplicated or inserted in reverse orientation. For instance, driver gene mutations in *DNMT3A* are found in up to 18 % of T-ALL and even in 31 % of AML patients. *IDH2* is detected in up to 9 % in T-ALL and 14 % in AML diagnosed people. In several cases, only driver mutations in DNTM3A or IDH2 are sufficient to initiate leukemia development, however, passenger mutations are necessary to develop the characteristic phenotype of the disease (Ley et al., 2013; Metzeler et al., 2016; Peirs et al., 2015).
Another form of genetic alterations are chromosomal translocations which induce two chromosomal double strand breaks in parallel and result in an exchange and a fusion of chromosomal fragments (Frohling and Dohner, 2008; Nambiar et al., 2008). The detailed molecular mechanism is not completely clear until now, but it is known that chromosomal translocations are early driver mutations in the development of acute leukemia. The breakpoint itself is either located very specifically or within a certain

breakpoint cluster region (BCR) mainly occurring in intronic genome regions. Two major explanations for the oncogenic potential of translocations exist: Either the function of the original gene is changed by creating a new oncogenic fusion protein or a potential oncogenic gene is placed under a strong promoter leading to an aberrant and increased activation. The chromosomal translocation generates a first, single “hit” and later additional mutations accumulate in the cell leading to cancer development (Greaves and Wiemels, 2003; Zheng, 2013).
As genetic alterations are found frequently in epigenetic regulators in acute leukemia, they represent an interesting target for new therapeutic drugs.

2.2.3 Epigenetic regulators as drug targets in acute leukemia

Several inhibitors were already developed and successfully tested in acute leukemia therapy targeting for example mutated DNMTs, IDHs or HDACs (Gallipoli et al., 2015; Peirs et al., 2015; Woods and Levine, 2015). Inhibition of mutated DNMTs was therapeutically implemented using cytosine analogs like 5-azacitidine (Vidaza) or 5-aza-2’-deoxycytidine (Decitabine). They incorporate into DNA during replication and transcription and lock the enzyme through covalent binding, thereby reversing DNMT-mediated methylation. During cancer development, protective genes like tumor suppressor genes are silenced by local hypermethylation. Using DNMT inhibitors, gene silencing is abrogated and important genes are activated again. However, detailed mechanistic insights and consequences on gene expression profiling still remain unclear and need to be investigated (Christman, 2002; Plass et al., 2013). Another type of inhibitors specifically targets mutant forms of *IDH1* and *2* with small molecules that block their enzymatic function. Experimental applications of small molecules lead to leukemia cell differentiation and decreased cell growth (Chaturvedi et al., 2013; Rohle et al., 2013).
HDACs and histone acetyltransferases (HATs) are antagonists in keeping the amount of DNA and histone acetylation at a moderate and healthy level. The epigenetic writer CBP is a member of the HAT family and mutations in this epigenetic regulator are known to be associated with acute leukemia. The recently developed inhibitor I-CBP112 targets the bromodomain (BD) of CBP leading to cell differentiation and impaired colony formation (Picaud et al., 2015). The BD is an essential protein domain for binding and reading acetylated lysine residues of epigenetically modified DNA and

histones and therefore serves as an interesting therapeutic option in treatment of acute leukemia (Fiskus et al., 2014; Herrmann et al., 2012; Taverna et al., 2007).
Another epigenetic regulator, mixed lineage leukemia (MLL), is often mutated in acute leukemia and therefore represents an attractive target for novel therapeutic approaches.

2.2.4 Mixed lineage leukemia as a global epigenetic regulator

The histone methyltransferase MLL is a global epigenetic regulator of initiation of gene transcription and is encoded by *the histone-lysine N-methyltransferase 2A (KMT2A)* gene. It is located on chromosome 11 at q23 and is the human homologue of Drosophila trithorax (TRX). The *MLL* gene, also known as *acute lymphoblastic leukemia gene 1* (*ALL1*), consists of 37 exons (Marschalek et al., 1997; Nilson et al., 1996). Depending on different existing splicing forms, the translated protein contains approximately 4,000 amino acids and a molecular weight of ~ 500 kDa. Eight different splicing forms are known until today, varying between 3,958 and 4,005 amino acids. Exon two, consisting of only 99 nucleotides, is spliced out in 66 % of all transcripts (Rossler and Marschalek, 2013).
The MLL protein is post-translationally cleaved into two parts: An N-terminal fragment with 320 kDa and a C-terminal fragment with 180 kDa. This reaction is catalyzed by an aspartic protease named Taspase1 (threonine aspartase). The sequence of the cleavage site is highly conserved at 2,616 amino acids for the first cleavage site and at 2,667 amino acids for the second. The protein is finally activated after heterodimerization of the N- and C-terminal MLL protein fragments (Hsieh et al., 2003a; Hsieh et al., 2003b; Yokoyama et al., 2002). Two phenylalanine/tyrosine rich sequence motifs, FYRN and FYRC, are inserted, one in each part of the cleaved protein to enable the correct conformational setting (Garcia-Alai et al., 2010). The proteolytically processed protein is then incorporated into a huge network of binding partners. Two classes of epigenetic regulators, writers and readers, are implemented in the fully assembled MLL complex (Nakamura et al., 2002).
The endogenous MLL function is not yet fully understood. It is known that MLL regulates multiple *Hox* genes, which are required for controlling the embryonic body plan and determine the formation of segmental structures. An $Mll^{-/-}$-deficient knock-out is lethal for mice during early embryogenesis and heterozygous $MLL^{+/-}$ disruption

causes aberrant *Hox* gene expression resulting into skeletal malformation and growth retardation in mice. Conditional $Mll^{-/-}$ knock-out mice have an impaired development of hematopoietic stem cells. Analysis of murine $MLL^{-/-}$-deficient embryonic bodies showed reduced expression of several *Hox* genes leading to the conclusion that MLL is required for establishing the hematopoietic system during embryonic development. Furthermore, MLL is important for stem cell self-renewal of bone marrow cells in adult mice (McMahon et al., 2007; Urano et al., 2005; Yu et al., 1998; Yu et al., 1995). Moreover, it has been shown that MLL not only activates, but also represses gene transcription. In murine fibroblast cells with $Mll^{-/-}$ knock-out, 66 % of genes were upregulated while 33 % were downregulated compared to wildtype cells (Attardi et al., 2000; Cogan et al., 2002; Schraets et al., 2003).

Functionally, MLL can be roughly divided into two parts: The N-terminal protein domain is responsible for chromatin binding and reading, whereas the C-terminal domain possesses enzymatic activity and directly acetylates and methylates histones (**Figure 3**). More in detail, MLL contains an AT hook domain at the N-terminus that enables binding to adenine/thymine-rich DNA in the minor groove. A CxxC motif, which specifically binds to unmethylated CpG and thereby recognizes epigenetic modifications of DNA, is located further downstream. Furthermore, MLL carries a methyl-CpG-binding domain (MBD) for binding and reading of hemi-methylated DNA, four plant homeodomains (PHD) and a BD. The C-terminal SET domain is required for methylation of H3K4 histone domains (Ballabio and Milne, 2012; Marschalek, 2016).

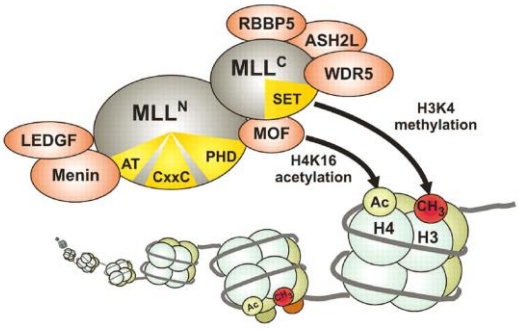

Figure 3: Schematic representation of the MLL complex
The MLL protein consists of an N-terminal and a C-terminal domain and is arranged in a network of binding partners. The SET domain of the C-terminal MLL performs histone methylation while the binding protein MOF acetylates histones. Reprinted with permission (Slany, 2009).

Many binding sites for partner proteins of MLL are found at the N- and C-terminal part. Menin (multiple endocrine neoplasia), a tumor suppressor protein, and LEDGF (lens

epithelium derived growth factor), a transcriptional coactivator, bind upstream of the AT hook domain at the N-terminus. Furthermore, several transcription factors bind to this region. A Polycomb group complex containing proteins like HDAC1/2 is located close to MBD and CBP. MOF (males absent on the first) are located further downstream at the C-terminal part. MOF is a specific H4K16 acetyltransferase, which induces histone charge neutralization and consequently loosens the chromatin. Finally, there are several SET domain core proteins, such as RBBP5 (retinoblastoma-binding protein 5) and ASH2L (absent, small or homeotic 2 like). These proteins are important for stabilization of the MLL conformation and therefore are required for efficient activity of its methyltransferase activity (Dou et al., 2005; Xia et al., 2003; Yokoyama et al., 2004).

Deregulation of MLL affects important cellular processes like proliferation and differentiation. Consequently, chromosomal translocations involving MLL have severe consequences on cellular development.

2.3 MLL rearrangements in acute leukemia

MLL is very often involved in chromosomal rearrangements leading to an aggressive form of leukemia with poor prognosis. In a study, in which almost 8,000 cases of AML and about 1,300 cases of ALL were analyzed in detail, an overall occurrence of 11q23 translocation was detected in 5.2 % of AML and 22 % of ALL patients. Moreover, incidence of MLL rearrangements correlates with age and is especially high in very young infants under the age of one year. Here, almost 60 % of AML and almost 70 % of ALL diagnosed babies bear a chromosomal translocation involving *MLL* (Behm et al., 1996; De Braekeleer et al., 2005; Hilden et al., 2006). The BCR of *MLL* is mainly found between intron 9 and 11 with few exceptions. Additionally, the localization of the *MLL* BCR is linked to age and correlates with clinical outcome of the patients. In adults, the BCR is positioned between intron 9 and 10 whereas it is predominantly located in intron 11 in infants (Broeker et al., 1996; Felix et al., 1998). Chromosomal rearrangements involving MLL serve as strong driver mutations in leukemogenesis, therefore very few additional mutations are detected in patients with acute leukemia. This indicates that MLL fused leukemia require only a small number of cooperating mutations compared to other acute leukemia initiating events (Ley et al., 2013).

Many different translocation partners are known for MLL and until now, over 80 direct fusion partners (MLL/X) and 120 reciprocal fusion partners (X/MLL) have been identified. In some cases, 3-way translocations involving three chromosomes are present, which lead to the unequal numbers for direct and reciprocal fusion partners. Patients analyzed for expression of fusion proteins do not always express both (fusion protein and reciprocal fusion protein) at the same time (Marschalek, 2016; Meyer et al., 2013a).

Although the spectrum of fusion partners is very broad, only few translocation partners are found in acute leukemia, most importantly AF4 (ALL1 fused gene on chromosome 4) and AF9 (ALL1 fused gene on chromosome 9) (**Figure 4**). It was shown that the fusion partner and the translocation locus are strongly age and subgroup dependent. AF4 is encoded by *AFF1* (*AF4/FMR2 family member 1*) and is the main fusion partner in ALL, which is found in 34 % of all MLL-rearranged patients. Furthermore, AF9, which is encoded by *MLLT3* (*myeloid/lymphoid or mixed-lineage leukemia translocated to chromosome 3*), is found in over 30 % of all AML patients with MLL-rearrangements (Krivtsov and Armstrong, 2007; Meyer et al., 2013a).

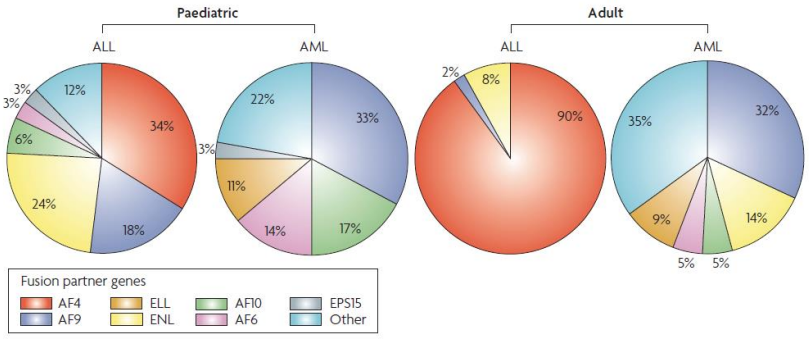

Figure 4: Schematic representation of the main fusion partners found in MLL-rearranged acute leukemia

Main fusion partners are shown for ALL and AML MLL-rearranged leukemia comparing their incidence in pediatric and adult patients. AF4 is predominantly associated with MLL-rearranged ALL, whereas AF9 is the main fusion partner in MLL-rearranged AML. Other frequent fusion partners like ENL, AF6 and AF10 are present in both pediatric and adult acute leukemia. AF, ALL1 fused gene on chromosome; ELL, Eleven-Nineteen Lysine-rich Leukemia; ENL, Eleven-Nineteen Leukemia; EPS15, Epidermal growth factor receptor substrate 15. Reprinted with permission (Krivtsov and Armstrong, 2007).

MLL plays an important role as global regulator of gene transcription, as previously described. Gene transcription involves the enzyme RNA polymerase II (Pol II) and is a tightly regulated process, at both the level of initiation and elongation. A super elongation complex (SEC) is required for successful elongation of transcription. SEC

is comprised of transcription factors, among them important fusion partners of MLL, AF4, AF9, and eleven-nineteen leukemia (ENL), together with the positive transcription elongation factor b (P-TEFb). Additionally, two more complexes are identified, SEC-like 2 (SEC-L2) and SEC-like 3 (SEC-L3), which contain AFF2 or AFF3, respectively. In each of them, the AFF protein is associated with P-TEFb, ENL and AF9. One of the key target genes of SEC is *MYC*, a strong proto-oncogene involved in proliferation and cell cycle control in many different tumors.

Taken together, not only MLL but also its main fusion partners play indispensable roles in regulation of gene transcription. Expression of fusion proteins involving these key players leads to aberrant transcriptional initiation and elongation (Lin et al., 2010; Luo et al., 2012; Yokoyama et al., 2010).

Therefore, MLL-rearranged leukemia requires the development of novel therapies, which could target numerous different proteins involved in the process of transcription's regulation. One potential target is LSD1, which has been shown to be important for maintenance of MLL target gene expression. Inhibition of LSD1 leads to an impaired colony-forming potential as well as reduced leukemia engraftment in immunodeficient mice. Small-molecule inhibitors like GSK2879552 are already in early clinical trials (Feng et al., 2016; Harris et al., 2012). Another target is the protein Menin, which is an oncogenic cofactor of the rearranged MLL and interacts with its N-terminal part. A recently developed small molecule inhibitor MI-2-2 shows strong growth inhibition and leads to cell differentiation in MLL-rearranged murine bone marrow cells (Grembecka et al., 2012; He et al., 2016). Several MLL fusion partners are associated in a SEC with pTEFb, as previously described. Specific pTEFb inhibitors like dinaciclib were successfully tested in preclinical models and successfully induce apoptosis and a decrease of MLL target genes (Baker et al., 2016; Cruickshank et al., 2017).

To gain a better understanding of the effect of fusion protein expression in acute leukemia, the main translocation partner of MLL in ALL, AF4, will be described more in detail in the following.

The main fusion partner of MLL in ALL, AF4, is also known as AFF1 (AF4/FMR2 family member 1). It is a member of the AFF family containing three more members, AFF2/FMR2 (fragile X mental retardation 2), AFF3/LAF4 (lymphoid nuclear protein related to AF4), and AFF4/ AF5q31 (ALL1 fused gene from 5q31). All four proteins are localized in the nucleus and are involved in transcriptional elongation as positive activators. They share several conserved domains, which may explain their functional

redundancy. One of the common domains, ALF (AF4/LAF4/FMR2), is responsible for the interaction with SIAH (seven in absentia homologues), an ubiquitin ligase, which promotes proteasomal protein degradation. Another C-terminal homologue domain is able to bind specific G-quadruplex RNA-forming structures (Bensaid et al., 2009; Melko et al., 2011; Oliver et al., 2004).

AF4 itself is located on chromosome 4 q21 and consists of 23 exons. The main BCR of *AF4* is localized between exon 3 and 7. The endogenous AF4 protein has a molecular weight of approximately 131 kDa (Nilson et al., 1997). It is ubiquitously expressed with a strong presence in the lymphoid organs. *Af4*$^{-/-}$ knock-out mice show an impaired development of B- and T-cells confirming the importance of the protein in lymphoid development (Chen et al., 1993; Isnard et al., 2000). The survival of mutant mice during embryogenesis might be due to partial compensation of gene loss by related genes of the AFF family. In robotic mice, an overexpression of Af4 is caused by a single point mutation (V280A) in the ALF domain leading to a disruption of the SIAH binding motif followed by a reduced proteasome degradation of mutant Af4. Beside defects in early T-cell maturation, these mice develop ataxia followed by Purkinje cell degeneration in the cerebellum. Thus, they are characterized by a strong loss of control in balance and motor coordination and are a useful tool to analyze AF4 overexpression in more detail (Bitoun and Davies, 2005; Isaacs et al., 2003).

It is known that AF4 plays a critical role in transcriptional elongation as a positive regulator of P-TEFb. Within this process, it recruits DOT1L (disruptor of telomeric silencing 1-like), a H3K79 methyltransferase, and thus acts as a mediator of histone methylation. This procedure is strictly controlled by phosphorylation of AF4, AF9 and ENL. The transcriptional activation of AF4 is negatively regulated by phosphorylation through P-TEFb. In contrast, AF4 is stabilized by complex formation with AF9 and ENL. Overexpression of AF4 as well as AF9 and ENL leads to enhanced activation of P-TEFb dependent transcription (Bitoun et al., 2007; Winters and Bernt, 2017).

In t(4;11)(q21,q23) translocated acute leukemia, the MLL gene, located on chromosome 11 q23, is translocated with the AF4 gene, located on chromosome 4 q21. Two in-frame fusion proteins MLL/AF4 and AF4/MLL are expressed in addition to the two endogenous proteins MLL and AF4. In MLL/AF4, the C-terminal part of MLL, which contains the SET domain for H3K4 histone methylation, is lost (**Figure 5**). Instead, the C-terminal part of the AF4 protein is present, which was described to be able to directly interact with proteins like AF9, ENL and DOT1L. This leads to a

complete change in the epigenetic labelling of histones, as DOT1L preferentially labels H3K79 (Krivtsov et al., 2008). The initiation and elongation of MLL target gene transcription is strongly enhanced by the fusion protein and changes in chromatin signature may even lead to re-expression of stem cell genes. MLL/AF4 may not be involved in the multiprotein complex of MLL at all due to missing protein domains but rather compete for DNA binding sites with its AT domain (Bursen et al., 2004).

The reciprocal fusion protein AF4/MLL contains the C-terminal part of MLL with all important domains required for heterodimerization and formation of the multiprotein complex. Therefore, AF4/MLL directly competes with endogenous MLL for the assembly into the complex with other binding partners and takes over its role as a global transcription regulator. Resulting from the fusion, functions of the whole protein complex are changed leading to altered gene expression (Schraets et al., 2003). It was reported that SIAH ligases only promote degradation of wildtype AF4, but could not initiate degradation of AF4/MLL (Bursen et al., 2004). In contrast to the endogenous proteins, fused protein complexes seem to have a prolonged half-life.

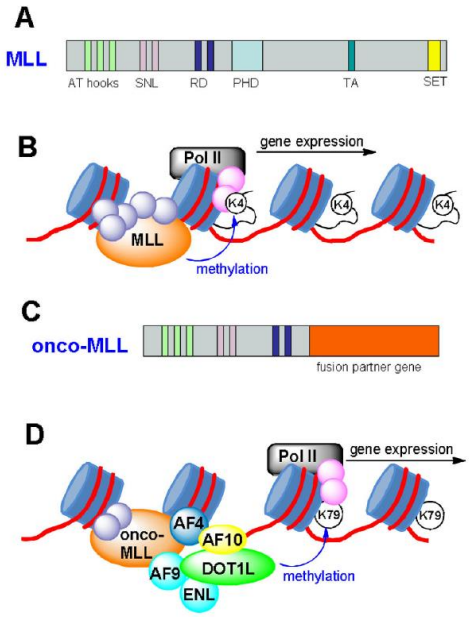

Figure 5: Schematic representation of the MLL structure comparing wildtype versus fused protein and its consequences on gene transcription

(A) The endogenous MLL contains all important protein domains. SNL, speckled nuclear localization domain; RD, repression domain; PHD, plant homeodomain; TA, transactivation domain; SET, H3K4 histone methyltransferase domain. **(B)** The role of wildtype MLL in initiating gene transcription and methylation of H3K4 via its SET domain. **(C)** After chromosomal translocation, the N-terminal part of MLL is fused in-frame to a fusion partner, for example AF4. **(D)** Aberrant function of the mutated MLL/AF4 fusion protein. Additional proteins are recruited and DOT1L can directly methylate H3K79 leading to a different epigenetic code and enhancing transcription of target genes. Reprinted with permission (Anglin and Song, 2013) .

Until today, it is not fully understood whether MLL/AF4 or AF4/MLL is the oncogenic driver. Around 20 % of patients diagnosed with MLL/AF4-rearranged acute leukemia lack an expression of the reciprocal AF4/MLL. A possible explanation is that AF4/MLL is only expressed during onset of the disease, but lost later on due to accumulation of other passenger mutations, which then complement the missing fusion protein (Bursen et al., 2004). Several research groups described that the expression of MLL/AF4 is sufficient to induce B-cell lymphoma and leukemia and that it initiates early onset of the disease in knock-in mouse models without requiring the reciprocal protein AF4/MLL (Chen et al., 2006; Krivtsov et al., 2008). Moreover, it was shown that inhibition of MLL/AF4 expression via siRNA in cell line cells led to impaired proliferation and clonogenicity. Additionally, apoptosis was induced by caspase-3-activation and a decrease of certain HOX genes was observed (Thomas et al., 2005). In contrast, MLL/AF4 alone did not induce acute leukemia after transplantation into mice, whereas the reciprocal protein led to the typical disease phenotype. Lentiviral overexpression of MLL/AF4 in human cord blood derived $CD34^+$ hematopoietic stem progenitor cells (HSPC) only enhanced repopulation and clonogenic potential, but was not sufficient to induce leukemogenesis. However, the latter experiments were performed in human cord blood cells, which might not be the appropriate model system for testing the gene function (Montes et al., 2011). Finally, a third group claims that both fusion proteins are required for initiation and maintenance of acute leukemia. Synergistic effects may lead to growth transformation and apoptosis resistance (Benedikt et al., 2011; Gaussmann et al., 2007). As it is controversially discussed in literature whether MLL/AF4 or AF4/MLL is the oncogenic driver, this question requires further investigation and represents an interesting question for further analyses.

2.4 RNA interference

RNA interference (RNAi) is an important, biological process to control gene expression of existing messenger RNAs (mRNA). Until today, over 300 microRNAs (miRNA), which inhibit gene translation of specific mRNAs by complementary binding followed by degradation of the mRNA, have been identified in humans. This provides a powerful platform to perform artificial silencing of target genes (Bousquet et al., 2013; Cullen, 2005; Fire et al., 1998).

2.4.1 Inhibition of gene expression by RNA interference

The natural pathway of RNAi was first discovered in 1998 in *Caenorhabditis elegans* and is based on a posttranscriptional gene switch-off. Long primary miRNA precursors (pri-miRNA) are transcribed by RNA polymerase II. Next, the pri-miRNA is cleaved by the enzyme Drosha, a ribonuclease III (RNase III) enzyme, ending up as a pre-miRNA with hairpin structure. Exportin 5, a nuclear export factor, is responsible for transporting the pre-miRNA into the cytoplasm. Dicer, another RNase III enzyme, recognizes and cleaves the pre-miRNA in the cytoplasm, which leads to a removal of the terminal loop and a release of a duplex intermediate. The resulting miRNA is then incorporated as a single-stranded RNA into the RNA-induced silencing complex (RISC). It functions as a template, the complementary mRNA is then cleaved with the help of a protein called Argonaute 2. This protein forms the enzymatically active core of the RISC and catalyzes target cleavage by a conserved aspartate – aspartate – glutamate triade. In summary, the RNAi process leads to a posttranscriptional downregulation of homologous mRNA expression (Cullen, 2004; Lee et al., 2002).

All three different RNA forms, which are found in the natural process, can be used as entry sites for artificial gene silencing. The first option, closest to the RISC, is mediated by double stranded synthetic small interfering RNA (siRNA). The siRNA particles are comparable to the natural miRNA and are directly integrated into the RISC, leading to downregulation of target genes. Successful experiments were performed using this technique, but displayed clear disadvantages concerning costs and transience (Elbashir et al., 2001). The second option are short-hairpin RNAs (shRNA), which are able to enter the natural pathway at an earlier stage equal to pre-miRNA. They can be introduced into the cells via expression plasmids and are transcribed by a RNA polymerase III. Unfavorable though are the low efficiency of single copy vectors and the different regulation of Pol III promoters, which might lead to saturation of the endogenous miRNA pathway and hence to shRNA induced toxicity in the cells (Brummelkamp et al., 2002; Paddison et al., 2002). The third approach represents an option to avoid disadvantages of the first two entry pathways and therefore provides the best tool for gene silencing. An artificial shRNA-mir is transcribed directly from the genome, using, if possible, a Pol II promoter and is processed in the same way as natural pri-miRNA, thus enhancing the efficiency of the processing and diminishing toxicity (Dickins et al., 2005; Silva et al., 2005) (**Figure 6**).

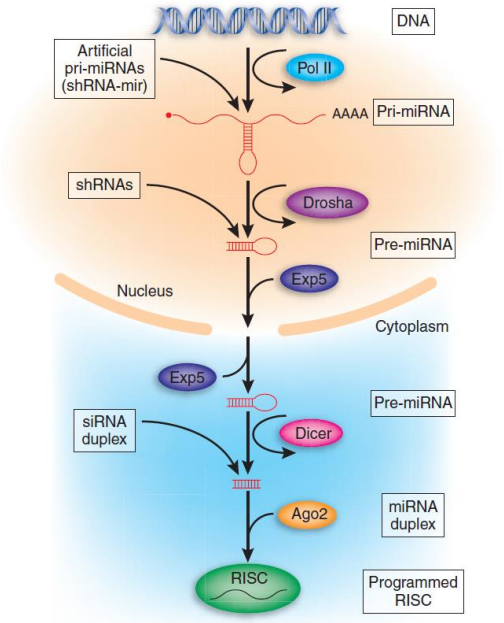

Figure 6: The natural way of RNA interference provides several entry sites for artificial gene silencing
In the biological miRNA pathway, pri-miRNA, transcribed by a Pol II, is processed in several consecutive steps by Drosha and Dicer and finally incorporated into the RISC complex to induce target mRNA degradation. The process is used for artificial gene silencing using shRNA-mir, shRNA or siRNA at different entry sites, respectively. Reprinted with permission (Cullen, 2005).

Novel systems that integrate specific knock-down target genes directly into the genome have already been successfully established. One approach is based on a miR30 backbone implemented with the desired shRNA, which is integrated in the genome (Fellmann et al., 2013; Fellmann et al., 2011). Inducible systems, either reversible - based on doxycycline dependent gene expression -, or irreversible - based on CreER^{T2}-regulated gene expression -, have been established and are described in literature (Stern et al., 2008; Wiznerowicz et al., 2006). Taken together, RNA interference represents an interesting pathway for artificial gene knock-down, which exploit existing biogenesis pathways in the cells.

2.4.2 An inducible CreER^{T2} system

Constitutive inhibition of gene expression via shRNA is a powerful technique to study non-essential target genes. In contrast, conditional knock-down strategies are required to investigate the role of those genes whose expression is necessary for cell proliferation and survival.
Inducible systems are an important technique to achieve a conditional knock-down. Two types of systems are available. While the inducing agent doxycycline is used in

reversible Tet-on Tet-off systems, tamoxifen is applied in irreversible Cre (cyclization recombination) systems (Wiznerowicz et al., 2006).

More in detail, Cre recombinase is a site-specific tyrosine recombinase enzyme, which was originally found in the bacteriophage P1. It catalyzes DNA recombination between two specific DNA recognition sites called loxP (locus of crossing [x-ing]-over of bacteriophage P1) sites. Different loxP sequences are known and all of them consist of a 34 base pair non-palindromic DNA sequence, which is naturally not found in mammalians. The sequence located between the two loxP sites is named floxed (flanked by loxP sites). Two different mechanisms can occur upon Cre activity: when both loxP sites are oriented in the same direction, the floxed sequence will be cut out, whereas it will be inverted when the loxP sites are orientated in opposite directions. This mechanism provides an important technique to induce deletions, insertions, inversions and translocations (Feil et al., 2009; Oberdoerffer et al., 2003; Zou et al., 1994). To receive an inducible system, Cre is fused to the hormone-binding part of the human estrogen receptor (ER) known as CreER. The optimized, highly sensitive version CreER^{T2} contains a triple mutation in the receptor ligand-binding domain (Feil et al., 1997; Indra et al., 1999). Without activation, CreER^{T2} is located in the cytoplasm bound to heat shock protein 90 (hsp90). Upon treatment with a synthetic 4-hydroxytamoxifen (4-OHT), this ligand binds to the ER, CreER^{T2} is released from hsp90 and thus can migrate into the nucleus. There, it recognizes loxP sites and catalyzes site-specific DNA recombination. Generally, this process is monitored by reporter genes with a switch of fluorochrome expression (**Figure 7**).

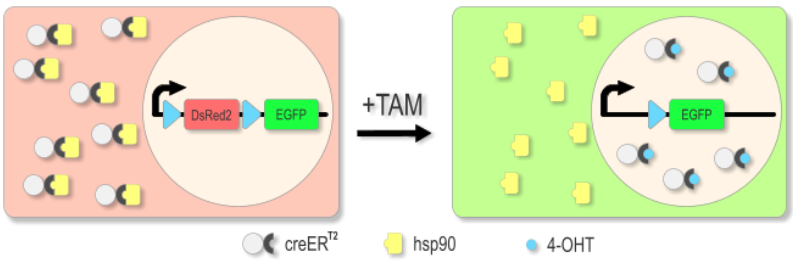

Figure 7: An inducible CreER^{T2} system
The Cre recombinase enzyme is fused to the human estradiol receptor (ER) and located in the cytoplasm where it is bound to heat shock protein 90 (hsp90). An improved CreER^{T2} version with three mutations in the ER ligand-binding domain is used. Upon tamoxifen treatment, 4-hydroxytamoxifen (4-OHT) binds to the ER, CreER^{T2} is released from hsp90 and migrates into the nucleus where it recognizes loxP sites and induces site-specific DNA recombination. Successful Cre recombinase activation is visualized by reporter gene expression changing from DsRed2 to eGFP. Reprinted with permission (Hans et al., 2009).

Inducible CreER^{T2} systems allow a controlled gene manipulation for both overexpression and knock-down. Conditional RNA interference is generated by flanking a miR30 cassette with different tandem loxP sites. Two differently mutated loxP sites, 2272 and 5171, are described by Oberdoerffer and colleagues and each of them can only recombine with the identical loxP partner sequence (Oberdoerffer et al., 2003; Siegel et al., 2001). The miR30 cassette allows shRNA transcription under a polymerase II promoter as described before. Therefore, a 22 nucleotide sense passenger strand targeting the gene of interest and its antisense guide strand are embedded in a fixed flank - loop - flank sequence within the miR30 backbone (Chang et al., 2013; Fellmann et al., 2013; Fellmann et al., 2011). To ensure the expression of the shRNA knock-down only upon tamoxifen induction, a so-called FLIP cassette is chosen as described by stern and colleagues (Stern et al., 2008). The FLIP cassette contains a constitutively expressed reporter gene, which is the gene for puromycin resistance and the surface marker Thy1.1 in this case, and an inverse miR30 cassette coupled to a second reporter gene, eGFP. Upon CreER^{T2} activation, the miR30 cassette and eGFP are inverted and expressed, whereas the constitutive marker is deleted. This process takes place in a two-step reaction, a reversible inversion followed by an irreversible deletion (Oberdoerffer et al., 2003; Stern et al., 2008; Ventura et al., 2004) (**Figure 8**).

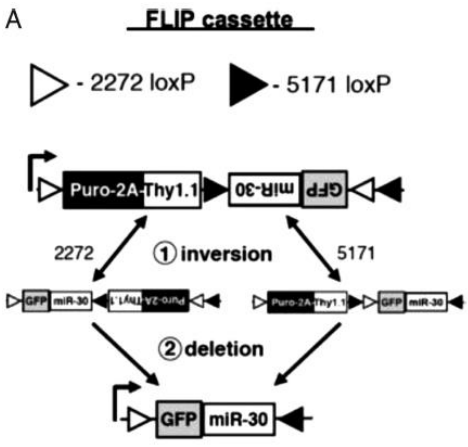

Figure 8: Design of a FLIP cassette for an inducible shRNA knock-down
Schematic representation of the FLIP cassette. Two differently mutated loxP sites, 2272 loxP and 5171 loxP, are inserted in the vector. The gene for puromycin resistance and the surface marker Thy1.1 are constitutively expressed. The flipping mechanism occurs in a two-step reaction, an inversion followed by a deletion. In the end, the fluorescent marker eGFP and the miR30 cassette are expressed. Reprinted with permission (Stern et al., 2008).

In contrast to constitutive knock-down systems, genes with important roles for cell viability and survival can be analyzed upon induction.

For instance, gene silencing of chromosomal translocation products is a highly interesting approach, as they have been reported to be very often essential alterations for cancer cells. Additionally, as the mRNA transcripts of translocated chromosomes provide a specific sequence not present in healthy non-rearranged cells, they are an ideal tumor specific target for leukemia treatment. The challenging aspect of applying RNA interference in targeted tumor therapy is the delivery of siRNA or shRNA into the desired cells.

2.4.3 Delivery systems for therapeutic RNA interference

For a successful therapeutic application of RNA interference, a stable and functional delivery system is required in addition to the knock-down system. Two application forms are possible for RNAi. In a systemic delivery approach, a packaging system is required to enter the organism and carry the RNA particles to the final destination. Vehicles are described in form of lipid nanoparticles, liposomes, polymers, or antibodies. Packaged RNA is injected directly into the tumor tissue, applied intravenously or via inhalator. This approach remains very challenging due to the first-pass effect of the liver and unsuccessful delivery systems for a certain target region. Both goals have to be fulfilled, reaching the correct target tissue and the specific cell type. The second delivery way is an *ex vivo* approach, meaning that aberrant cells are taken from the patient, genetically manipulated *ex vivo* and re-transplanted into the patient. As naked uptake of RNA is very rare, lentiviral systems or physical methods like electroporation are used to achieve highly efficient cell engineering. Until today, mainly siRNA has been used for therapeutic application, having the disadvantages of being expensive and transient, as previously described. Fewer trials have been described for shRNA, claiming a critical role of virally delivered, persisting shRNA without sufficient knowledge about off-target effects. Therefore, further optimization of delivery systems and more insights into detailed molecular mechanisms are highly required to achieve an efficient treatment perspective of leukemia in patients (Borkhardt and Heidenreich, 2004; He et al., 2014; Jyotsana et al., 2017; Tiemann and Rossi, 2009).

2.5 Patient derived xenograft mouse models in acute leukemia

Due to limited treatment options, acute leukemia is still a challenging disease of the hematopoietic system with poor prognosis and risk of relapse (Bassan and Hoelzer, 2011; Pui et al., 2008). Mouse model systems are highly required since aspirates of acute leukemia patients do not proliferate *in vitro* and leukemia cells die after several days in cultivation. Working with established acute leukemia cell line cells is not an optimal model system as these cells often maintain additional, unphysiologic mutations and other alterations, which do not exist in patient leukemia cells (Petitjean et al., 2007). Animal models provide an important tool in human acute leukemia research as they are used to amplify and analyze individual leukemia samples. In contrast to syngeneic models, in which mice with a functional immune system are used, xenograft mice lack a functional immune system (Jacoby et al., 2014). Up to now, the patient derived xenograft (PDX) mouse model presents the system, which studies human ALL and AML in a highly patient-related approach *in vivo*. Aspirates or peripheral blood from patients are injected into immunocompromised mice and engraft with a disease course similar to patients. Restricted amount of patient derived material is amplified upon cell proliferation in the living organism. Human leukemia cells are then re-isolated from the spleen and bone marrow and further passaged in mice after reinjection. In contrast to cell line cells, this model preserves the tumor heterogeneity and the subclonal profile of the leukemia. Therefore, it reflects specific characteristics of human acute leukemia and is used for studies on stem cells, evolution, niche, or subclones. Tumor cell interaction with the microenvironment and related signaling play an important role in leukemogenesis and are mimicked and investigated with this animal model (Ebinger et al., 2016; Lock et al., 2002; Paczulla et al., 2017; Townsend et al., 2016; Woiterski et al., 2013).

The PDX mouse model was first described in 1989 and has been continuously improved until today (Kamel-Reid et al., 1989). In the beginning, mice homozygous for severe combined immunodeficiency (SCID) were used as mouse models in leukemia research. As engraftment rates were poor, non-obese diabetic (NOD)/SCID mice were generated showing a better engraftment rate due to higher immunodeficiency. Next, a mutation in the interleukin-2 receptor gamma (IL2Rγ) chain was added to obtain NOD/SCID/gamma (NSG) mice lacking mature B- and T-cells as well as natural killer cells. High engraftment rates of human acute leukemia cells were observed with this

mouse model (Agliano et al., 2008; Baersch et al., 1997; Ito et al., 2002; Shultz et al., 2005).

In ALL, numerous PDX models exist for pediatric patient studies, whereas less is known about xenografting adult ALL cells. As this seems to be challenging, studies suggest to pretreat mice using for example total body irradiation or chemotherapy (Notta et al., 2011; Patel et al., 2014).

An improved model is described by Gopalakrishnapillai and colleagues, which used null alleles for the major histocompatibility complex class I beta2-microglobulin (β2m) named NSG-B2m. 100 % engraftment rates were achieved without preconditioning in both cell line cells and primary samples, which provides good reasons to work with this model in advanced leukemia studies (Gopalakrishnapillai et al., 2016).

2.6 Genetically engineered mouse models

In our lab, we additionally established genetically engineered PDX (GEPDX) cells using lentiviral vector systems in parallel to genetically engineered mouse models (GEMM) (Hauer et al., 2014; Walrath et al., 2010). Lentiviral transduction enables to molecularly manipulate PDX cells, which are subsequently called GEPDX cells. For instance, the lentiviral constructs contain genes for expression of fluorochromes such as eGFP or mCherry to label positively transduced cells and to monitor cells by flow cytometry. Besides, a lentiviral luciferase reporter gene enables bioluminescence imaging (BLI) to monitor tumor growth reliably and sensitively *in vivo* (Jones et al., 2017; Terziyska et al., 2012; Vick et al., 2015). Moreover, studies on intracellular signaling pathways are performed on a molecular level with the help of GEPDX cells.

Taken together, PDX mouse models are highly relevant to study tumor biology and to develop new treatment options in acute leukemia.

Overall, acute leukemia associated with MLL rearrangements causes an aggressive disease in patients. MLL acts as an important epigenetic regulator in cells and its chromosomal translocation MLL/AF4 influences major cellular processes in gene activation and repression. However, it is still unclear, if MLL/AF4 is an oncogenic driver mutation in leukemia cells (Bursen et al., 2010; Krivtsov et al., 2008; Montes et al., 2011). Therefore, the importance of MLL/AF4 for tumor cell growth and survival needs to be further investigated.

2.7 Objectives

Chromosomal rearrangements are frequently found as driver mutations in acute leukemia patients associated with bad prognosis and poor survival. A frequent translocation leading to an aggressive form of the disease is the MLL-rearranged subtype t(4;11) MLL/AF4. As the breakpoint sequence is only present in leukemia cells and absent in healthy non-tumor cells, it represents an ideal cancer specific target for new therapeutic approaches.

The overall aim of the present work was to analyze the importance of the chromosomal translocation MLL/AF4 for tumor growth and survival of acute leukemia cells including for patient derived xenograft (PDX) cells *in vivo*.

The first aim was to engraft and amplify primary samples with the chromosomal translocations t(4;11) MLL/AF4 and further translocations in our PDX mouse model and to analyze them in detail. In this context, molecular manipulation of rearranged PDX samples was performed using lentiviral vector systems.

The second aim was to silence MLL/AF4 using a breakpoint specific approach and a constitutive competitive system.

The third aim was to establish an inducible knock-down system, which could be used in competitive *in vivo* assays due to monitoring of distinct cell subpopulations applying suitable fluorochrome markers. This system was finally applied to investigate whether the fusion protein MLL/AF4 plays an essential role for growth of ALL cells line cells as well as PDX ALL cells *in vivo*.

3. Material

3.1 Patient material

Fresh bone marrow (BM) or peripheral blood (PB) samples from adult patients with acute lymphoblastic leukemia (ALL) were obtained from the Department of Medicine III, University Hospital, LMU Munich, Germany (samples ALL-210, ALL-223, ALL-224, ALL-225, ALL-352, ALL-360, ALL-363, ALL-389), or from the Department of Medicine III – Hematology, Oncology and Palliative Care, Rostock University Medical Center, Rostock, Germany (samples ALL-256, ALL-262, ALL-589, ALL-590, ALL-815, ALL-816, ALL-817 and ALL-818).

Aspirates from adult acute myeloid leukemia (AML) patients were obtained from the Department of Medicine III, University Hospital, LMU Munich, Germany (AML-388, AML-393, AML-669).

Pediatric ALL samples were obtained from the ALL-BFM study group in Kiel (ALL-703, ALL-704, ALL-705, ALL-706, ALL-707, ALL-762, ALL-763), from the Dr. von Haunersches Kinderspital, Ludwig-Maximilian Universität, Munich, Germany (ALL-199), or from the University children hospital in Zürich, Switzerland (ALL-265).

Samples from pediatric patients with AML were obtained from the university Kinderklinik, Tübingen, Germany (AML-346).

3.2 Mice

Non-obese diabetes (NOD) severe combined immune deficiency (scid) gamma (NOD.Cg-*Prkdc*^{scid} *Il2rg*^{tm1Wjl}/SzJ, NSG) mice were obtained from the Jackson Laboratory (Bar Harbour, ME, USA). These mice have NOD/ShiLtJ as a genetic background and show severe immunodeficiency caused by the combination of two mutations. The scid mutation is located in the DNA repair complex protein Prkdc and leads to a lack of mature B- and T-cells. The second mutation is a complete null allele of the interleukin 2 receptor common gamma chain (IL2rg^{null}) inactivating cytokine signaling and generating dysfunctional natural killer (NK) cells (Shultz et al., 2005; Shultz et al., 1995).

3.3 Cell lines

All listed cell lines were tested monthly for mycoplasma infection.

Table 1: Cell lines

Name	Description	Source
NALM-6	human B-cell precursor leukemia	DSMZ: ACC 128
SEM	human B-cell precursor leukemia	DSMZ: ACC 546
HEK-293	human embryonic kidney cells	DSMZ: ACC 305
MS-5	murine stromal cells	DSMZ: ACC 441

3.4 Bacterial strains

Table 2: Bacterial strains

Name	Description	Source
Escherichia coli (E. coli) DH5α	F^- Φ80*lac*ZΔM15 Δ(*lac*ZYA-*arg*F) U169 *rec*A1 *end*A1 *hsd*R17 (rk^-, mk^+) *pho*A *sup*E44 λ^- *thi*$^-$1 *gyr*A96 *rel*A1	Thermo Fischer Scientific, Waltham, MA, USA

3.5 Plasmids

Table 3: Plasmids

Name	Description	Source
pRSV-Rev	plasmid 12253; lentiviral packaging plasmid	Addgene, Cambridge, MA, USA
pMDLg/pRRE	plasmid 12251; lentiviral packaging plasmid	Addgene, Cambridge, MA, USA
pMD2.G	plasmid 12259; envelope expressing plasmid	Addgene, Cambridge, MA, USA
pCDH-EF1α-eFFly-T2A-mtagBFP	EF1α promoter; expression of eFFly and mtagBFP	cloned by Michela Carlet
pCDH-EF1α-eFFly-T2A-eGFP	EF1α promoter; expression of eFFly and eGFP	cloned by Michela Carlet
pCDH-SFFV-dsRED-miR30_Renilla	SFFV promoter; expression of shRNA targeting Renilla and dsRED	cloned by Jenny Vergalli
pCDH-SFFV-dsRED-miR30_MLL/AF4_1	SFFV promoter; expression of shRNA targeting MLL/AF4 and dsRED	cloned for this study

Name	Description	Source
pCDH-SFFV-dsRED-miR30_MLL/AF4_2	SFFV promoter; expression of shRNA targeting MLL/AF4 and dsRED	cloned for this study
pCDH-SFFV-GLuc-T2A-CreERT2-P2A-mCherry	SFFV promoter; expression of GLuc, $CreER^{T2}$ and mCherry	cloned by Michela Carlet
pCDH-SFFV-FLIP cassette-mtagBFP-eGFP-miR30_Renilla	SFFV promoter; expression of mtagBFP; expression of shRNA targeting Renilla and eGFP after tam induction	cloned by Michela Carlet
pCDH-SFFV-FLIP cassette-mtagBFP-eGFP-miR30_MLL/AF4_1	SFFV promoter; expression of mtagBFP; expression of shRNA targeting MLL/AF4 and eGFP after tam induction	cloned for this study
pCDH-SFFV-FLIP cassette-mtagBFP-eGFP-miR30_MLL/AF4_2	SFFV promoter; expression of mtagBFP; expression of shRNA targeting MLL/AF4 and eGFP after tam induction	cloned for this study
pCDH-SFFV-FLIP cassette-iRFP-T-Sapphire_Renilla	SFFV promoter; expression of iRFP; expression of shRNA targeting Renilla and T-Sapphire after tam induction	cloned by Michela Carlet

3.6 Antibodies

Table 4: Antibodies

Name	Immune species	Application	Source
anti-CD33 PE; clone WM-53; #555450	human	FCM: 1:17	BD Bioscience, Heidelberg, Germany
anti-CD38 PE; clone HB7; #345806	human	FCM: 1:10	BD Bioscience, Heidelberg, Germany
anti-CD45 APC; clone HI30; #555485	human	FCM: 1:10	BD Bioscience, Heidelberg, Germany
anti-CD45 APC; clone: 30-F11; #103112	mouse	FCM: 1:10	Biolegend, San Diego, CA, USA
mouse IgG1 APC isotype control; clone MOPC-21; #555751		FCM: 1:10	BD Bioscience, Heidelberg, Germany

Name	Immune species	Application	Source
mouse IgG1 APC isotype control; clone MOPC-21; #400119		FCM: 1:10	Biolegend, San Diego, CA, USA
mouse IgG1 PE isotype control; clone MOPC-21; #559320		FCM: 1:17	BD Bioscience, Heidelberg, Germany
mouse IgG1 PE isotype control; clone MOPC-21; #400140		FCM: 1:10	Biolegend, San Diego, CA, USA

3.7 Enzymes

3.7.1 Restriction endonucleases

Table 5: Restriction endonucleases

Name	Restriction site	Source
BglII	A ▼ GATCT TCTAG ▲ A	New England Biolabs, Frankfurt am Main, Germany
EcoRI HF	G ▼ AATTC CTTAA ▲ G	New England Biolabs, Frankfurt am Main, Germany
NotI HF	GC ▼ GGCCGC CGCCGG ▲ CG	New England Biolabs, Frankfurt am Main, Germany
PmeI	GTTT ▼ AAAC CAAA ▲ TTTG	New England Biolabs, Frankfurt am Main, Germany
SalI	G ▼ TCGAC CAGCT ▲ G	New England Biolabs, Frankfurt am Main, Germany
SpeI	A ▼ CTAGT TGATC ▲ A	New England Biolabs, Frankfurt am Main, Germany
XbaI	T ▼ CTAGA AGATC ▲ T	New England Biolabs, Frankfurt am Main, Germany
XhoI	C ▼ TCGAG GAGCT ▲ C	New England Biolabs, Frankfurt am Main, Germany

3.7.2 Enzymes

Name	Source
GoTaq G2 DNA Polymerase	Promega, Madison, WI, USA
Pfu Polymerase	Thermo Fischer Scientific, Waltham, MA, USA
Quantiscript Reverse Transcriptase	Qiagen, Venlo, NL
T4 DNA Ligase	Thermo Fischer Scientific Waltham, MA, USA

3.8 Standard size ladders

Name	Source
DNA ladder mix	Thermo Fischer Scientific, Waltham, MA, USA

3.9 Oligonucleotides

3.9.1 Oligonucleotides for short-hairpin RNA

Table 6: Oligonucleotides for shRNA

Number	Name	Sequence 5’ -> 3’
454	Ren-s	TCGAGAAGGTATATTGCTGTTGACAGTGAGCGCAGGAATTATAATGCTTATCTATAGTGAAGCCACAGATGTATAGATAAGCATTATAATTCCTATGCCTACTGCCTCGG
455	Ren-as	AATTCCGAGGCAGTAGGCATAGGAATTATAATGCTTATCTATACATCTGTGGCTTCACTATAGATAAGCATTATAATTCCTGCGCTCACTGTCAACAGCAATATACCTTC
673	miR30MLL/AF4_1s	TCGAGAAGGTATATTGCTGTTGACAGTGAGCGCAAGAAAAGCAGACCTACTCCATAGTGAAGCCACAGATGTATGGAGTAGGTCTGCTTTTCTTTTGCCTACTGCCTCGG
674	miR30MLL/AF4_1as	AATTCCGAGGCAGTAGGCAAAAGAAAAGCAGACCTACTCCATACATCTGTGGCTTCACTATGGAGTAGGTCTGCTTTTCTTGCGCTCACTGTCAACAGCAATATACCTTC
683	miR30MLL/AF4_2s	TCGAGAAGGTATATTGCTGTTGACAGTGAGCGCACCAAAAGAAAAGCAGACCTATAGTGAAGCCACAGATGTATAGGTCTGCTTTTCTTTTGGTTTGCCTACTGCCTCGG
684	miR30MLL/AF4_2as	AATTCCGAGGCAGTAGGCAAACCAAAAGAAAAGCAGACCTATACATCTGTGGCTTCACTATAGGTCTGCTTTTCTTTTGGTGCGCTCACTGTCAACAGCAATATACCTTC

3.9.2 PCR primer for finger printing of mitochondrial DNA

Table 7: PCR primer for finger printing of mitochondrial DNA

Number	Name	Sequence 5’ -> 3’
456	mtReg-F1	TCCACCATTAGCACCCAAAGC
457	mtReg-R1	TCGGATACAGTTCACTTTAGC
458	mtReg-F3	CGCACCTACGTTCAATATTAC
459	Mt-Reg-R3	GGGTGATGTGAGCCCGTCTAA

3.9.3 qPCR primer

Table 8: qPCR primer

Number	Name	Sequence 5’ -> 3’
546	HPRT1-for	TGATAGATCCATTCCTATGACTGTAGA
547	HPRT1-rev	CAAGACATTCTTTCCAGTTAAAGTTG
816	MLL_for(MLLAF4)	AAGTTCCCAAAACCACTCCTAGT
817	AF4_rev(MLLAF4)	GCCATGAATGGGTCATTTCC
818	MLL_1_rev(MLL)	GATCCTGTGGACTCCATCTGC
838	AF4_for(AF4)	TTGGACACTGTGGTTATGCAG
1178	AF4_rev(endo AF4)	TAGGTCTGCTCAACTGACTGAG

3.10 Buffers

Buffer	Components
Annealing buffer	50 mM Hepes 100 mM NaCl pH 7.4
DNase I buffer	20 mM Tris-HCl 1 mM $MgCl_2$ 50 % Glycerol pH 7.5

PBE (PBS with EDTA)	1x PBS 0.5 % BSA 5 mM EDTA
10x PBS (phosphate buffered saline)	1.37 M NaCl 27 mM KCl 100 mM Na_2HPO_4 x $7H_2O$ 18 mM KH_2PO_4 pH 7.3
1x PBS	137 mM NaCl 2.7 mM KCl 10 mM Na_2HPO_4 x $7H_2O$ 1.8 mM KH_2PO_4 pH 7.3
HBG (HEPES buffered glucose)	20 mM HEPES, pH 7.1 5 % glucose w/v
50x TAE buffer (Tris-acetate-EDTA)	2 M Tris-HCl 50 mM EDTA 1 M acetic acid pH 8.5
TFB I (transformation buffer I)	100 mM KCl 10 mM $CaCl_2$ 30 mM K-Acetate 50 mM $MnCl_2$ 15 % glycerine 98 % pH 5.8
TFB II (transformation buffer I)	10 mM KCl 75 mM $CaCl_2$ 10 mM MOPS 15 % glycerine 98 % pH 7.0

3.11 Media and solutions

Name	Components
α-MEM complete (MS-5 cells)	α-MEM (500 ml) 10 % FCS 1 % L-glutamine
DMEM complete (HEK-293 cells)	DMEM (500 ml) 10 % FCS 1 % L-glutamine
IMEM complete (SEM cells)	IMEM (500 ml) 10 % FCS 1 % L-glutamine

RPMI complete (NALM-6 cells)	RPMI 1640 10 % FCS 1 % L-glutamine
DD medium (AML PDX cells)	StemPro-34 medium (50 ml) 2.6 % Nutrient Supplement 1 % Pen/Strep 1 % L-glutamine 2 % FCS 0.01 % recombinant human FLT-3 ligand 0.02 % recombinant human SCF 0.02 % recombinant human TPO 0.02 % recombinant human IL-3
Patient medium (PM) (ALL PDX cells)	RPMI 1640 (500 ml) 20 % FCS 1 % L-glutamine 1 % Pen/Strep 0.2 % gentamycin
PM^{+++} (ALL PDX cells)	PM (50 ml) 0.6 % ITS 1 % sodium-pyruvate 0.0434 % α-Thioglycerol
LB agar	4 g SELECT peptone 140 2 g yeast extract 4 g NaCl 6 g Agar-Agar Kobe I up to 400 ml with ddH_2O
LB medium	8 g SELECT peptone 140 4 g yeast extract 8 g NaCl up to 800 ml with ddH_2O

3.12 Chemicals and reagents

Name	Source
α-MEM	Gibco, San Diego, CA, USA
α-Thioglycerol (α-TG)	Sigma-Aldrich, St. Louis, MO, USA
Acetic-acid	Merck Millipore, Darmstadt, Germany
Agar-Agar Kobe I	Carl Roth, Karlsruhe, Germany
Agarose	Biozym Scientific GmbH, Hessisch Oldendorf, Germany
Ampicillin 25 mg/ml	Sigma-Aldrich, St. Louis, MO, USA
Baytril (2.5 %)	Bayer, Leverkusen, Germany
BSA	Carl Roth, Karlsruhe, Germany

$CaCl_2$	Sigma-Aldrich, St. Louis, MO, USA
Ciprobay antibiotics 400 mg/200 ml	Bayer, Leverkusen, Germany
Coelenterazine	Synchem OHG, Felsberg, Germany
Corn oil	Sigma-Aldrich, St. Louis, MO, USA
CutSmart buffer	New England Biolabs, Frankfurt am Main, Germany
D-Luciferin	BIOMOL GmbH, Hamburg, Germany
DMEM	Gibco, San Diego, CA, USA
DMSO	Sigma-Aldrich, St. Louis, MO, USA
DNA loading dye 6x	Thermo Fischer, Scientific, Waltham, MA, USA
DNase I	Roche, Mannheim, Germany
DNase I buffer	Roche, Mannheim, Germany
dNTP mix	Thermo Fischer, Scientific, Waltham, MA, USA
dNTPs (10 mM each)	Biozym Scientific GmbH, Hessisch Oldendorf, Germany
EDTA (0.5 M)	Lonza, Allendale, USA
Ethanol 100 %	AppliChem GmbH, Darmstadt, Germany
Ethanol, technical grade	AppliChem GmbH, Darmstadt, Germany
FACS Lysing Solution 10x	BD Bioscience, Heidelberg, Germany
FCS (Fetal calf serum)	Biochrome, Berlin, Germany
Ficoll-Paque™ PLUS	GE Healthcare, Freiburg, Germany
Gentamicin	Lonza, Allendale, USA
Glucose (20 %)	Braun, Melsungen, Germany
Glycerol (> 99 %)	Sigma-Aldrich, St. Louis, MO, USA
GoTaq G2 colourless Master Mix	Promega, Madison, WI, USA
GoTaq G2 green Master Mix	Promega, Madison, WI, USA
HCl (32 %)	Merck Millipore, Darmstadt, Germany
Heparin	Ratiopharm, Ulm, Germany
HEPES (1 M)	Gibco, San Diego, CA, USA
IMEM	Gibco, San Diego, CA, USA
Isopropyl alcohol	Merck Millipore, Darmstadt, Germany
ITS (Insulin-Transferrin-Selenium)	Gibco, San Diego, CA, USA
K-Acetate (> 99.5 %)	Sigma-Aldrich, St. Louis, MO, USA

KCl	Merck Millipore, Darmstadt, Germany
KH_2PO_4	Merck Millipore, Darmstadt, Germany
L- Glutamine	Gibco, San Diego, CA, USA
LentiBOOST	Sirion Biotech, Martinsried, Germany
LightCycler 480 Probes Master	Roche, Mannheim, Germany
$MgCl_2$ x $6H_2O$ (> 99 %)	Carl Roth, Karlsruhe, Germany
Midori green advance	Biozym Scientific GmbH, Hessisch Oldendorf, Germany
$MnCl_2$ x $4H_2O$	US Biological, Swampscott, MA, USA
MOPS (> 99.5 %)	Sigma-Aldrich, St. Louis, MO, USA
Na_2HPO_4 x $7H_2O$	Sigma-Aldrich, St. Louis, MO, USA
NaCl	Carl Roth, Karlsruhe, Germany
NEAA (non essential amino acids) 100x	Gibco, San Diego, CA, USA
Penicillin/streptomycin 5,000 U/ml	Gibco, San Diego, CA, USA
Peptone (SELECT peptone 140)	Gibco, San Diego, CA, USA
Polybrene 2 mg/ml	Sigma-Aldrich, St. Louis, MO, USA
Recombinant human Flt-3 ligand	R&D Systems, Minneapolis, USA
Recombinant human IL-3	PeproTech, Rocky Hill, USA
Recombinant human SCF	PeproTech, Rocky Hill, USA
Recombinant human TPO	PeproTech, Rocky Hill, USA
RLT buffer	Qiagen, Venlo, NL
RPMI-1640	Gibco, San Diego, CA, USA
StemPro-34 medium	Thermo Fischer, Scientific, Waltham, MA, USA
StemPro-34 Nutrient supplement	Thermo Fischer, Scientific, Waltham, MA, USA
Sodium pyruvate (100 mM)	Sigma-Aldrich, St. Louis, MO, USA
Tamoxifen	Sigma-Aldrich, St. Louis, MO, USA
Tris (> 99.9 %)	Carl Roth, Karlsruhe, Germany
Trypan blue	Sigma-Aldrich, St. Louis, MO, USA
Trypsin (0.5 % Trypsin-EDTA)	Invitrogen, Karlsruhe, Germany
Turbofect	Thermo Fischer, Scientific, Waltham, MA, USA
Universal ProbeLibrary Probes	Roche, Mannheim, Germany
Water (DNase- and RNase-free)	Sigma-Aldrich, St. Louis, MO, USA

Yeast extract	Carl Roth, Karlsruhe, Germany

3.13 Kits

Name	Source
CloneJET PCR cloning kit	Thermo Fischer, Scientific, Waltham, MA, USA
Mouse cell depletion kit	Miltenyi, Bergisch Gladbach, Germany
NucleoSpin gel and PCR clean-up	Macherey Nagel, Duren, Germany
NucleoSpin Plasmid EasyPure	Macherey Nagel, Duren, Germany
NucleoBond Xtra Midi Plus	Macherey Nagel, Duren, Germany
QiAmp DNA Mini Kit	Qiagen, Venlo, NL
QuantiTect Reverse Transcription kit	Qiagen, Venlo, NL
RNase-free DNase set	Qiagen, Venlo, NL
RNeasy mini kit	Qiagen, Venlo, NL

3.14 Consumables

Name	Source
Amicon Ultra 15 centrifugal filter units	Merck Millipore, Darmstadt, Germany
Cell strainer	Greiner bio-one, Frickenhausen, Germany
Centrifuge tubes (15 ml, 50 ml)	Greiner bio-one, Frickenhausen, Germany
Cryotubes (1.8 ml)	Greiner bio-one, Frickenhausen, Germany
Eppendorf tubes (1.5 ml, 2 ml)	Eppendorf, Hamburg, Germany
Erlenmeyer flasks (1 l)	SCHOTT AG, Mainz, Germany
Examination gloves	Microflex, Reno, NV, USA
FACS tubes (5 ml)	Corning Incorporated, Corning, NY, USA
Filter Steriflip (0.45 µm)	Merck Millipore, Darmstadt, Germany
Filter tips (10 µl, 20 µl, 200 µl, 1,000 µl)	STARLAB, Hamburg, Germany
Filterunit Millex-HV 0.45 µm	Merck Millipore, Darmstadt, Germany
Glass bottles (100 ml, 500 ml, 1 l)	SCHOTT, Stafford, UK
Inoculation loops	Sarstedt, Nümbrecht, Germany
LightCycler 480 Multiwell plate 96	Roche, Mannheim, Germany
LS columns	Miltenyi, Bergisch Gladbach, Germany
Microvette, Lithium-Heparin (100 µl)	Sarstedt, Nümbrecht, Germany

Multiwell Plate 96 for LightCycler 480	Roche, Mannheim, Germany
Needles RN G32 PST3 51MM	Hamilton, Reno, NV, USA
Parafilm laboratory film	Kisker Biotech GmbH, Steinfurt, Germany
PCR tubes	Eppendorf, Hamburg, Germany
Pipette tips (10 µl, 20 µl, 200 µl, 1,000 µl)	Eppendorf, Hamburg, Germany
PureYield™ Binding/Clearing Columns	Promega, Madison, WI, USA
QiaShredder	Qiagen, Venlo, NL
Rotilabo syringe filters 0.22 µm	Carl Roth, Karlsruhe, Germany
Round bottom tubes (14 ml)	Corning Incorporated, Corning, NY, USA
Round bottom tubes (5 ml) with lid or with cell strainer cap	Corning Incorporated, Corning, NY, USA
Sealing Foil for LightCycler 480	Roche, Mannheim, Germany
Serological pipettes (5 ml, 10 ml, 25 ml)	Greiner bio-one, Frickenhausen, Germany
Soft wipes	Kimberly-Clark Europe, Surrey, UK
Surgical disposable scalpel	Braun, Melsungen, Germany
Tali™ cellular analysis slides	Invitrogen, Karlsruhe, Germany
Tissue culture dishes (100 x 20 mm)	BD Bioscience, Heidelberg, Germany
Tissue culture flasks (25 cm^2, 75 cm^2)	Greiner bio-one, Frickenhausen, Germany
Tissue culture plates (6-, 12-, 24-, 48-, 96- well)	Corning Incorporated, Corning, NY, USA
Tube Top Filter 50 ml; 0.45 µm	Corning Incorporated, Corning, NY, USA
Vacuum disposable filtration system	Merck Millipore, Darmstadt, Germany

3.15 Hardware and Equipment

Name	Source
Axioplan fluorescence microscope	Zeiss, Jena, Germany
BD Calibur	BD Bioscience, Heidelberg, Germany
BD FACSAria III	BD Bioscience, Heidelberg, Germany
BD LSRFortessa	BD Bioscience, Heidelberg, Germany
Calibration Check pH-meter HI 221	HANNA Instrument, Vöhringen, Germany
Centrifuge Rotanta 460R	Andreas Hettich GmbH, Tuttlingen, Germany
CO_2 Induction Systems	Quietek, New York, USA
Electrophoresis system	Biozym Scientific GmbH, Hessisch Oldendorf, Germany

ErgoOne multi-channel pipettes	STARLAB, Hamburg, Germany
ErgoOne single-channel pipettes	STARLAB, Hamburg, Germany
Freezer (-20 °C)	Siemens, München, Germany
Freezer HERA HFU (-80 °C)	Thermo Fischer Scientific Waltham, MA, USA
Freezing container Mr. Frosty	Thermo Fischer Scientific Waltham, MA, USA
Fridge (4 °C)	Bosch GmbH, Stuttgart, Germany
Gamma cell 40 CS-137 irradiation	Best Theratronics, Ottawa, Canada
Gel documentation E-box VX2	Peqlab, Erlangen, Germany
Hera Cell incubator 150i	Thermo Fischer Scientific Waltham, MA, USA
Innova 44 shaking incubator	New Brunswick Scientific, Enfield, CT, USA
IVIS Lumina II Imaging System	Caliper Life Sciences, Mainz, Germany
Labeling BMP51	Brady, Milwaukee, WI, USA
Laminar Flow SAFE 2000	Thermo Fischer Scientific Waltham, MA, USA
LightCycler 480 II	Roche, Mannheim, Germany
Light microscope 550 1317	Zeiss, Jena, Germany
Microbiological incubator B 6060	Heraeus, Hanau, Germany
Microcentrifuge 5417C	Eppendorf, Hamburg, Germany
Microscale 2001 MP2	Sartorius, Göttingen, Germany
Nanodrop 1000	PeqLab, Erlangen, Germany
Neubauer improved counting chamber	Brand, Wertheim, Germany
Pipette controller Accu-jet pro	Brand, Wertheim, Germany
Rocking platform	VWR, Radnor, PA, USA
Tali™ cytometer	Invitrogen, Carlsbad, CA, USA
Thermocycler primus 25 advanced	PeqLab, Erlangen, Germany
Thermoleader Heat block	Kisker Biotech GmbH, Steinfurt, Germany
UV cleaner	Kisker Biotech GmbH, Steinfurt, Germany
Vortex-Genie 2	Scientific Industries, Bohemia, NY, USA
Water bath WNB 14	Memmert GmbH, Schwabach, Germany
Water purification system Aquintus	membraPure GmbH, Berlin, Germany

3.16 Software

BD FACS Diva software v8.0.1

Clone Manager 7

Endnote X8

FlowJo V10

Graph Pad Prism 6

LightCycler 480 software 1.5.1

Living Image software 4.4

Microsoft Office

MyIMouse Databank

4. Methods

4.1 Ethical issues

4.1.1 Working with patient derived material

Human material was obtained from clinical diagnostic leftover before treatment was started. Fresh bone marrow and peripheral blood from acute leukemia patients were collected and used for this study. Written informed consent was obtained from all patients and from parents/carers in the cases where the patients were minors. The study was performed in accordance with the ethical standards of the responsible committee on human experimentation (written approval by the Ethikkommission des Klinikums der Ludwig-Maximilian-Universität (LMU) München, Germany Ethikkommission@med.unimuenchen.de, April 2008, number 068-08 and October 2010, number 222-10) and with the Helsinki Declaration of 1975, as revised in 2000.

4.1.2 Working with animals

Non-obese diabetes (NOD) severe combined immune deficiency (scid) gamma (NSG) mice were obtained from The Jackson Laboratory (Bar Harbour, ME, USA). The mice were kept under specific pathogen-free conditions in the research animal facility of the Helmholtz Zentrum München and had free access to drinking water and food. Constant room temperature and 12 hour day-night light cycle were maintained in the animal facility. All animal trials were performed in accordance with the current ethical standards of the official committee on animal experimentation (written approval by Regierung von Oberbayern, poststelle@reg-ob.bayern.de, September 2010, number 55.2-1-54-2531-95-10, October 2012, number 55.2-1-54-2531.6-10-10 and August 2016, number 55.2-1-54-2532.0-56-2016). As soon as clinical signs of sickness were detected (over 60 % leukemia cells in the peripheral blood or exterior abnormalities), mice were sacrificed. If leukemia cells did not engraft, mice were sacrificed and analyzed not later than 25 weeks after cell injection.

4.2 The xenograft mouse model of individual acute leukemia

Immunocompromised animals enable the engraftment and amplification of human hematopoietic stem cells (Andre et al., 2010). A xenograft mouse model for individual acute leukemia has been established in the laboratory and was used for this study

(Kamel-Reid et al., 1989; Shultz et al., 2005; Terziyska et al., 2012; Vick et al., 2015). Peripheral blood or bone marrow cells from patients with acute leukemia were resuspended in sterile filtered PBS and injected into the tail vein of NSG mice to amplify cells. Mice were fed with drinking water containing 0.01 % Baytril to prevent infections.

4.2.1 Engraftment and amplification of primary patient cells

10^7 primary tumor cells from acute leukemia patients were transplanted into 2 - 4 NSG mice per primary sample. Therefore, peripheral blood or bone marrow aspirates were resuspended in 100 µl autoclaved and filtered PBS and injected into the tail vein. Specific pathogen-free conditions in the research animal facility of the Helmholtz Zentrum München were used for animal maintenance.

Engraftment was determined by blood sampling and staining for human CD45 and human CD38 in the blood (4.2.5). Mice were sacrificed when specific time points of experiments were reached, when advanced leukemia was detected via blood measurement or as soon as first signs of illness were observed. Human leukemia cells were isolated from bone marrow and spleen and typically contained > 90 % human cells in full-blown leukemia mice. In contrast to other groups, cell transplantation was performed in the absence of preconditioning by total body irradiation (Patel et al., 2014; Terziyska et al., 2012). After successful engraftment of primary samples, patient derived xenograft (PDX) cells were amplified by passaging in mice. For re-transplantation, $5x10^6$ - 10^7 isolated cells were reinjected into 2 - 4 new NSG mice.

4.2.2 Sacrification of mice

Mice were sacrificed either when blood measurement displayed leukemia, at certain time points of experiments, or as soon as first clinical signs of illness were detected (rough fur, hunchback, reduced motility). A CO_2 facility from Quietek CO_2 Induction Systems was used to sacrifice mice. The animals were placed into a specific cage (v = 7.67 l), which was connected to the CO_2 system (100 %) of the house through the lid. Mice were treated in two-steps, first they were anesthetized with a CO_2 flow rate of 10 % (750 ml/min) for 1 min. Subsequently, the CO_2 flow rate was increased to 30 % (2250 ml/min) for 4 min to kill the animals. Clinical death was confirmed and mice were used for organ dissection and further analysis.

4.2.3 PDX cell isolation from bone marrow and spleen

Human cells were obtained from bone marrow (BM) and spleen. After mouse sacrification (4.2.2), spleen and bones containing the bone marrow (sternum, backbone, femur, tibiae and hips) were isolated.

Spleen was homogenized using a 70 µm cell strainer and cells were collected in 30 ml PBS. For human cell purification, a Ficoll gradient centrifugation was performed by underlying the cell suspension carefully with 10 ml Ficoll and subsequent centrifugation (30 min, 400 g, RT, without rotor break). After this procedure, mononuclear cells were located in the interphase above the Ficoll, whereas erythrocytes and granulocytes were found at the bottom. Lymphocytes were carefully aspirated with a Pasteur pipette and washed twice in PBS (10 min, 400 g, RT). The supernatant was discarded and the cell pellet was resuspended in 10 ml PBS or patient medium (PM). The amount of cells was counted with a Neubauer counting chamber (4.3.3) and cells were stored short-time at 4 °C.

To isolate BM cells, bones were crushed in PBS using porcelain mortar and pestle. Cell suspension was filtered through a 70 µm cell strainer and washed twice with PBS (10 min, 400 g, RT). The supernatant was discarded and the cell pellet was resuspended in 10 ml PBS or PM. Cell number was determined with the help of a Neubauer counting chamber (4.3.3) and cells were stored short-time at 4 °C, respectively.

4.2.4 Mitochondrial fingerprinting

Mitochondrial fingerprinting was applied to confirm individual sample identity (Hutter et al., 2004). For each PDX sample, a repetitive finger printing of mitochondrial DNA was determined by polymerase chain reaction (PCR). A reference sequence of primary samples or the earliest available passage was prepared and used for sample authentication of later passages. 10^7 cells were collected for DNA extraction, which was conducted according to the manufacturer's instructions of the Qiagen QIAamp DNA Blood Mini Kit. Purified DNA concentration was measured at the Nanodrop and stored at -20 °C until experiments were continued.

PCR was performed in 50 µl batches using the following reaction:

Table 9: PCR composition for mitochondrial fingerprinting PCR

Compound	Volume [µl]
5x reaction buffer (colourless)	10
DNA (300 ng)	1
Primer mix (456 + 457 or 458 + 459) 10 pmol/µl each	5
dNTPs (10 mM)	1
GoTaq	0.25
H_2O	32.75

The following parameters were set for running the mitochondrial PCR:

Table 10: Cycler parameters for mitochondrial fingerprinting PCR

PCR step	Temperature	Time	Cycles
Initial denaturation	95 °C	2 min	1
Denaturation	94 °C	30 s	35
Annealing	60 °C	30 s	
Elongation	72 °C	30 s	
Final elongation	72 °C	5 min	1
Final hold	8 °C	∞	1

PCR products were purified with the Qiagen MiniElute 70 - 7,000 bp kit according to manufacturer's instructions and send for sequencing (100 ng/µl) at GATC (Biotech, Konstanz, Germany) using the same primer pair as applied in the PCR approach. In case the first primer pair 456 and 457 did not show clear unique pattern of single nucleotide polymorphisms (SNP), a second primer pair 458 and 459 was used instead. The sequence was compared with the original sample set from an early passage and would be considered as correct, if both samples showed the sample fingerprint pattern. Otherwise, cells were trashed and work was continued with a sample, which still contained the correct sample identification.

4.2.5 Monitoring leukemia growth *in vivo* by blood measurement

To determine the amount of human cells within the peripheral murine blood, 50 µl blood were collected from the tail vein with a heparin coated glass capillary. The blood was directly placed into an Eppendorf tube containing 5 µl heparin and gently mixed. Subsequently, the blood was stained with anti-murineCD45 APC (1:10) and anti-humanCD38 PE (1:10) in ALL samples or with anti-humanCD45 APC (1:10) and anti-umanCD33 PE (1:17) in AML samples. Samples were vortexed and incubated for 30 min at RT in the absence of light. Next, 1 ml FACS Lysing Solution was added per sample and incubated for 15 min at RT to lyse erythrocytes. If the mixture was not clear afterwards, the lysis step would be repeated. Samples were washed twice with FACS buffer (5 min, 300 g, RT) and measured at the FACS Calibur (4.4.6). Percentages of human cells within the murine peripheral blood were analyzed using FlowJo Software.

4.2.6 Bioluminescence *in vivo* imaging

Engraftment and growth of PDX acute leukemia cells was monitored *in vivo* in mice by bioluminescence imaging (Barrett et al., 2011; Bomken et al., 2013; Rabinovich et al., 2008; Terziyska et al., 2012). PDX cells were genetically engineered (4.4) to express Gaussia luciferase (GLuc) or enhanced Firefly luciferase (eFFly). Mice were anesthetized by inhalation anesthesia. Therefore, an empty mouse cage was connected with an isoflurane supply and flooded with 5 L/min for 1 min. Up to four mice were transferred into the chamber and as soon as mice were anesthetized, flow rate was reduced to 1.5 L/min. 100 µg Coelenterazine (GLuc) or 4.5 mg D-Luciferin (eFFly) were injected into the tail vein of immobilized mice after anesthetization. The substrate Coelenterazine was dissolved in methanol containing 32 % HCl to a final concentration of 10 mg/ml and shortly before application diluted in HBG buffer. D-Luciferin was dissolved in PBS to a final concentration of 30 mg/ml. Pictures were taken directly after injection (field of view: 12.5 cm, binning: 8, f/stop: 1 and open filter setting) and analyzed using Living Image Software 4.4.

4.2.7 Tamoxifen treatment *in vivo* in PDX cells

For inducible competitive assays in PDX cells *in vivo* 4-Hydroxytamoxifen, the active metabolite of tamoxifen, was used. The cytostatic drug belongs to the class of estrogen

receptor antagonists and is used in therapy against estrogen receptor positive breast cancer (Abukhdeir et al., 2008; Fisher et al., 1998; Osborne et al., 2000). A 10 mg/ml stock solution of tamoxifen was prepared by dissolving 10 mg of tamoxifen in 10 % filtered ethanol and 90 % filtered corn oil under sterile conditions. After vortexing, the solution was placed at 55 °C and vortexed frequently, until all the tamoxifen had dissolved completely. Mice were treated with tamoxifen by gavage, while control animals received a solution consisting of 10 % ethanol and 90 % corn oil. As tamoxifen is sensitive towards light, all work was performed under dark conditions. If mice were not treated directly, tamoxifen would be stored at -20 °C up to 2 weeks and heated to 37 °C prior to administration.

4.2.8 Constitutive competitive transplantation assay *in vivo*

A constitutive competitive transplantation assay *in vivo* was performed to monitor the growth behavior of two PDX cell populations expressing different shRNAs. PDX cells were transduced with lentiviruses (4.4.4) and positive cells enriched by FACS (4.4.5). Sorted cells were counted (4.3.3) and directly mixed in a 1:1 ratio. Total numbers of the cell mixture depended on the amount of sorted cells and varied between 2,000 and 15,000 cells. Before *in vivo* injection, the ratio of the mixed cells was checked by flow cytometry (4.4.6). Leukemia cell growth in mice was monitored by bioluminescence *in vivo* imaging as described (4.2.6) and first mice were sacrificed and analyzed as soon as a positive signal was detected. For late time points, mice were kept until human leukemia cells were detected via blood measurement (4.2.5). PDX cells were re-isolated from bone marrow or spleen as described (4.2.3) and the composition of the cell mixture was analyzed by flow cytometry (4.4.6).

4.2.9 Inducible competitive transplantation assay *in vivo*

An inducible system for competitive transplantation assays *in vivo* provides the advantage of determining the time point of starting the shRNA expression upon tamoxifen treatment. In addition, genetically engineered PDX cells were amplified by passaging in mice and thus, high cell numbers were available to start an experiment. Two cell populations expressing different fluorochromes were counted (4.3.3) and mixed in a 1:1 ratio. Prior to injection into mice, the correct mixing ratio was confirmed by flow cytometry (4.4.6). Human cell growth *in vivo* was followed up by

bioluminescence imaging as described (4.2.6) and tamoxifen treatment was started as soon as mice showed positive signals in imaging or at a defined time point. Mice were divided into two groups, the control group was treated with corn oil, whereas the experimental group received tamoxifen as described (4.2.7). Mice were sacrificed at different time points and human cells, extracted from murine bone marrow or spleen were analyzed using flow cytometry (4.4.6).

4.3 *In vitro* cell culture of PDX cells and cell lines

4.3.1 Freezing of PDX cells and cell lines

Cells were frozen for long time storage at -80 °C or in liquid nitrogen at -190 °C. Standardly, PDX cells were frozen in aliquots containing 10^7 or $5x10^7$ cells. After determining the correct cell number (4.3.3), cells were centrifuged in ice-cold PBS containing 2 % FCS (5 min, 300 g, 4 °C). The supernatant was discarded and the cell pellet dissolved in cold FCS. The same volume of freezing medium (80 % FCS, 20 % DMSO v/v) was added dropwise and 1 ml cell suspension was pipetted into each cryovial. All tubes were collected in a special freezing container, which allowed a cooling rate of -1 °C/min, and placed into the -80 °C freezer. After 24 h, cryotubes were transferred into appropriate boxes for either short-term storage at -80 °C or long-term storage in liquid nitrogen.

4.3.2 Thawing of PDX cells and cell lines

Frozen PDX cells were thawed according to the protocol of Dominique Bonnet to achieve high cell viability and to increase engraftment rates in mice (Bonnet, 2008). Cryovials were incubated for 1 min at 37 °C to thaw the contained cells. 100 µl DNase (1 mg/ml) were added dropwise to the cells, which then were gently mixed and incubated for 1 min. The cell suspension was transferred into a falcon tube and 1 ml FCS was added dropwise. After gentle mixing and 1 min incubation, 10 ml PBS/2 % FCS were added slowly. Again, the cell suspension was incubated for 1 min and PBS/2 % FCS was slowly added up to 30 ml. After centrifugation (5 min, 200 g, 4 °C) the cell pellet was resuspended in 1 ml PBS/2 % FCS. Clumped cells were filtered through a 70 µm cell strainer. Cell number was detected using a Neubauer counting chamber (4.3.3) and cells were used for *in vivo* and *in vitro* experiments.

Cell line cells were thawed rapidly at 37 °C and transferred into a 15 ml falcon containing 9 ml PBS/2 % FCS. After centrifugation of the cell suspension (5 min, 400 g, RT), the supernatant was discarded and cells were resuspended in the appropriate medium containing 1 % Pen/Strep. Viable cells were counted using the Tali cell counter and transferred into a new culture flask.

4.3.3 Determination of cell numbers and staining of apoptotic cells

The Neubauer counting chamber was used to determine the number of living PDX cells. 10 µl adequately diluted cells were pipetted into the hemocytometer chamber and counted under a light microscope. The cell number of one quarter is representative for 0.1 µl cell suspension, as one corner quarter has an area of 1 mm^2 and a height of 0.1 mm. Trypan blue staining was used to distinguish living and dead cells. Therefore, cell suspension was mixed 1:1 (v/v) with 0.4 % trypan blue and 10 µl were pipetted into the chamber. Dead cells were selectively coloured blue, as the dye could penetrate their cell membrane, whereas living cells remained colourless. All four corner quarters were counted and the counted cell number was divided by four to receive the mean of counted cells. The total cell number was calculated with the following approach:

$$\text{total cell number} = \text{mean of counted cells} \times \text{dilution factor} \times 10^4 \text{ cells/ml}$$

To determine the number of viable cells in cell lines, the Tali cell counter was used. Cells were mixed well and collected in a falcon tube. Adherent cells were detached from the flask beforehand using trypsin. After centrifugation (5 min, 400 g, RT), cells were resuspended in the appropriate medium and 25 µl were pipetted into a Tali cellular analysis slide. Cell sample slide was inserted into the Tali cell counter and cell number was calculated in cells/ml.

4.3.4 *In vitro* cultivation of PDX cells and cell lines

Fresh and thawed PDX cells were maintained short-term *in vitro* in 6-well plates. Therefore, ALL cells were cultivated in PM^{+++} medium and AML cells in DD medium, respectively. Cells were cultured with a cell density of $2x10^6$ cells/ml. Cells were cultivated at 37 °C with 5 % CO_2 and 0.5 ml/well fresh medium were added each day.

All cell lines used in this study are listed in **Table 1**. Suspension cell lines were cultured in 25 cm^2 or 75 cm^2 flasks in 10 ml or 20 ml medium at 37 °C with 5 % CO_2. Cells were grown at a concentration of 0.5 to 2x10^6 cells/ml and split 1:10 every 2 to 3 days to have steady numbers of cell density. IMEM complete medium was used for SEM cells and RPMI complete medium for NALM-6 cells (3.11). Adherent cell lines were cultured in 75 cm^2 flasks specific for adherent cells in 10 ml medium at 37 °C with 5 % CO_2. Cells were confluent after 2 to 3 days and split 1:10 by removing the old medium and washing the attached cells with PBS. Then, 2 ml trypsin were added onto the cells and incubated at 37 °C. As soon as the cells detached, the reaction was stopped by adding 2 ml fresh medium and resuspended and splitted them accordingly. Fresh medium was added up to a total volume of 10 ml. HEK-293 cells were cultured in DMEM complete medium and the murine stromal cell line MS-5 was grown in α-MEM complete medium (3.11).

4.3.5 *Ex vivo* cultivation of transduced PDX ALL cells in co-culture

To increase the cell viability of transduced PDX ALL cells *ex vivo*, a co-culture system was used in this study. The supernatant of confluent MS-5 cells from a 75 cm^2 flask was removed and cells were washed carefully with PBS. Cells were detached using 2 ml trypsin and incubated for 5 min at 37 °C. The reaction was stopped adding 2 ml fresh medium and detached cells were collected in a falcon tube. After centrifugation (5 min, 400 g, RT), cells were resuspended in fresh medium and counted with the Tali cell counter (4.3.3). Murine stromal cells were seeded in 6-well plates to a final density of 300,000 cells per well in 2 ml α-MEM complete medium and cultured overnight at 37 °C. After 24 h, cells were irradiated at 52.6 cGy/min for 2 h (63 Gy). The cell line medium was removed and PDX cells were placed onto the feeder cells with a final concentration of 2x10^6 cells/ml in PM^{+++} medium. 0.5 ml fresh PM^{+++} medium were added each day and cells were sorted using FACS after 5 days *in vitro* (4.4.5). The co-culture was only needed to cultivate transduced PDX ALL cells, as transduced AML cells showed a better viability *ex vivo* and therefore were directly cultured in DD medium in 6-well plates.

4.3.6 Tamoxifen treatment *in vitro* in cell lines

For inducible competitive assays *in vitro*, cell lines were treated with 4-hydroxytamoxifen, which is the active metabolite of tamoxifen. 5 mg of lyophilized 4-hydroxytamoxifen were dissolved in 2.5 ml 100 % ethanol and vortexed until the solution was clear. This 5 mM stock solution was aliquoted into tubes containing 10 µl and stored at -80 °C. Stock solutions were only stored up to 2 months at -80 °C, as tamoxifen would begin to precipitate afterwards. Then, stock solutions were trashed and new lyophilized tamoxifen powder was solved. Stock solution aliquots were diluted in PBS directly before treating the cells. For cell line experiments, cells were seeded with a density of $1.5x10^6$ cells in 3 ml total medium and treated with tamoxifen accordingly. Different tamoxifen concentrations were used in a range of 40 nM to 120 nM in parallel to find out optimal experimental conditions. As tamoxifen is sensitive towards light, all work was done under dark conditions.

4.3.7 Constitutive competitive assay *in vitro* in cell lines

A constitutive competitive assay was performed to analyze the growth behavior of two cell populations with different shRNA expression patterns. Cell populations were genetically engineered to express different fluorescent markers, mixed in a 1:1 ratio and seeded with a density of $0.5x10^6$ cells/ml in 1 ml total volume in a 12-well plate. Plates were incubated at 37 °C with 5 % CO_2 and cell growth was monitored twice per week by flow cytometry (4.4.6). Cells were split every 2 to 3 days according to cell density (4.3.4) and cultured up to 30 days.

4.3.8 Inducible competitive assay *in vitro* in cell lines

For inducible competitive experiments *in vitro*, two cell populations distinguishable by the expression of different fluorescent markers were mixed in a 1:1 ratio with a density of $1.5x10^6$ cells in 3 ml total volume in a 6-well plate. Samples were treated with tamoxifen as described (4.2.7). Control assays were performed without tamoxifen treatment. Cells without genetic engineering were treated with tamoxifen to detect tamoxifen toxicity. To analyze $CreER^{T2}$ toxicity, cells that solely expressed $CreER^{T2}$ were treated with tamoxifen. Plates were incubated at 37 °C with 5 % CO_2 and cell growth was monitored for four weeks. Cells were measured twice per week using flow

cytometry (4.4.6) and split according to cell density every 2 to 3 days. Additionally, specific fluorochrome expressing cell populations were isolated by FACS (4.4.5), mRNA was extracted (4.6.11), reverse transcribed into cDNA (4.6.12) and used for qRT-PCR analysis (4.6.13) at defined time points.

4.4 Genetic engineering of PDX cells and cell lines

4.4.1 Enrichment of PDX cells

Magnetic-activated cell sorting (MACS) was applied to enrich human leukemia cells from the murine bone marrow and to remove murine cells. In principal, microbeads antibodies bind to specific cluster of differentiation (CD) surface antigens of the human cell populations. Hence, labelled cells are separated with a column placed in a permanent magnetic field. For this purpose the mouse cell depletion kit (MCDK) was used to gather enough human cells for analyzing or sorting (4.4.5 and 4.4.6) when the leukemia burden in the mouse was still at a very low level. Cells were isolated from the total bone marrow of one mouse (4.2.3), filtered through a 70 µm cell strainer and centrifuged (5 min, 400 g, RT). After resuspending the cell pellet in 3 ml PBS containing 0.5 % BSA, 100 µl mouse cell depletion beads were added and mixed. The approach was incubated for 15 min at 4 °C on a tube roller and afterwards, 10 ml PBS/0.5 % BSA were added. The cell suspension was filtered again through a 70 µm cell strainer and was equally distributed between two LS columns. The MCDK procedure was conducted according to the manufacturer's instructions and human leukemia cells were finally collected in a falcon tube, centrifuged (5 min, 400 g, RT) and resuspended in PBS.

4.4.2 Lentivirus production using HEK-293 packaging cells

Third generation lentiviruses were used for genetic engineering of PDX leukemia cells and cell lines (Dull et al., 1998; Zufferey et al., 1999). The required components are split onto four separate plasmids for safety reasons. Two packaging plasmids, pMDLg/pRRE and pRSV-Rev, contain the viral genes coding for GAG, POL and REV. A third plasmid named pMD2.G contains the viral gene for the envelope protein VSV-G. The DNA or shRNA of interest is encoded on the transfer plasmid (**Figure 9**).

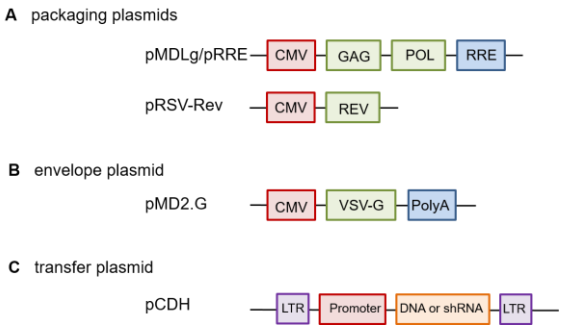

Figure 9: Schematic representation of third generation lentiviral plasmids used in this study
(A) The packaging plasmids contain the viral genes GAG, POL and REV. **(B)** The envelope plasmid contains the viral gene VSV-G coding for a structural protein. **(C)** The transfer plasmid contains the DNA or shRNA of interest. CMV, cytomegalovirus; RRE, Rev Response Element; VSV-G, vesicular stomatitis virus G; LTR, Long Terminal Repeats.

For the production of lentiviruses, the adherent packaging cell line HEK-293 was used (3.3). The old medium was removed and adherent cells were washed with PBS. 2 ml trypsin were added and the flask placed at 37 °C for 1 – 2 min to detach the cells. 2 ml DMEM complete medium were added, cells resuspended and collected in a falcon tube. After centrifugation (5 min, 400 g, RT), the cell pellet was dissolved in fresh medium and cells were counted with the Tali cell counter (4.3.3). Next, 7.5 - 10x10^6 cells were seeded into a new 75 cm^2 flask in 10 ml DMEM complete medium. The next day, cell confluency was checked under the light microscope and cell transfection was performed when cells reached 50 - 80 % confluency. For each 75 cm^2 flask one Eppendorf tube was prepared with the following components: 1 ml DMEM without FCS, 2.5 µg of packaging plasmid 392, 5 µg of 393, 1.25 µg of pMD2.G and 2.5 µg of the desired transfer vector. In a final step, 24 µl turbofect were added dropwise and the mixture was incubated for 20 min at RT. In the meantime, the old medium of HEK-293 cells was exchanged by fresh DMEM complete medium. The DNA suspension was added dropwise to the adherent cells and incubated for 72 h at 37 °C and 5 % CO_2. After 3 days, the supernatant of two equal flasks was collected in a 50 ml falcon and centrifuged (5 min, 400 g, RT) to remove remaining cells. If the desired vector expressed fluorochromes, flasks were checked under the fluorescent microscope for colour expression. The supernatant was filtered through 0.45 µm filters to exclude small cell particles. Subsequently, the virus suspension was concentrated by ultrafiltration in Amicon-Ultra 15 centrifugal filter units (30 min, 2,000 g, RT) to a final volume of 200 – 250 µl and was stored at -80 °C in aliquots of 20 µl. Each produced lentiviral virus was tested on NALM-6 cells and the virus titer was determined (4.4.3).

4.4.3 Lentiviral titer determination

The titer of each produced lentivirus was determined in NALM-6 cells. Therefore, NALM-6 cells were collected in a falcon tube, centrifuged (5 min, 400 g, RT), resuspended in fresh RPMI complete medium and counted (4.3.3). Five wells of a 24-well plate were prepared containing $0.5x10^6$ cells in 0.5 ml medium. 8 µg/ml polybrene were pipetted into each well and virus was added in ascending concentrations (0 µl, 1 µl, 3 µl, 10 µl, 25 µl). Plates were incubated for 72 h at 37 °C with 5 % CO_2. Then, cells were washed 3x with PBS (5 min, 400 g, RT) to remove remaining virus particles and dissolved in RPMI complete medium. The amount of positive transduced cells was analyzed by flow cytometry and the virus titer was calculated as follows:

$$\text{virus titer} = \left(\frac{\text{F} * \text{Z}}{\text{V}}\right) \text{TU/ml}$$

F: percentage of positive transduced cells
Z: cell number at infection
V: volume of virus in ml

Efficient virus titers used in this study were in a range of 10^8 - 10^9 TU/ml and led to a transduction rate > 80 % in NALM-6 cells. If the tested lentivirus showed a worse transduction quality, the virus was trashed and not used for further experiments.

4.4.4 Lentiviral transduction of PDX cells and cell lines

Third generation lentiviral vector systems were used for genetic engineering of PDX (GEPDX) cells and cell lines (4.4.1). For lentiviral transduction of PDX cells, $10x10^6$ cells were plated in 1 ml/well in a 6-well plate. For both, ALL and AML PDX cells, patient medium (PM) without additional ingredients was used (3.11). The transduction enhancer polybrene was added with a final concentration of 8 µg/ml to decrease the charge repulsion between virus and cell and thereby, increasing the transduction efficiency (Davis et al., 2002; Davis et al., 2004). 20 µl concentrated virus carrying the desired transgene were added per well to achieve a final multiplicity of infection between 300 - 1300. Cells were incubated for 24 h at 37 °C with 5 % CO_2. The next

day, cells were collected and washed three times with PBS (5 min, 400 g, RT) to remove viral particles. PDX cells were either directly injected into the mouse or cultivated additionally using a co-culture for ALL PDX cells *in vitro* (4.3.5). To prepare cells for *in vivo* injection, they were resuspended in 100 µl sterile filtrated PBS. Transduction rate of PDX cells was determined using flow cytometry (4.4.6).
For lentiviral transduction of cell lines, $1.5x10^6$ cells were plated in 1 ml/well in a 6-well plate using the appropriate medium (4.3.4). The rest of the procedure was performed as described for PDX cells. Positive transduction of cell lines was monitored via transgene expression using flow cytometry (4.4.6).

4.4.5 Enrichment of GEPDX cells and cell lines by fluorescence-activated cell sorting

GEPDX cells expressing a fluorescent colour were enriched by fluorescence-activated cell sorting (FACS) using the BD FACSAria III and the instrumental settings listed in **Table 11**.

Table 11: Filter settings of the BD FACSAria III

Laser	Excitation (nm)	Longpass filter	Bandpass filter (Emission)	Parameter
Violet laser	405		450/40 510/50	CFP AmCyan
Blue laser	488	655 505	695/40 530/30 488/10	PerCP/CyF5.5 FITC, GFP SSC
Yellow/Green laser	561	600 570	610/20 586/15	mCherry DsRED
Red laser	633	735 690	780/60 710/50	APC/Cy7 Alexa Fluor 700

Cells were either thawed (4.3.2), taken fresh directly from the mouse (4.2.3) or from co-culture 5 days after lentiviral transduction (4.3.5). A final concentration of $10x10^6$ cells/ml was prepared and filtered before sorting, using a round bottom tube with cell

strainer cap. Sorted cells were collected in a 15 ml falcon tube containing 3 ml patient medium. A 100 µm nozzle was used for the sorting procedure and sorting was performed either with the instrument setting “Purity” when transduction rate was high or with the adjustment “Yield” when transduction rate was low. Sorted PDX cell populations were centrifuged (5 min, 400 g, RT), resuspended in sterile filtrated PBS for injection into mice or used for subsequent experiments.

Cell lines were mostly sorted fresh from *in vitro* cell culture and processed in the same way as PDX cells (**Figure 10**). The appropriate medium was used for each cell line (4.3.4). Generally, cell lines showed high transduction rates > 50 % upon genetic engineering with lentiviruses and therefore, they were always sorted with the adjustment “Purity”. As the sorting procedure was a semi-sterile process, cell lines were subsequently cultured adding 1:200 ciprobay antibiotics for 1 week.

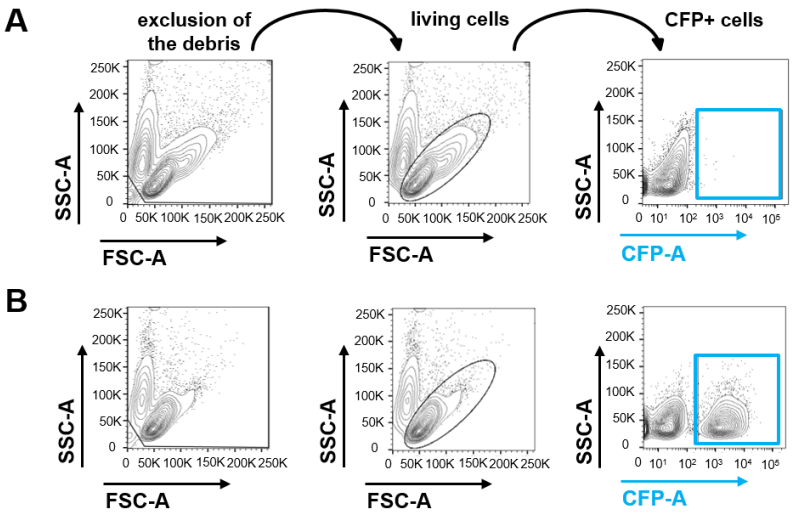

Figure 10: Gating strategy to enrich genetically engineered cells
Cell debris and dead cells were excluded and viable cells were gated using forward scatter against side scatter (FSC/SSC). **(A)** Non-transduced cells were used as a negative control for fluorescent colour expression. **(B)** Genetically engineered cells expressed fluorochromes, for example mtagBFP, which was monitored by CFP. Positively transduced cells were enriched by FACS.

4.4.6 Analysis of PDX cells and cell lines using flow cytometry

Flow cytometry analysis was performed with a BD LSRFortessa. Laser and filter settings for the detection of fluorescent proteins (eGFP, iRFP, mCherry, mtagBFP, T-Sapphire) and other fluorochromes (APC, FITC, PE, PerCP/Cy5.5) are indicated in **Table 12**. Cell debris and dead cells were excluded by gating to only monitor living cell populations (**Figure 10**).

Table 12: Filter settings of the BD LSRfortessa

Laser	Excitation (nm)	Longpass filter	Bandpass filter (Emission)	Parameter
Violet laser	405	475	525/50 450/50	AmCyan mtagBFP
Blue laser	488	600 505	695/40 530/30 488/10	PerCP/Cy5.5 FITC, GFP SSC
Yellow/Green laser	561	750 685 635 600 570	780/60 710/50 670/30 610/20 585/15	PE/Cy7 PE/Cy5.5 PE/Cy5 mCherry PE
Red Laser	640	750 710	780/60 730/45 670/14	APC/Cy7 Alexa Fluor 700 APC/Cy7

4.5 Microbiology methods

4.5.1 Generation of competent *E.coli* DH5α cells

For generation of competent *E.coli* DH5α cells transformation buffer I (TFB I) and transformation buffer II (TFB II) were prepared accordingly (3.10). A 3 ml culture of DH5α bacteria was prepared with LB medium and incubated overnight at 37 °C. 100 ml fresh LB medium were inoculated with 1 ml of the overnight culture and incubated at 37 °C until an OD_{600} of 0.4 - 0.5 was reached. As bacterial growth behaves exponential, the OD_{600} was frequently checked with a photometer starting approximately 1h after inoculation. As soon as the appropriate OD_{600} was detected, the bacteria suspension was put on ice for 2 min to cool down. The bacteria suspension was divided into two 50 ml falcon tubes and centrifuged (5 min, 400 g, 4 °C) in a pre-cooled centrifuge. After discarding the supernatant, each pellet was resuspended in 15 ml TFB I buffer and incubated 5 min on ice. Again, the bacteria suspension was centrifuged (5 min, 400 g, 4 °C) in a pre-cooled centrifuge and after discarding the

supernatant, both pellets were pooled together and resuspended in 4 ml TFB II buffer. The bacteria suspension was aliquoted in small batches of 50 µl in sterile 1.5 ml Eppendorf tubes and stored at -80 °C.

4.5.2 Culture and storage of competent *E.coli* DH5α cells

E.coli DH5α cells were cultured in LB medium at 37 °C. After transformation with plasmid DNA (4.5.3), cells were cultured with 50 µg/ml ampicillin either in LB_{amp} medium or on LB_{amp} agar plates (3.11). Glycerol stocks of *E.coli* DH5α cells were prepared for long-term storage. Therefore, 100 µl glycerol were mixed with 900 µl of an overnight culture prepared as previously described (4.5.1), frozen by 30 min incubation on ice and stored at -80 °C.

4.5.3 Heat shock transformation of competent *E.coli* DH5α cells

To introduce plasmid DNA into chemically competent *E.coli* DH5α cells, heat shock transformation was performed. Either 50 - 100 ng purified plasmid DNA (4.6.10) or 5 µl ligation product (4.6.7) were pipetted to 50 µl *E.coli* DH5α bacteria that had thawed on ice. After gentle mixing, the cells were incubated 30 min on ice and subsequently subjected to 42 °C for 90 s. Afterwards, cells were quickly put back onto ice and incubated for 2 min. 400 µl LB_0 medium were added and the whole bacteria suspension was incubated for 45 - 60 min in a shaker at 37 °C. LB_{amp} agar plates were pre-warmed at 37 °C and 100 µl bacteria suspension were plated. Plates were incubated up-side-down overnight at 37 °C and checked for colonies the next day.

4.5.4 Single colony picking

Agar plates were incubated overnight at 37 °C after heat shock transformation (4.5.3) and analyzed for colony growth the next day. Single colonies were picked using an inoculation loop and either 2 ml LB_{amp} in a 24-well plate or 5 ml LB_{amp} in a round bottom tube were inoculated. LB_{amp} medium was supplemented with 50 µg/ml ampicillin using 50 mg/ml antibiotics stock solution. Bacteria cells were incubated for 24 h at RT or on a shaker overnight at 37 °C. Afterwards, *E.coli* DH5α cells were directly used for plasmid preparation or stored short-term for up to one day at 4 °C.

4.5.5 Culture and storage of transformed *E.coli* DH5α cells

E.coli DH5α cells, which were transformed with plasmid DNA, were cultured in LB_{amp} medium containing 50 µg/ml ampicillin (4.5.4). The bacteria suspension was incubated on a shaker overnight at 37 °C. For long-term storage, 900 µl cell suspension were mixed with 100 µl glycerol, incubated 30 min on ice and stored at -80 °C.

4.6 Molecular biology methods

4.6.1 Polymerase chain reaction

Polymerase chain reaction (PCR) was done to amplify coding sequences of interest using a DNA plasmid as a template. The PCR approach was pipetted according to the following composition (**Table 13**).

Table 13: Composition for polymerase chain reaction

Compound	Volume/amount
Template DNA	50 ng
dNTPs (10 mM)	2 µl
5x GoTaq buffer	10 µl
Primer for (100 pmol/µl)	1 µl
Primer rev (100 pmol/µl)	1 µl
GoTaq DNA polymerase	1 µl
ddH_2O	up to 50 µl

DNA was amplified during the run of the following PCR program (**Table 14**):

Table 14: Cycler parameters for polymerase chain reaction

PCR step	Temperature	Time	Cycles
Initial denaturation	95 °C	2 min	1
Denaturation	95 °C	30 s	35
Annealing	50 - 60 °C	30 s	
Elongation	72 °C	1 min/kb	
Final elongation	72 °C	5 min	1
Final hold	8 °C	∞	1

Annealing temperature and elongation time were adjusted for each experiment depending on the melting temperature of the primer and the DNA fragment length of the PCR product. The success of the PCR was controlled by agarose gel electrophoresis (4.6.3). Eventually, DNA bands were cut out and purified (4.6.4).

4.6.2 Purification of PCR products

To purify PCR products, the NucleoSpin Plasmid EasyPure Kit was used according to manufacturer's protocol. In brief, the PCR product was mixed with the binding buffer and the whole suspension was loaded onto a silica membrane provided by the manufacturer. After a few washing steps, the membrane was dried and DNA was eluted in 30 µl ddH_2O pre-heated to 70 °C. Concentration of the DNA was determined with the Nanodrop (4.6.14) and samples were stored at -20 °C.

4.6.3 Agarose gel electrophoresis of DNA

After PCR or DNA digestion, mixed solutions of DNA fragments were separated according to their size by agarose gel electrophoresis. Depending on the size of the DNA fragment, 1 - 3 % (w/v) agarose gels were prepared by dissolving agarose powder in 1x TAE buffer accordingly. Therefore, the agarose powder was mixed with 1x TAE buffer and heated in the microwave. As soon as the solution appeared completely clear, it was cooled down to ~ 55 °C and 12 µl Midori Green were added to 100 ml agarose solution (0.12 %). The mixture was placed into a gel chamber and a comb was added for pocket formation. The gel hardened in approximately 30 min and

was then placed into a gel electrophoresis chamber, which was filled with 1x TAE buffer. The comb was removed afterwards. Samples were prepared by mixing them with 6x DNA-loading dye and loaded into the pockets. Additionally, a 1 kb DNA ladder mix was added to determine the fragment size afterwards. Agarose gel electrophoresis was performed at 90 V for 50 – 70 min, checking the gel run in between. Separated DNA bands became visible when exposed to UV light. Pictures of the agarose gel were taken and appropriate bands were cut out (4.6.4).

4.6.4 DNA extraction of agarose gels

DNA fragments were separated by agarose gel electrophoresis (4.6.3) and cut out under the UV light. To purify DNA fragments out of agarose gel slices, the NucleoSpin gel and PCR clean-up Kit was used according to manufacturer's protocol. After melting the gel in the appropriate buffer via incubation at 50 °C for 10 min, the solution was placed onto a column provided by the manufacturer. The DNA fragments were bound to the silica membrane by centrifugation (30 s, 11,000 g, RT) and washed several times. In the end, purified DNA was eluted with 30 µl RNAse-free water and concentration was measured at the Nanodrop (4.6.14). DNA samples were stored at -20 °C.

4.6.5 Digestion of DNA with specific restriction enzymes

DNA digestion with restriction endonucleases was conducted for both analytical and preparative purposes. Plasmid DNA was digested with specific restriction enzymes applying the following approach (**Table 15**) and a total volume of 30 µl per approach.

Table 15: composition for restriction digestion of DNA

Component	Volume/amount
Plasmid DNA	~ 2 µg
Restriction enzyme I	1 µl
Restriction enzyme II	1 µl
Restriction enzyme buffer (10x)	3 µl
ddH_2O	up to 30 µl

Samples were incubated for 60 min at 37 °C to perform the restriction digestion. Afterwards, the process efficiency was visualized via agarose gel electrophoresis (4.6.3). Non-digested and single-digested plasmid DNA were used as controls. Eventually, DNA bands were cut out and purified using the NucleoSpin gel and PCR clean-up Kit (4.6.4).

4.6.6 Annealing of oligonucleotides

Synthesized complementary oligonucleotides were annealed to double-stranded DNA using the following approach (**Table 16**).

Table 16: Composition for annealing of oligonucleotides

Compound	Volume [µl]
Annealing buffer	18
Sense oligonucleotide (100 pmol/µl)	1
Anti-sense oligonucleotide (100 pmol/µl)	1

Samples were mixed and the annealing reaction was performed in a thermocycler using the following settings (**Table 17**):

Table 17: Cycler parameters for oligonucleotide annealing

Temperature	Time
90 °C	5 min
70 °C	10 min
70 °C	ramp down -0.5 °C/20 s (from 70 °C to 37 °C)
37 °C	
16 °C	20 min
4 °C	30 min

Annealed oligonucleotides were stored at -20 °C or directly used for ligation into a plasmid backbone (4.6.7). To control successful annealing to double-stranded DNA, a 3 % agarose gel was poured (4.6.3) and samples were prepared as follows (**Table 18**):

Table 18: Composition for controlling the annealing process

Compound	**Volume [µl]**	
	Control (single-strand oligonucleotide)	**Sample (annealed oligonucleotide)**
oligonucleotide	0.5	2
DNA-loading dye (6x)	2	2
ddH_2O	9.5	8

Agarose gel electrophoresis was analyzed under UV light. Annealed double-stranded oligonucleotides possess higher molecular weight compared to single-stranded oligonucleotides and thus, the visible bands showed different heights.

4.6.7 Ligation of oligonucleotides into vectors

Either annealed oligonucleotides (4.6.6) or digested and purified DNA fragments (4.6.5) were ligated into vectors. The plasmid backbone was digested with the same restriction enzymes used for the insert and purified after separation on an agarose gel (4.6.5). For the ligation, a 1:3 ratio of vector to insert was used and the appropriate insert amount for 100 ng vector was calculated with the help of a ligation calculator (http://www.promega.com/a/apps/biomath/index.html?calc=ratio):

$$\text{amount of insert (g)} = \text{molar ratio } \left(\frac{\text{insert}}{\text{vector}}\right) * \text{amount of vector (g)} * \text{lenths ratio } \left(\frac{\text{insert}}{\text{vector}}\right)$$

The ligation approach was pipetted according to the following scheme (**Table 19**):

Table 19: Composition for ligating oligonucleotides into vectors

Compound	Volume/amount
Plasmid DNA	100 ng
Insert DNA	calculated
T4 DNA ligase	1 µl
T4 DNA ligase buffer (10x)	1 µl
ddH_2O	up to 10 µl

Additionally, a ligation mix without insert was prepared to check for plasmid re-ligation and to control for false positive bacteria growth after transformation. Samples were mixed and incubated either at 22 °C for 2 h or at 16 °C overnight. Ligated samples were stored at -20 °C or directly used for transformation into competent *E. coli* DH5α bacteria (4.5.3).

4.6.8 Colony PCR

Colony PCR was done to analyze whether transformed *E.coli* DH5α bacteria (4.5.3) with plasmid DNA contained the insert of interest. Single colonies growing on LB_{amp} agar plates were selected with an inoculation loop and 2 ml LB_{amp} medium placed in a 24-well plate were inoculated. Bacteria suspension was incubated at RT during the day and 2 µl were taken for the colony PCR. To conduct the colony PCR, the components listed in **Table 20** were used and a master mix was prepared mixing all reagents except the bacteria suspension. The 24-well plates were stored short-term at 4 °C.

Table 20: PCR composition for colony PCR

Compound	Volume [µl]
5x reaction buffer (green)	4
dNTPs (10 mM)	0.4
forward primer (100 pmol/µl)	0.8
reverse primer (100 pmol/µl)	0.8

Compound	Volume [µl]
GoTaq G2 DNA polymerase	0.125
ddH_2O	11.875
Bacteria suspension	2

The colony PCR was run with the following parameters:

Table 21: Cycler parameters for colony PCR

PCR step	Temperature	Time	Cycles
Initial denaturation	95 °C	2 min	1
Denaturation	95 °C	30 s	35
Annealing	52 °C	2 min	
Elongation	72 °C	1 min	
Final elongation	72 °C	5 min	1
Final hold	8 °C	∞	1

To analyze whether plasmid DNA contained the correct insert, PCR products were checked on a 1 % agarose gel (4.6.3).

4.6.9 Plasmid DNA extraction by minipreparation

Minipreparation was performed to isolate plasmid DNA from 5 ml overnight cultures of *E.coli* DH5α bacteria (4.5.4). Cells were centrifuged (5 min, 2640 g, 4 °C) and plasmid DNA was purified with the NucleoSpin Plasmid EasyPure Kit according to the manufacturer's instructions. The system was based on cell lysis followed by lysate clearing with a silica-membrane-based column. After few washing steps, the plasmid DNA was eluted in 50 µl 70 °C pre-heated nuclease-free water and the concentration was measured using a Nanodrop (4.6.14). The DNA was stored short-term at 4 °C and long-term at -20 °C.

4.6.10 Plasmid DNA extraction by midipreparation

Plasmid DNA was isolated by midipreparation to achieve high purity and high amounts of the vector. Therefore, 100 ml LB_{amp} medium were inoculated with 1 ml bacteria culture (4.5.4) and incubated overnight at 37 °C on a shaker. Cell suspension was centrifuged (10 min, 3810 g, 4 °C) and plasmid DNA was purified using the NucleoBond Xtra Midi Plus Kit according to manufacturer's instructions. In the end, the plasmid DNA was dissolved in 100 µl 70 °C pre-heated nuclease-free water and the concentration was determined (4.6.14). For short-term storage, DNA was placed at 4 °C and for long-term storage at -20 °C.

4.6.11 RNA extraction

RNA isolation from cell lines and PDX cells was performed using the Qiagen RNeasy kit. Cells were counted (4.3.3) and up to 10^6 cells were taken for one approach. Cells were washed once in 10 ml PBS (5 min, 400 g, RT) and processed according to manufacturer's instructions. In brief, cells were lysed with a provided buffer and the lysate was filtered through QIAshredder spin columns to remove cellular particles. The sample was homogenized in ethanol and transferred onto silica gel membranes using provided RNeasy columns. Additionally, a DNAse digestion step was included using Qiagen RNAse-free DNAse set after manufacturer's instructions to purify the RNA and remove genomic DNA. Next, RNA was washed several times and eluted with 30 µl RNAse-free water. RNA concentration was measured at the Nanodrop (4.6.14) and samples were stored at -20 °C.

4.6.12 Complementary DNA synthesis

Isolated RNA from PDX cells and cell lines (4.6.11) was applied as a template to perform reverse transcription and to generate complementary DNA (cDNA). The QuantiTect Reverse Transcription kit was used according to manufacturer's protocol. In the first step, a genomic DNA elimination step was done according to **Table 22** using a total volume of 14 µl.

Table 22: Composition of the genomic DNA elimination reaction

Compound	Volume/amount
gDNA wipeout buffer 7x	2 µl
Template RNA	max. 1 µg
RNAse-free water	up to 14 µl

Samples were incubated for 2 min at 42 °C and placed on ice. The approach for reverse transcription was prepared with the compositions listed in **Table 23** in a total volume of 20 µl per sample.

Table 23: Composition of the reverse transcription approach

Component	Volume [µl]
Quantiscript Reverse Transcriptase	1
Quantiscript RT buffer 5x	4
RT primer mix	1
RNA mix from **Table 22**	14

Samples were incubated for 15 min at 42 °C and subsequently for 3 min at 95 °C to inactivate the reverse transcriptase enzyme. 80 µl RNAse-free water were added per sample and cDNA stored at -20 °C.

4.6.13 Quantitative real-time PCR

The expression level of mRNA in PDX cells and cell lines was analyzed by quantitative real-time PCR (qRT-PCR) with the Roche LightCycler 480 Probe system according to manufacturer's instructions. Each approach was prepared as listed in **Table 24**.

Table 24: Composition of qRT-PCR

Component	Volume [µl]
Mastermix	10
Primer for+rev (0.4 µM each)	1
Probe	0.2
cDNA	5
ddH_2O	3.8

Each experiment contained three negative controls, a cDNA-free composition, an approach with mRNA instead of cDNA and a single primer mix. HPRT1 gene was chosen as a housekeeping gene to normalize the expression of the gene of interest (GOI). All samples were pipetted in duplicates to calculate average values. To monitor the quantitative real-time PCR (qRT-PCR), a LightCycler 480 II was taken and the reaction measured with the following settings listed in **Table 25**:

Table 25: Cycler parameters for qRT-PCR with the Roche probe system

PCR step	Temperature	Time	Cycles	Ramp rate [C°/s]
Preincubation	95 °C	10 min	1	
Amplification	95 °C	10 s	45x	4.4
	60 °C	30 s		2.2
	72 °C	1 s		4.4
Cooling	40 °C	30 s	1	2.2

Gene expression level of the GOI was detected with the ΔΔCp analysis normalizing to the house keeping gene HPRT1 (reference).

$$\text{gene expression} = \frac{2^{-\Delta\text{Cp knock-down (GOI}-\text{reference)}}}{2^{-\Delta\text{Cp control (GOI}-\text{reference)}}}$$

GOI: gene of interest

Cp: crossing point

4.6.14 Determination of DNA and RNA concentration and quality

The spectrophotometer Nanodrop1000 was applied to quantify DNA and RNA concentrations and to determine the sample purity in this study. 1.5 µl sample were loaded onto the detector and measured at 260 nm (A_{260}), which is the absorbance maximum of nucleic acids. Additionally, the ratio of absorbance at 260 nm and 280 nm was detected to assess the purity of the nucleic acid. Pure DNA showed a ratio of ~ 1.8, whereas pure RNA had an A_{260}/A_{280} value of ~ 2.0.

4.6.15 DNA Sequencing

Sanger sequencing was performed to confirm DNA sequences of cloned plasmids. DNA plasmids were purified as described (4.6.9 and 4.6.10) and concentration was determined with a spectrophotometer (4.6.14). A total volume of 15 µl with a concentration of 50 ng/µl was pipetted for each DNA sample and 10 µl of the appropriate primer were prepared with a final concentration of 10 pmol/µl. Alternatively, common primers offered by the company were used. Samples were sent for sequencing and the results were checked the next day.

4.7 Statistics

To determine the significance of differences between control and knock-down cells or to compare frozen and fresh cell viability, a two-tailed unpaired t-test was conducted. If variances differed significantly, Welch's correction was applied. All analysis was calculated with the Graph Pad Prism 6 software.

5. Results

In acute leukemia patients, chromosomal translocations are associated with dismal prognosis. Here, we aimed at evaluating the role of the fusion protein MLL/AF4 for survival of patient derived xenografts growing *in vivo*. In this regard, we engrafted patient samples carrying chromosomal rearrangements in severely immunodeficient mice and established a novel knock-down system targeting the fusion breakpoint.

5.1 Establishing patient derived ALL xenografts with chromosomal translocations

To analyze the importance of fusion proteins for tumor cell survival, we first collected samples with chromosomal rearrangements from acute leukemia patients. As primary cells do not proliferate *in vitro* and die after few days in culture, our lab established the individualized xenograft mouse model (4.2) (Castro Alves et al., 2012; Terziyska et al., 2012; Vick et al., 2015). NOD/scid gamma (NSG) mice lacking B-cells, T-cells and natural killer cells allow reliable engraftment and amplification of human leukemia cells. Re-isolated cells are subsequently called patient derived xenograft (PDX) cells and enable to work with acute leukemia cells of different genetic backgrounds (Barth et al., 2014; Jacoby et al., 2014; Shultz et al., 2005; Woiterski et al., 2013).

5.1.1 Engraftment of primary patient cells with chromosomal translocations

In contrast to pediatric acute lymphoblastic leukemia (ALL), cell engraftment of adult ALL cells remains challenging (Jones et al., 2017; Townsend et al., 2016). Therefore, we first aimed to engraft primary adult ALL cells with chromosomal rearrangements in NSG mice. In this project, I aimed at working with two different types of translocations, BCR/ABL (breakpoint cluster region/Abelson murine leukemia viral oncogene homolog) and MLL/AF4 (mixed lineage leukemia/ALL1 fused gene from chromosome 4).

Primary samples from 15 adult ALL patients carrying either t(9;22) BCR/ABL (n = 10) or t(4;11) MLL/AF4 (n = 5) were obtained from collaborating clinicians from adult hemato-oncology in either Munich or Rostock and transplanted into NSG mice. Clinical data and sample characteristics of the patients are listed in **Table 26**.

Table 26: Clinical data of adult ALL patients and sample characteristics.

UPN	Subtype	Age (years)	Gender	Disease stage	Sample type	Major cytogenetic group
ALL-352	adult	67	m	diagnosis	PB	t(4;11)
ALL-389	adult	43	f	diagnosis	BM	t(4;11)
ALL-816	adult	52	f	diagnosis	PB	t(4;11)
ALL-817	adult	74	f	diagnosis	PB	t(4;11)
ALL-818	adult	47	m	diagnosis	PB	t(4;11)
ALL-209	adult	61	f	relapse	BM	t(9;22)
ALL-210	adult	35	f	diagnosis	BM	t(9;22)
ALL-223	adult	48	f	diagnosis	PB	t(9;22)
ALL-224	adult	70	f	diagnosis	PB	t(9;22)
ALL-256	adult	41	f	diagnosis	PB	t(9;22)
ALL-262	adult	42	m	diagnosis	BM	t(9;22)
ALL-360	adult	33	f	diagnosis	BM	t(9;22)
ALL-363	adult	66	m	diagnosis	PB	t(9;22)
ALL-589	adult	44	m	diagnosis	BM	t(9;22)
ALL-590	adult	84	m	diagnosis	PB	t(9;22)

The presence of chromosomal rearrangements was confirmed by both FISH and PCR analysis in most samples. ALL, acute lymphoblastic leukemia; BM, bone marrow; PB, peripheral blood; UPN, unique patient number; f, female; m, male.

If possible, samples were transplanted directly at the day of bone marrow aspiration without prior freezing/thawing process. Otherwise, primary cells were frozen and thawed applying optimized protocols (4.3.1 and 4.3.2). No preconditioning such as chemotherapy or irradiation was applied to the mice prior to cell transplantation.

13 out of 15 adult ALL samples successfully engrafted in NSG mice and 9 samples led to a lethal leukemia burden in mice within 100 days manifested in at least 70 % human blasts in the bone marrow (**Figure 11**). In total, 8 out of 10 t(9;22) and 5 out of 5 t(4;11)

primary samples engrafted, arguing for a high and reliable engraftment of adult rearranged ALL cells without requirement of animal preconditioning. This stands in marked contrast to literature describing high engraftment rates only after animal pretreatment by total body irradiation (Notta et al., 2011; Patel et al., 2014).

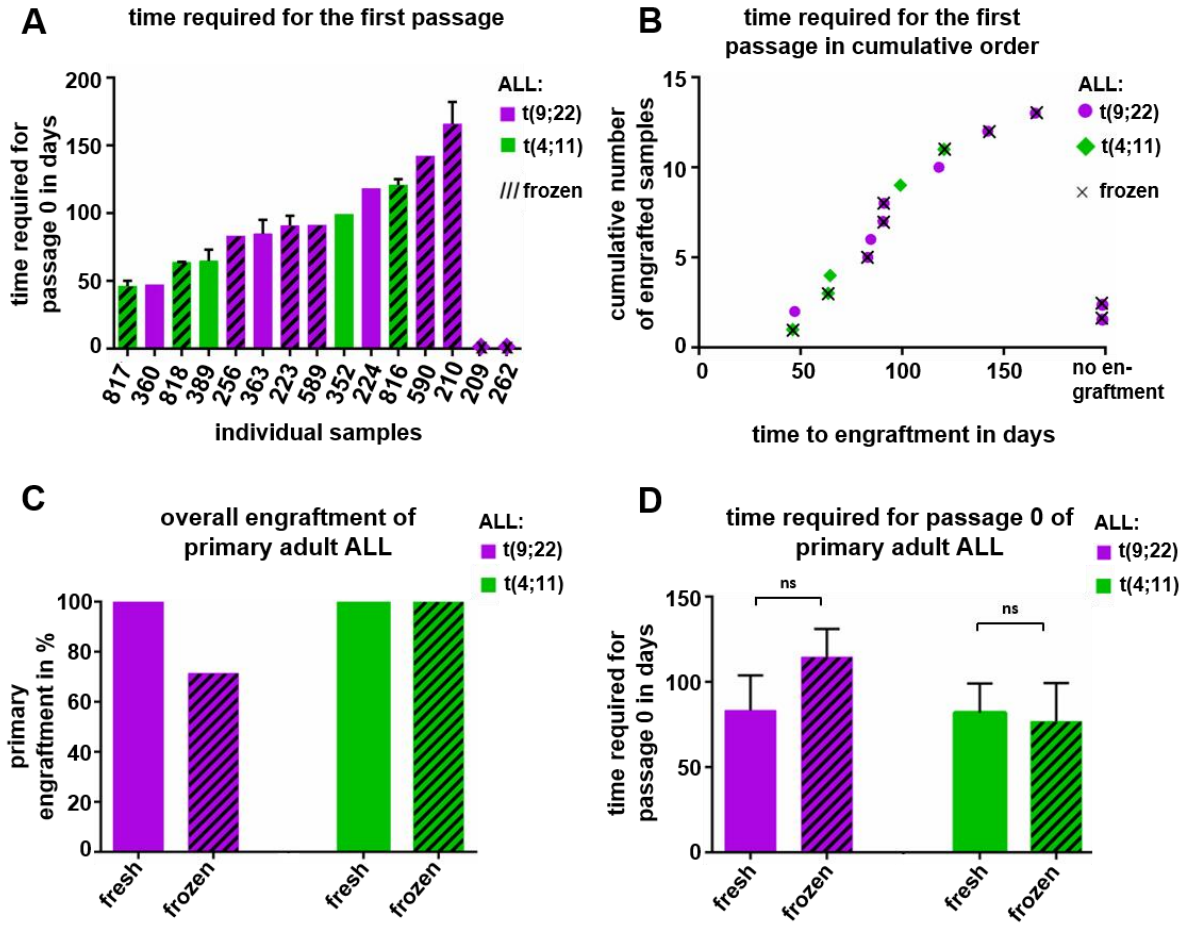

Figure 11: Primary adult rearranged ALL samples reliably engraft in NSG mice
A, **B**: Time required for the first passage of primary adult rearranged PDX ALL samples is shown individually (**A**: numbers indicate unique patient numbers (UPN); **B**: in cumulative form). **C**: Mean overall engraftment of primary adult rearranged ALL samples **D**: Mean time required for passage 0 of primary adult rearranged ALL samples. Samples after a freezing/thawing cycle are indicated with stripes or crosses. Reprinted with permission (Heckl et al., 2018).

More in detail, 5 out of 5 (100 %) directly transplanted samples and 8 out of 10 (80 %) frozen/thawed samples engrafted (**Figure 11C** and **Supplementary Table 28**). This indicates a reduced engraftment ability after freezing/thawing procedures, which is probably ascribable to a decreased cell viability. Moreover, frozen/thawed primary samples required longer time periods to induce deadly leukemia after primary sample injection (102.2 days) compared to directly transplanted cells (82.6 days).

Next, passaging time of BCR/ABL-rearranged samples defined as the time from cell injection until deadly leukemia was tracked over five passages. A decrease was visible over passaging in all samples. A strong reduction was observed for two samples, ALL-210 and ALL-590, which showed very long passaging times in the beginning and adjusted to average time levels after the initial two passages. All samples manifested constant passaging times after the first 2 - 3 passages (**Figure 12**).

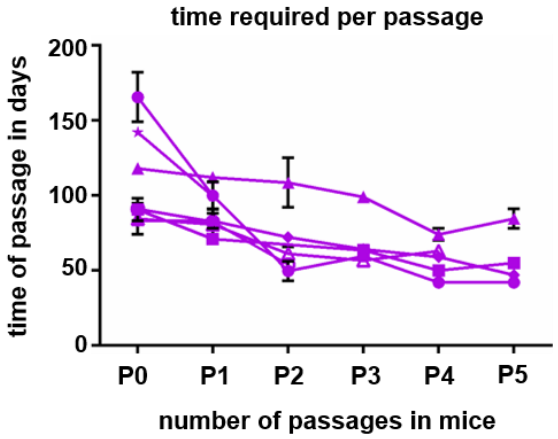

Figure 12: Passaging time of individual samples with BCR-ABL rearrangement over several passages
● ALL210; ■ ALL223; ▲ ALL224; ◆ ALL256; △ ALL363; ○ ALL589; ★ ALL590. Sample 360 is not shown, as mice of P0 and P1 were taken down due to sickness before receiving a positive blood measurement. Reprinted with permission (Heckl et al., 2018).

In summary, primary adult rearranged ALL samples were engrafted with high efficiency and reliability showing engraftment rates similar to pediatric ALL samples described in literature. Woiterski and colleagues achieved 90 % positive engraftment of primary pediatric acute leukemia samples in mice within 7 – 10 weeks after injection (Woiterski et al., 2013).

5.1.2 Genetic engineering of PDX cells by lentiviruses

Genetic engineering of PDX cells provides a powerful tool to study the molecular biology of the disease in detail. Genetically engineered PDX (GEPDX) cells were successfully established in our lab and enable transgene expression, for example of fluorochromes or luciferases, in PDX cells (4.4) (Ebinger et al., 2016; Terziyska et al., 2012; Vick et al., 2015) (**Figure 13**).

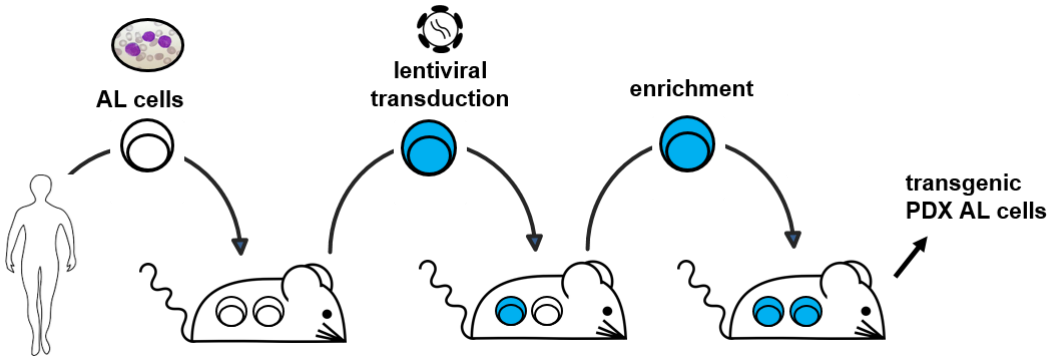

Figure 13: Generation of genetically engineered patient derived xenograft cells
Primary cells from acute leukemia patients were engrafted in immunodeficient NSG mice. After re-isolation from bone marrow and spleen, cells were genetically engineered using lentiviruses and enriched by FACS. Reprinted with permission (Heckl et al., 2018).

Recombinant expression of luciferase enables bioluminescent *in vivo* imaging, which allows monitoring of disease progression in living animals using PDX cells with recombinant luciferase expression. Furthermore, labelling leukemia cells with fluorescent markers is highly useful for subsequent cell enrichment by sorting and data analysis. Therefore, lentiviral constructs were used containing a fluorochrome, for example eGFP or mtagBFP, which were directly visible by flow cytometry (**Figure 14**). All inserts of lentiviral constructs used in this study and their origin are listed in **Supplementary Table 29**.

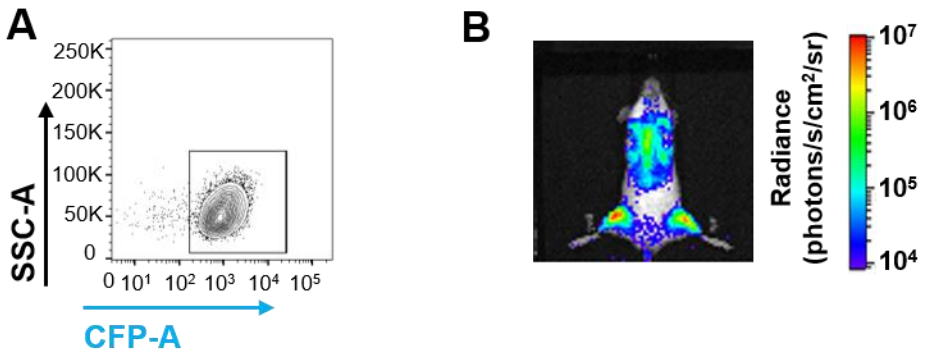

Figure 14: Transgenic PDX cells
A: Lentiviral constructs contained a fluorochrome, for example mtagBFP. After lentiviral transduction, cells were enriched using fluorescence-activated cell sorting (FACS). Successful enrichment was confirmed by flow cytometry. **B**: Genetically engineered PDX cells expressing a luciferase were monitored by bioluminescence *in vivo* imaging.

Genetic engineering was performed by a third generation lentivirus vector system (4.4.2). The viral genome directly integrates into the genome of the recipient cells leading to a stable transgene expression. PDX cells were transduced with lentiviruses, kept 24 h in culture and directly injected into NSG mice (**Figure 15A**). PDX samples

with high cell viability *ex vivo* were kept 5 days *in vitro* in culture after lentiviral transduction. Fluorochrome expression upon genetic engineering enabled subsequent fluorescence-activated cell sorting (FACS) prior to reinjection into mice (**Figure 15B**). When possible, freshly transduced cells were kept in culture for another five days in order to allow expression of the recombinant marker and direct cell enrichment by flow cytometry before cell amplification in mice.

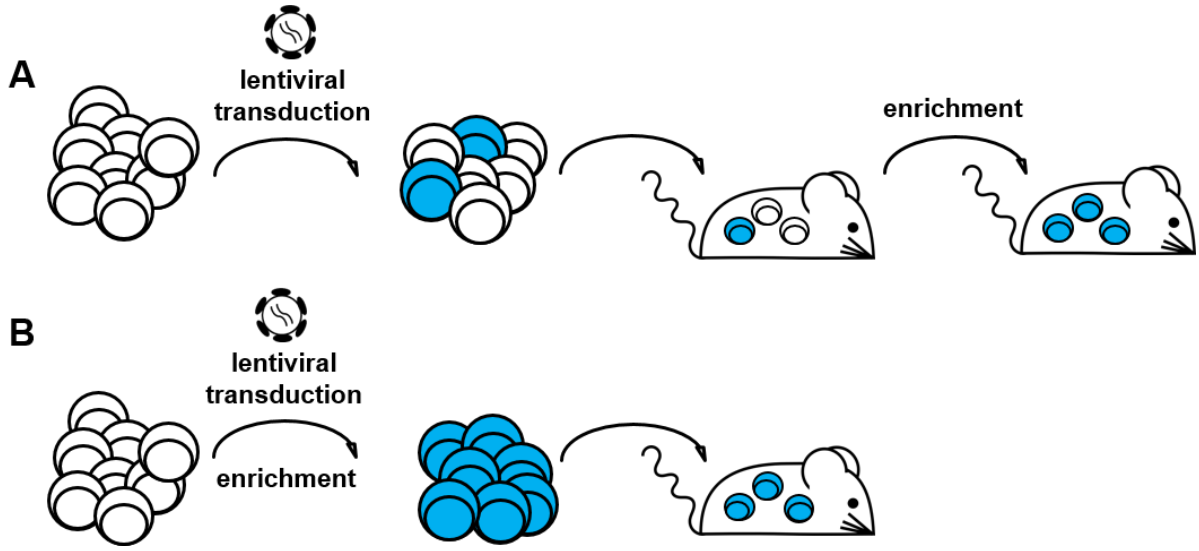

Figure 15: Genetic engineering of patient derived xenograft cells
A: PDX cells were transduced with lentiviruses, kept 24 h in culture and injected into NSG mice. After one mouse passage, GEPDX cells were enriched by FACS and reinjected. **B**: PDX cells were lentivirally transduced and kept 5 days *in vitro* in culture. GEPDX were sorted by FACS and injected into NSG mice.

In addition to adult ALL PDX samples, which were engrafted in our lab, pediatric MLL-rearranged ALL and adult MLL-rearranged acute myeloid leukemia (AML) PDX samples were used in this study. Non-rearranged samples were taken as a control. Details on clinical data and sample characteristics are listed in **Supplementary Table 30**.

High cell viability of PDX samples was desired *in vitro* to enable enrichment by cell sorting prior to reinjection of the cells into donor mice. In general, PDX cells do not proliferate *in vitro* and a co-culture system using irradiated MS-5 feeder cells was applied to increase cell survival and viability in culture (4.3.5). A minimum of five days *in vitro* cultivation was necessary to detect transgene expression after lentiviral transduction. Despite co-culture, several MLL-rearranged PDX ALL samples showed very low cell viability *in vitro* after five days, a consequence of the freezing/thawing procedure and subsequent lentiviral transduction (**Figure 16**). However, this was not

the case for MLL-rearranged PDX AML samples or non-rearranged PDX ALL samples. Three MLL-rearranged pediatric PDX samples, ALL-704 (MLL/AF9), ALL-706 (MLL/AF4) and ALL-707 (MLL/AF4), showed less than 10 % living cells *in vitro* after 5 days in culture. Therefore, working with freshly isolated cells was highly recommended for these samples.

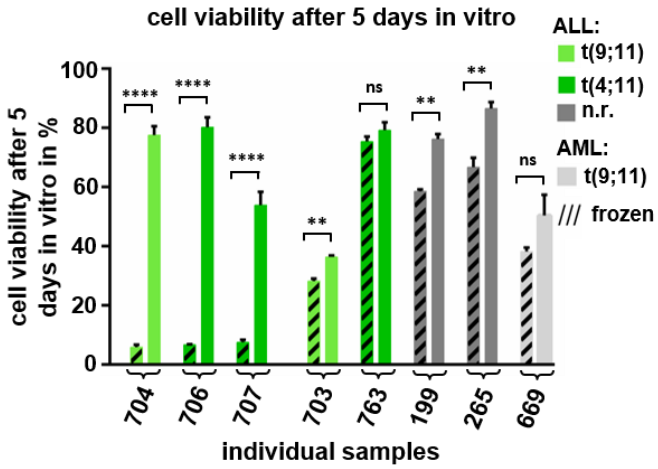

Figure 16: Cell viability of MLL-rearranged PDX cells after 5 days *in vitro* in culture
Samples were either freshly isolated from mice (plain) or underwent freezing/thawing procedure (stripes). Several fresh MLL-rearranged samples showed significantly increased viability compared to thawed cells. Reprinted with permission (Heckl et al., 2018).

In contrast to leukemia cell lines, PDX cells are difficult to transduce. So far, genetic engineering using lentiviruses represents the most promising method to achieve GEPDX cells. Both adult and pediatric rearranged PDX cells showed very little susceptibility towards lentiviral transduction and had transduction efficiencies of around 5 % (**Figure 17**). BCR/ABL and MLL-rearranged adult ALL PDX cells had a 10-fold lower transduction rate compared to MLL-rearranged adult AML PDX cells (5 % versus 50 %) (**Figure 17A**). Similar results were observed for pediatric MLL-rearranged ALL PDX cells with lentiviral transduction rates of less than 5 % in contrast to pediatric non-rearranged ALL and AML PDX cells with a transduction rate between 30 % and almost 90 % (**Figure 17B**).

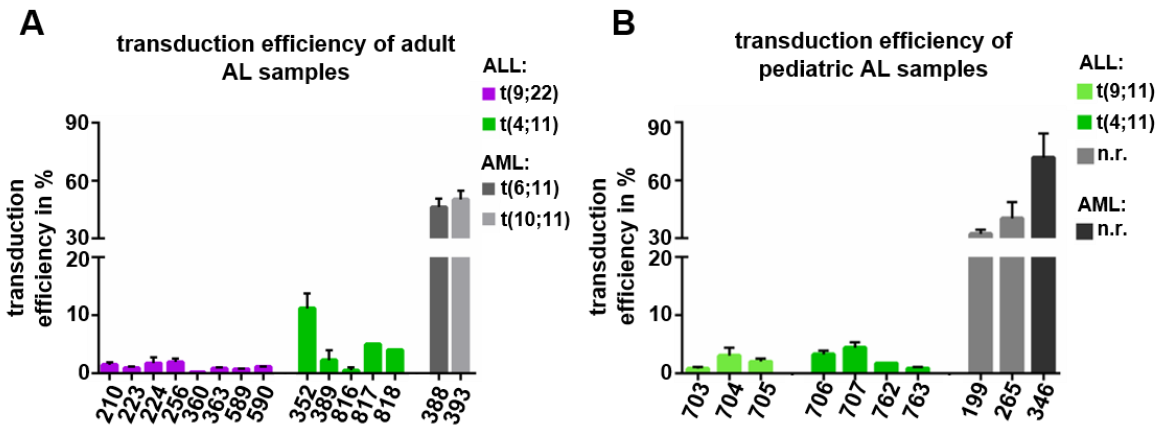

Figure 17: Transduction efficiencies of PDX samples
PDX samples were lentivirally transduced and kept *in vitro* in culture for 5 days. Successful transduction rate was measured by flow cytometry detecting the recombinant fluorochrome. **A**: Transduction efficiency of adult ALL samples with chromosomal rearrangement was very low compared to adult rearranged AML samples. **B**: Transduction efficiency of pediatric MLL-rearranged ALL samples was very low compared to pediatric non-rearranged samples. Reprinted with permission (Heckl et al., 2018).

In our lab, we use an established lentiviral transduction enhancer, polybrene, for lentiviral transduction. Additionally, I performed several experiments in order to optimize the transduction efficiency of difficult PDX samples. To this aim, I tested lentiBOOST, a recently developed lentiviral transduction enhancer especially recommended for cells, which are hard to transduce. I did not detect any improvement of the transduction efficiency after this application (data not shown).
Nevertheless, lentiviral transduction was feasible for all rearranged PDX samples enabling the establishment of GEPDX models for further experiments. Enrichment of transgenic cells by FACS successfully overcame the challenges of low transduction rates.

5.1.3 Establishing a breakpoint specific PCR

As the MLL rearrangement is very frequent in ALL patients and associated with dismal prognosis, we focused on the chromosomal translocation t(4;11) MLL/AF4 and investigated its role in leukemia growth and development. Successfully engrafted and amplified PDX samples were sequenced for precise breakpoint analysis. PDX ALL samples with the identical MLL/AF4 breakpoint sequence on mRNA level were grouped. In total, five PDX samples, ALL-352, ALL-706, ALL-707, ALL-762 and ALL-763 were collected upon sequencing (**Figure 18**). Additionally, the SEM cell line harbors the identical rearrangement and breakpoint and was selected to establish and

validate methods *in vitro*. Subsequent experiments were performed *in vivo* in PDX cells. Detailed characteristics of the primary adult and pediatric ALL samples are listed in **Table 26** and in **Table 30**.

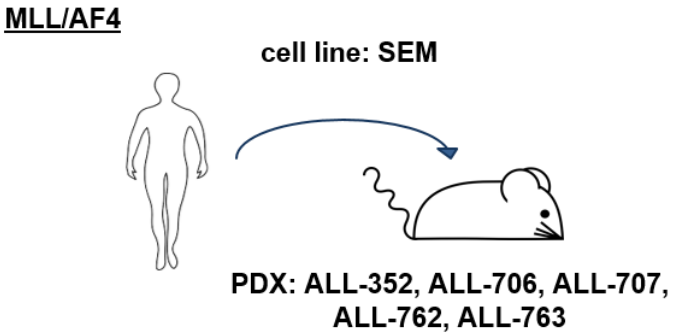

Figure 18: PDX samples and SEM cell line with equal MLL/AF4 fusion breakpoint on mRNA level
The same MLL/AF4 breakpoint sequence on mRNA level was detected for ALL-352, ALL-706, ALL-707, ALL-762, ALL-763 PDX cells and for SEM cell line cells.

The average time of the selected PDX samples to cause deadly leukemia in mice varied between 42 days (ALL-707) and 112 days (ALL-352) (**Table 27**). As short passaging times were favorable to generate transgenic PDX cells, ALL-707 (42 days), ALL-763 (43 days) and ALL-706 (62 days) were chosen for further experiments.

Table 27: Sample characteristics of MLL/AF4-rearranged ALL PDX samples used for the main experiments.

UPN	cytogenetic group	mean passaging time (1 - 2x10^6 cells/mouse)	mean transduction efficiency
ALL-352	MLL/AF4	112 days	11.2 %
ALL-706	MLL/AF4	62 days	3.3 %
ALL-707	MLL/AF4	42 days	4.4 %
ALL-762	MLL/AF4	73 days	1.7 %
ALL-763	MLL/AF4	43 days	0.8 %

For all three samples, re-passaging of PDX cells and preservation by freezing at -80 °C was possible and enabled generation of a large stock of PDX leukemia cells for further experiments. ALL-763 showed a remarkably high viability *ex vivo* even after freezing/thawing procedure containing 75.3 % viable cells after 5 days *in vitro* (**Figure**

16). However, transduction rate was very poor (0.8 %) and transgenic samples had to be enriched by FACS in two consecutive rounds. In contrast, ALL-707 and ALL-706 had very few viable cells after 5 days *in vitro* (6.7 % and 7.5 %, respectively) and therefore, working with freshly isolated cells was preferred. All PDX samples obtained transduction efficiencies under 10 %, assessing single integrations of the lentiviral genome in the recipient ALL cells (Charrier et al., 2011; Christodoulou et al., 2016; Cooper et al., 2011).

By sequencing, I further characterized the MLL/AF4 fusion breakpoint. The breakpoint in the MLL gene, which is localized on chromosome 11, was located in the intron region between exon 9 and 10. In the AF4 gene, which is localized on chromosome 4, the breakpoint occurred in the intron region between exon 3 and exon 4. Upon chromosomal translocation, two genomic fragments were exchanged leading to a fusion of the 5' part of MLL to the 3' end of AF4 on genomic level. After transcription into mRNA, exon 9 of MLL was directly fused to exon 4 of AF4, resulting in an in-frame fusion protein upon translation (**Figure 19A**). Additionally, the reciprocal fusion gene is formed fusing the 5' part of AF4 to the 3' end of MLL. The transcribed mRNA fuses exon 3 of AF4 to exon 10 of MLL (not shown).

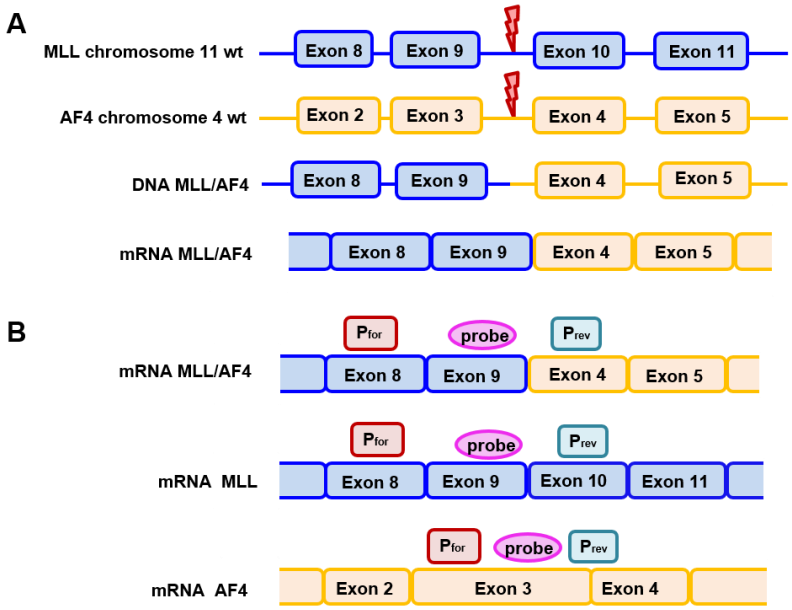

Figure 19: Schematic representation of the chromosomal translocation and localization of the fusion breakpoint in the MLL/AF4-rearranged samples
A: The MLL breakpoint is located between exon 9 and 10 in the MLL gene and the AF4 breakpoint is located between exon 3 and 4 of the AF4 gene. After transcription of the fusion DNA, exon 9 of MLL is directly connected to exon 4 of AF4. **B**: Specific qPCR was designed to monitor MLL/AF4 fused mRNA besides endogenous MLL and AF4 mRNA. P, primer; for, forward; rev, reverse.

In order to investigate the expression levels of both endogenous and translocated genes on mRNA level, quantitative real-time PCR (qRT-PCR) was performed exploiting the Roche Probe system (4.6.13). Specific primers were used to distinguish between MLL/AF4 fusion mRNA and endogenous gene mRNA of MLL and AF4, respectively. Therefore, a primer pair detecting the breakpoint region on mRNA level was selected to validate the amount of MLL/AF4 mRNA. To detect the endogenous mRNA, a specific sequence not present in the rearranged mRNA was taken for primer setting (**Figure 19B**). This setup enabled the quantification of each of the three genes MLL, AF4 and MLL/AF4 separately on mRNA level and allowed to validate the efficiency of the knock-down.

First, primer pairs were successfully tested in SEM cell line cells showing presence of all three genes, MLL, AF4 and MLL/AF4. PDX samples ALL-706 and ALL-707 were additionally tested positive for the MLL/AF4 rearrangement. In contrast and as expected, non-rearranged NALM-6 cell line cells did not show a positive signal for MLL/AF4. The housekeeping gene HPRT1 was used as positive control, while ddH_20 was added instead of cDNA as a negative control (**Figure 20**).

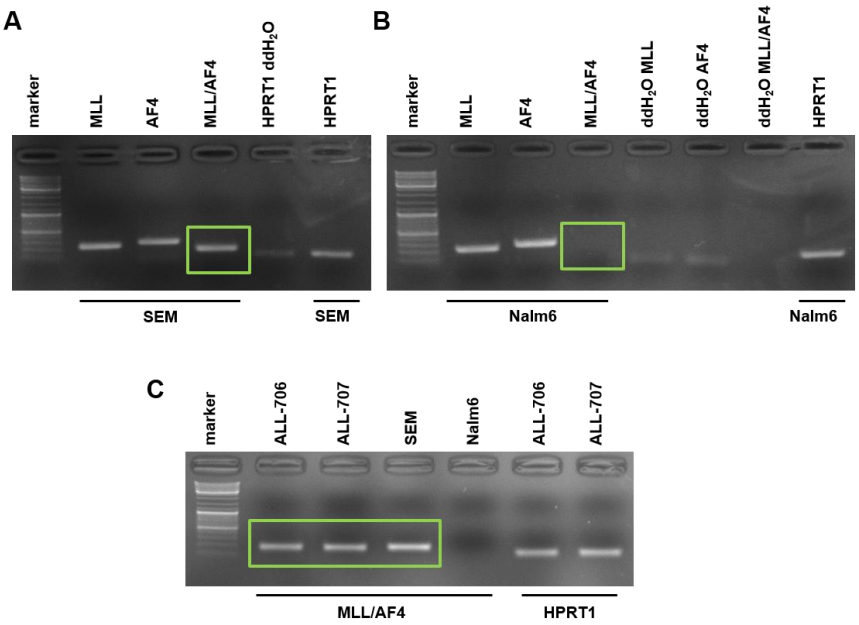

Figure 20: Fusion mRNA was detected in MLL/AF4-rearranged PDX cells and in SEM cells
A: The endogenous genes MLL and AF4 and the fused gene MLL/AF4 were detected in SEM cell line cells containing the MLL/AF4 translocation. **B**: NALM-6 cell line cells without chromosomal translocation only showed bands for the endogenous genes MLL and AF4. HPRT1 gene detection was used as a positive control. ddH_2O was used instead of cDNA in all negative controls. **C**: The fused gene MLL/AF4 was detected in both ALL-706 and ALL-707 besides SEM cell line cells.

Taken together, MLL-AF4 specific qRT-PCR was successfully established, hence allowing the easy detection of endogenous and rearranged MLL in the following experiments.

In summary, I successfully engrafted adult ALL cells with chromosomal rearrangements in immunodeficient mice and applied them for genetic engineering to study the importance of chromosomal translocations especially focusing on MLL/AF4.

5.2 Targeting MLL/AF4 using a competitive knock-down system

The aim of my experiments was to understand whether or not ALLs with fusion of MLL/AF4 would rely on its expression and MLL/AF4 would have an essential function for these ALLs. Therefore, I aimed at knocking down MLL/AF4.

5.2.1 Generation of transgenic cells

As first approach, I applied a competitive knock-down system. This system had already been established in the lab by my supervisor Dr. Michela Carlet. A competitive approach allows to directly compare the knock-down effect of a target gene with control cells and enables an easy readout of the experiment.
Cells were divided into two groups at the beginning and transduced with different constructs to distinguish control and MLL/AF4 knock-down cells by fluorochrome expression. One group of cells was transduced with a construct expressing a monomeric tag blue fluorescent protein (mtagBFP), whereas the other group of cells was labelled with a construct expressing an enhanced green fluorescent protein (eGFP). Fluorochrome expression was important not only to distinguish the two competing cell populations but also to enrich the positively transduced cells by FACS. Both constructs of the first transduction round contained an EF1α promoter and a gene for enhanced firefly (eFFly) luciferase, which is a codon-optimized form of firefly luciferase (**Figure 21A**). Transgenes were connected using the linker T2A or P2A to ensure equimolar expression. In the second transduction step, both populations received a similar construct in order to induce a knock-down. Here, an SFFV (spleen focus-forming virus) promoter was applied to achieve a strong knock-down efficiency. A fluorochrome, *discosoma species* red fluorescent protein (dsRED) was chosen as reporter gene and directly coupled to the miR30 cassette containing an shRNA either

targeting Renilla for the control group or MLL/AF4 for the knock-down of the gene of interest (**Figure 21B**). As an important control, dsRED expression of the control cells and the cells with a knock-down of MLL/AF4 was checked and showed identical intensities for both cell groups (**Figure 21C**).

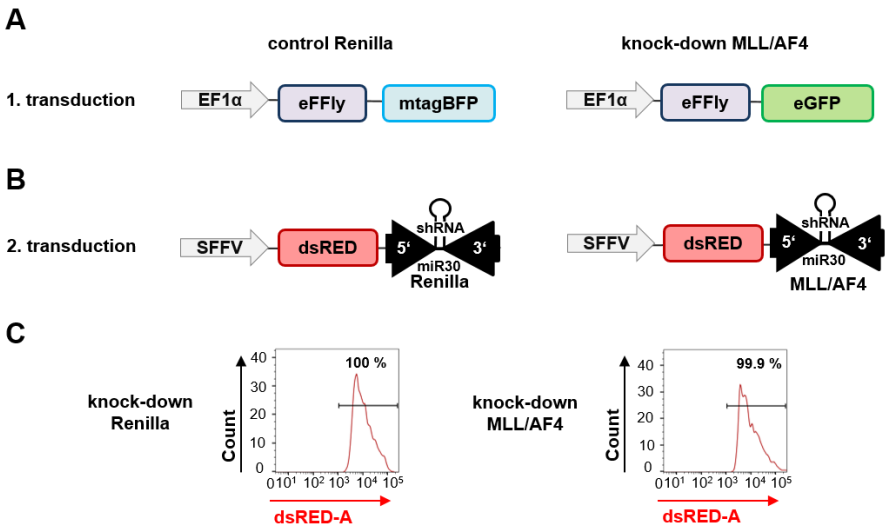

Figure 21: Schematic representation of the constitutive knock-down system
Schematic representation of the lentiviral constructs used in the constitutive knock-down system. Cells were transduced in two consecutive rounds. **A:** In the first round, cells were transduced with a construct containing the luciferase enhanced firefly and a gene for fluorochrome expression, which was mtagBFP for control cells and eGFP for cells with the knock-down of MLL/AF4. **B:** In the second round, cells received a construct containing a gene for dsRED expression coupled to the miR30cassette, which contained an shRNA targeting Renilla for control cells or an shRNA targeting MLL/AF4 for the knock-down cells. **C:** DsRED expression showed identical intensities for cells with control (left) or verum (right) knock-down sequence. SFFV, spleen focus-forming virus promoter; eFFly, enhanced firefly; mtagBFP, monomeric tag blue fluorescent protein; eGFP, enhanced green fluorescent protein; dsRED, discosoma sp. red fluorescent protein; shRNA, short-hairpin RNA.

Transduction was performed in two consecutive rounds. First, cells were transduced with the luciferase construct depicted in **Figure 21A** and enriched by FACS. In a second round, cells were transduced with the dsRED-miR30 construct and enriched by FACS again (**Figure 21B**). Double transgenic cells expressed either mtagBFP and dsRED (control cells) or eGFP and dsRED (knock-down MLL/AF4). As all transgenic cells expressed dsRED, cells were first gated on dsRED$^+$ to monitor the expression of the shRNA in the analysis. As important control, expression of dsRED had to be of identical intensity between cells with control or verum knock-down sequence as described before (**Figure 21C**). Afterwards, cells were gated on mtagBFP versus eGFP to monitor the two different cell populations.

In brief, double transgenic cells of the constitutive competitive knock-down system were generated and were applied for further experiments in the following.

5.2.2 Selecting suitable sequences for breakpoint specific MLL/AF4 knock-down

The first challenge was to find an effective knock-down sequence, as the fusion breakpoint should be addressed specifically without targeting each of the two wildtype proteins. As the fusion breakpoint of MLL/AF4 is a defined sequence in the gene, the selection of different candidates was restricted to this specific locus. This approach severely limited the range of putative knock-down sequences.

Six sequence candidates targeting the fusion breakpoint of MLL/AF4 were designed and cloned into the miR30 background. Therefore, 22 nucleotide sense passenger strands targeting MLL/AF4 and their antisense guide strands were embedded in a fixed flank - loop - flank sequence within the miR30 backbone as described by Fellmann and colleagues (Fellmann et al., 2013; Fellmann et al., 2011).

We proceeded with the selection of potent shRNA sequences targeting MLL/AF4. To this aim, six sequence candidates targeting the fusion breakpoint on mRNA level were designed and implemented into the miR30 background as described above. To select the most efficient shRNA sequence, SEM cells were used, which harbor the MLL/AF4 fusion, and both double transgenic subpopulations were generated. Competitive cell line experiments were performed mixing the two differently labelled cell populations. Cells expressing the different target sequences were seeded and collected for analysis at two different time points, day 3 and day 10. To validate the knock-down efficiency, shRNA expressing SEM cell line cells were sorted at day 3 and day 10 and mRNA expression level of MLL/AF4 was examined by qRT-PCR using the primer pair “816 + 817” (4.6.13). The two most potent sequences (KD 1 and KD 2) were identified (**Figure 22A**). A first reduction of MLL/AF4 mRNA was already visible at day 3 upon knock-down (47.47 % for KD1 and 70.24 % for KD 2). Full knock-down efficiency was monitored at day 10 showing a decrease of MLL/AF4 mRNA to 25.49 % for KD 1 and to 43.79 % for KD 2. Sequence KD 1 was selected as it induced the most efficient knock-down. In addition, NALM-6 cells without MLL/AF4 translocation were used as a control in this assay and showed no MLL/AF4 expression as expected (**Figure 22B**). Reducing the mRNA expression of MLL/AF4 with sequence KD 1 to 25.49 % is not such a strong knock-down as described for other target genes in literature, but no better sequence was possible as the shRNA design was restricted to the fusion breakpoint (Lee et al., 2014; Singh et al., 2008). Detailed sequences of the applied primers are listed in **Table 8**. As a next step, the expression levels of the endogenous

genes MLL and AF4 were checked at day 10 to ensure that they were not affected by the knock-down of MLL/AF4. Therefore, the mRNA expression levels of the wildtype MLL and AF4 were analyzed by qRT-PCR (MLL primer “816 + 818”; AF4 primer “838 + 1178”). None of the two endogenous genes neither MLL nor AF4 did show an off-target effect caused by the knock-down of MLL/AF4. This led to the conclusion that both wildtype proteins MLL and AF4 were not affected by the knock-down and expression level was identical as in control cells. NALM-6 cells without chromosomal translocation were applied as a control and did not show an effect of the MLL/AF4 knock-down on the two endogenous genes MLL and AF4, neither (**Figure 22C**).

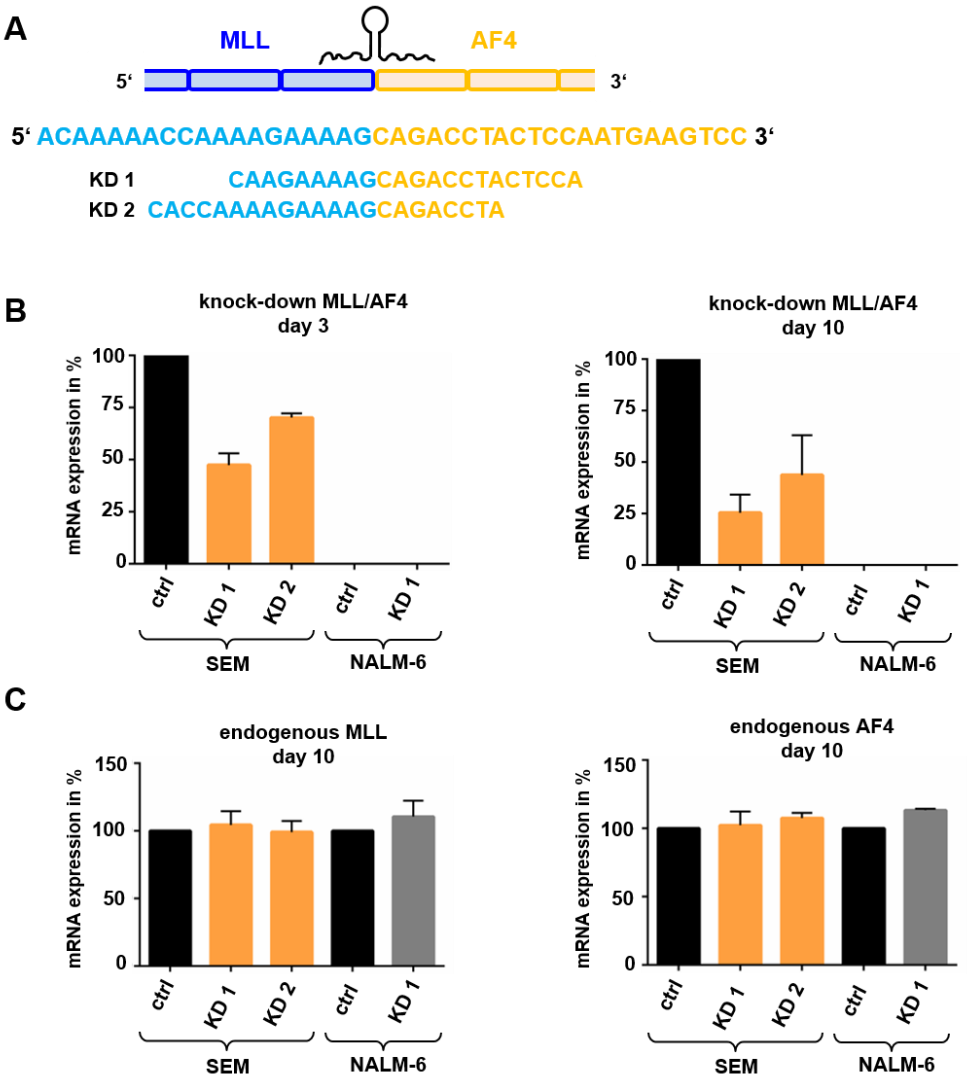

Figure 22: Validation of shRNA candidate sequences targeting MLL/AF4
A: Knock-down sequences targeted the fusion breakpoint of the MLL/AF4 mRNA. Two potent candidates KD 1 and KD 2 were chosen. **B**: MLL/AF4 mRNA expression level was analyzed by qRT-PCR. KD 1 was selected as the most potent shRNA and KD 2 as second most potent shRNA in SEM cell line cells. NALM-6 cell line cells were used as a negative control. **C:** qPCR data did not show an off-target effect on endogenous MLL or AF4 neither in SEM cell line cells nor in NALM-6 cells. KD, knock-down; eGFP, enhanced green fluorescent protein; ctrl, control.

In summary, shRNA candidates were designed and implemented into the miR30 background. Two potent sequences were successfully selected after testing the knock-down efficiency in SEM cell line cells. No off-target effects of the MLL/AF4 knock-down were seen in the expression level of the endogenous genes MLL and AF4. The best MLL/AF4 knock-down sequence will now be applied to analyze the importance of MLL/AF4 in PDX cells *in vivo*.

5.2.3 Generation of GEPDX cells for a constitutive competitive knock-down system *in vivo*

To perform competitive experiments in PDX cells *in vivo*, freshly isolated cells were taken and transduced with the luciferase construct as described before. GEPDX cells were enriched by FACS and amplified by passaging in mice. After lentiviral transduction with the dsRED-miR30 construct, PDX cells were kept 5 days *in vitro* using co-culture to express the transgene dsRED (4.3.5). Both groups, control Renilla and knock-down MLL/AF4, were then directly mixed and sorted in parallel for mtagBFP$^+$/dsRED$^+$ or eGFP$^+$/dsRED$^+$, respectively. Clear differentiation according to fluorochrome expression enabled mixing before sorting, which had the advantage of reducing the sorting time. Moreover, cell populations were processed in exactly the same manner avoiding side-effects on engraftment or growth ability. Equal cell numbers were sorted for both cell populations and re-counted (4.3.3). Transgenic PDX cells were mixed 1:1 and injected into eight mice (**Figure 23**).

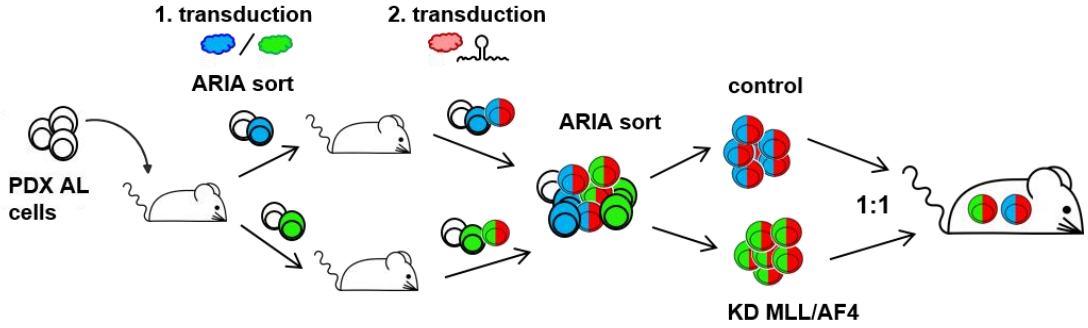

Figure 23: Generation of GEPDX cells for a constitutive knock-down system
Transgenic PDX cells were generated for a constitutive competitive system transducing in two consecutive rounds. First, PDX cells were transduced with a construct containing a gene for mtagBFP (control group) or eGFP (knock-down MLL/AF4) fluorochrome expression. GEPDX cells were enriched by FACS and passaged in mice. After re-isolation, PDX cells were transduced with the second construct, which contained the gene for dsRED expression coupled to the miR30 cassette. The control group received a miR30 cassette expressing an shRNA targeting Renilla, whereas an shRNA targeting MLL/AF4 was applied to the knock-down cells. Cells were sorted after five days *in vitro*, mixed 1:1 and directly injected into mice. AL, acute leukemia; PDX, patient derived xenograft; KD, knockdown.

In total, the constitutive competitive system was established in three different PDX ALL cells, ALL-706, ALL-707 and ALL-763.

Consistently and as described before, transduction rates were very low (0.5 % for ALL-706 and ALL-707), especially for PDX ALL-763 (0.2 %) and low cell numbers were injected after enrichment by flow cytometry (2,000/mouse for ALL-706 and ALL-763, 15,000/mouse for ALL-707). Injected cell numbers were dependent on transduction efficiency and sorting outcome. Due to low injected cell numbers, time until leukemia disease was manifested in the animals followed by mice sacrification was extended (up to 80 days) in comparison to passaging times described before (**Table 27**). Bioluminescence *in vivo* imaging was used to monitor successful engraftment and tumor growth in mice and blood measurement was applied to determine the time point of sacrificing the mice (4.2.5 and 4.2.6) (**Figure 24**).

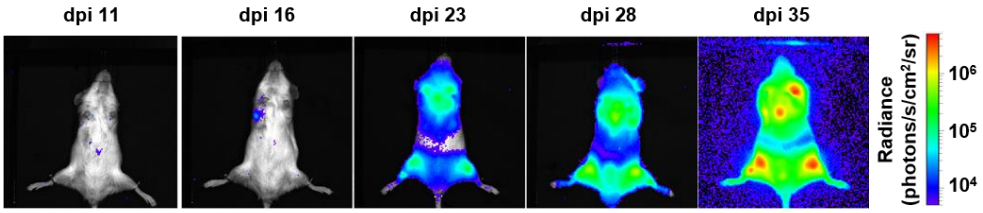

Figure 24: Leukemia growth in mice was monitored using bioluminescence *in vivo* imaging
Competitive PDX samples were injected into NSG mice and tumor growth monitored using bioluminescence *in vivo* imaging. The first mice were taken down as soon as a positive imaging signal was detected (eFFly: 10^6 bioluminescence photons/second). Data shown representatively for PDX ALL-707. dpi, days post injection. Reprinted with permission (Heckl et al., 2018).

The first mice were taken down as soon as a positive *in vivo* imaging signal was detected (eFFly: 10^6 bioluminescence photons/second) and a mouse cell depletion kit (MCDK) was applied to isolate the few human PDX cells out of the murine bone marrow cells (4.4.1). As injected cell numbers were very low, not all injected cells engrafted in mice and thus, mice without positive engraftment were monitored up to 100 days until they were taken down and re-analyzed.

5.2.4 Silencing of MLL/AF4 induced a growth disadvantage in PDX ALL cells *in vivo*

After successfully transplanting transgenic PDX ALL cells for the constitutive competitive system into NSG mice, I was interested in the growth behavior of PDX cells with the knock-down of MLL/AF4. Therefore, the ratio of the mixture of the two

competing GEPDX cell populations was analyzed by flow cytometry before injection into the mice and after re-isolation of the bone marrow or spleen. As described before, cells were first gated on dsRED$^+$ to monitor the expression of the shRNA and second on mtagBFP versus eGFP to monitor the two competing cell populations. The correct mixing was examined by flow cytometry before injection into mice to ensure a 1:1 ratio of the two differently labelled cell populations containing either a knock-down targeting Renilla or the gene of interest MLL/AF4. Here, the injected mixture ratio of 1:1 was visualized (**Figure 25A**). After several weeks in the mouse, cells were isolated from the bone marrow or spleen and analyzed by flow cytometry as described. I detected very few remaining eGFP$^+$ cells at the end of the experiment, whereas the cell amount expressing mtagBFP was very high (0.44 % versus 99.56 %). Gating on PDX cells with a high intensity of dsRED indicating a strong knock-down effect even led to a more drastic distribution of 0 % eGFP$^+$ versus 100 % mtagBFP$^+$, representatively shown for PDX cells of one mouse at day 73 injected with ALL-707 (**Figure 25B**). These data suggest that silencing of MLL/AF4 induced a strong growth disadvantage in PDX cells *in vivo*. The effect caused by the MLL/AF4 knock-down was visible in all three PDX ALL samples independently of the time point of analysis (**Figure 25C**). For ALL-707 and ALL-763, cells engrafted successfully in seven mice, whereas cells only engrafted in four mice for ALL-706.

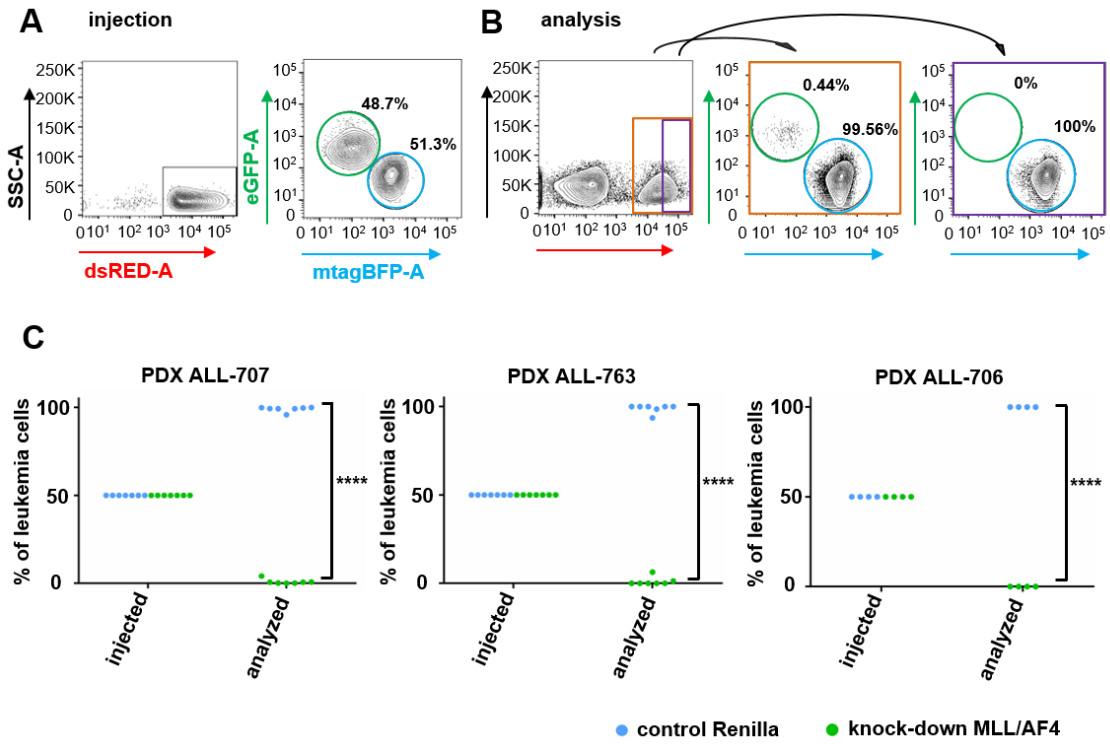

Figure 25: A constitutive knock-down of MLL/AF4 showed a growth disadvantage in PDX cells
A: PDX cells were injected 1:1 mixing control cells containing an shRNA targeting Renilla (mtagBFP$^+$/dsRED$^+$) with cells containing an shRNA targeting MLL/AF4 (eGFP$^+$/dsRED$^+$). Cells were pre-gated on living cells using forward scatter against side scatter (FSC/SSC). Then, cells were gated for dsRED expression followed by mtagBFP versus eGFP expression. Data shown representatively for PDX ALL-707. **B**: Analyzed mice showed a strong decrease of cells with the MLL/AF4 knock-down (eGFP$^+$/dsRED$^+$). Decrease was even stronger gating for high dsRED expression. **C**: The experiment was performed with three different PDX samples ALL-706, ALL-707 and ALL-763. Each dot represents a competitive cell population (mtagBFP or eGFP) in one mouse.

These data show a strong growth disadvantage for leukemia cells upon MLL/AF4 knock-down in PDX cells *in vivo* and strongly emphasize the importance of the fusion protein for the growth of the leukemia cells.

5.3 Targeting MLL/AF4 using an inducible competitive knock-down system

So far, we had shown that a constitutive knock-down of the MLL/AF4 fusion product induced a major growth disadvantage for PDX ALL cells growing in mice. The final aim of our approach is to molecularly mimic clinical anti-leukemia treatment in a model as closely related to the patient as possible. When used to mimic the therapeutic situation in patients, a constitutive knock-down approach suffers the limitation that the knock-down occurs very early at the start of the disease and at very low tumor burden directly after cell transplantation. To overcome this obstacle, we went further and

developed inducible molecular systems that mimic the clinical situation better as they allow unmanipulated tumor growth followed by a therapeutic intervention at advanced disease stages.

An inducible system based on the Cre recombinase offered the advantage to switch on the knock-down at a certain time point. Generally, the Cre enzyme recognizes specific sites in the genome called loxP (locus of crossing [x-ing]-over of bacteriophage P1) and catalyzes site-specific recombination between identical loxP sequences, as previously described (Feil et al., 2009; Oberdoerffer et al., 2003; Zou et al., 1994). In our system, we used the highly sensitive fusion protein CreER^{T2}. Here, the coding region of the Cre recombinase is fused to the ligand-binding domain of the human estrogen receptor (ER) and an optimized version containing a triple mutation in the receptor ligand-binding domain is present (Feil et al., 1997; Indra et al., 1999).

5.3.1 An inducible knock-down system with three fluorochromes

As a basis to establish an inducible competitive knock-down system, I improved an inducible non-competitive system, which had already been established in the lab. Design of the vectors and the cloning strategy had been done by Dr. Michela Carlet in cooperation with Prof. Dr. Marc Schmidt-Supprian.

Principally, the inducible three colour system consisted of two different vectors and lentiviral transduction was performed in two consecutive rounds. To achieve high gene expression and good knock-down efficiency in the cells, a strong viral promoter, SFFV, was applied for both constructs. The first construct contained the gene for CreER^{T2} expression coupled to the reporter gene mCherry for enrichment by flow cytometry. Additionally, a gene for Gaussia luciferase expression (GLuc) was located directly after the SFFV promoter. Transgenes were connected using the linker T2A or P2A to ensure equimolar expression. The second construct constitutively expressed a reporter gene coding for the fluorescent protein mtagBFP to enable cell enrichment of positively transduced cells. Cells additionally received a FLIP cassette containing the shRNA embedded in a miR30 background coupled to the fluorochrome eGFP. This cassette was cloned in the antisense direction between loxP sites. Two differently mutated loxP sites, 2272 loxP and 5171 loxP, were flanking the system and were only able to be recombined with the identical partner sequence by the CreER^{T2} recombinase (Hans et al., 2009; Stern et al., 2008) (**Figure 26A**). Silencing of the target gene was taking

place after induction of the system and specific recombination of the loxP sites. The miR30 background allows shRNA expression under a polymerase II promoter and directly couples it to transgene expression. Moreover, this system is supposed to process shRNA with high efficiency and low toxicity (Cullen, 2005).

The induction of the treatment occurs upon tamoxifen. Addition of tamoxifen to the cells releases the recombinase CreER^{T2} from heat shock proteins (Hsps) into the cytoplasm and enables the enzyme to migrate into the nucleus. Inside the nucleus, the CreER^{T2} recognizes the differently mutated loxP sites and combines the identical partner sequences according to their orientation and localization. Here, we used a two-step recombination system, starting with a reversible inversion followed by an irreversible deletion based on the FLIP system described by Stern and colleagues (Stern et al., 2008). After the flipping, cells expressed the shRNA, which was coupled to the reporter eGFP in the correct reading direction (**Figure 26B**).

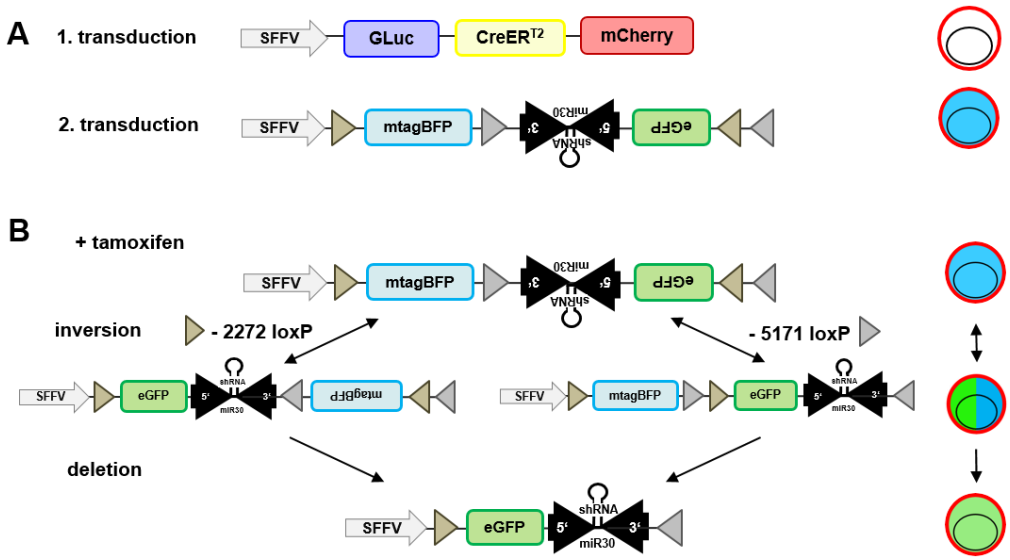

Figure 26: Schematic representation of the lentiviral constructs of the inducible three colour system

A: Cells were transduced in two consecutive rounds. The first construct contained genes for the expression of a Gaussia Luciferase, for expression of CreER^{T2} and for the fluorochrome mCherry. The second construct was a FLIP construct constitutively expressing mtagBFP. The miR30 cassette expression was coupled to eGFP and inserted in an inverted direction. **B**: Two differently mutated loxP sites, 2272 loxP and 5171 loxP, were integrated in the FLIP cassette and only able to recombine with the identical sequence upon CreER^{T2} activation. The flipping occurred in a two-step reaction, a reversible inversion followed by an irreversible deletion. In the end, eGFP was expressed coupled to the shRNA expression. SFFV, spleen focus-forming virus; GLuc, Gaussia luciferase, CreER^{T2}, Cre recombinase estrogen receptor T2; mtagBFP, monomeric blue fluorescent protein; eGFP, enhanced green fluorescent protein; shRNA, short-hairpin RNA.

To analyze the inducible three colour system, a gating strategy was established and applied to all further experiments. In a first step, cell debris and dead cells were

excluded monitoring forward scatter (FSC) against side scatter (SSC). Viable cells were selected and then gated on mCherry positive cells representing all cells with CreER^{T2} expression. In a next step, the FLIP construct was visualized gating for mtagBFP against eGFP expression. Cells, which were positively transduced with the FLIP construct, constitutively expressed mtagBFP. After FACS, almost all cells were located in the lower right gate and positive for mtagBFP, but still negative for eGFP. The leakiness of the system was very low, showing < 1% cells expressing eGFP without induction. Upon tamoxifen activation, cells started to express the miR30 cassette, visualized by eGFP expression. As mtagBFP had a half life time of approximately five days, cells shifted first to the upper right gate and still expressed the blue fluorochrome (Subach et al., 2011). Only after several days, cells got single positive for eGFP expression and were monitored in the upper left gate (**Figure 27**).

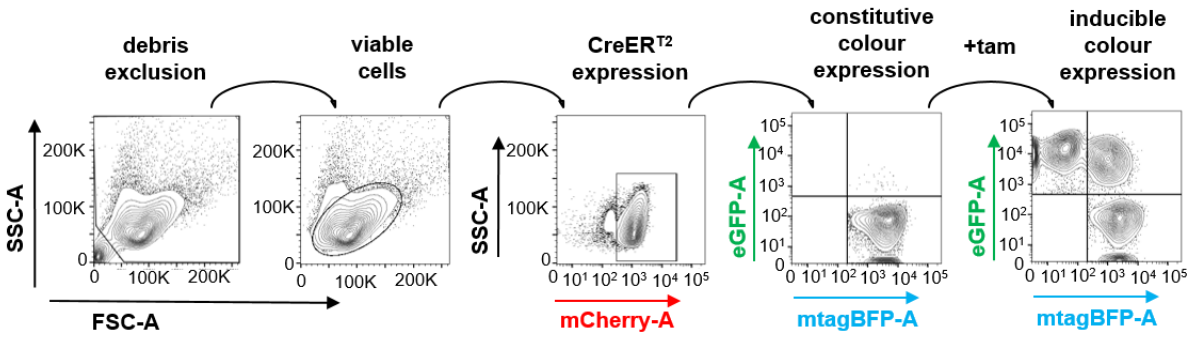

Figure 27: Gating strategy of the inducible three colour system
Cells were first gated by forward scatter (FSC) against side scatter (SSC). After exclusion of debris, living cells were selected and gated on mCherry positive cells to monitor cells with CreER^{T2} expression. Next, the FLIP construct was gated using mtagBFP versus eGFP. Cells constitutively expressed mtagBFP and showed eGFP expression upon tamoxifen treatment.

In the following, only the last gating step will be shown to monitor the cell behavior upon knock-down induction after tamoxifen treatment.

The inducible knock-down system was applied to SEM cell line cells to analyze the importance of MLL/AF4 for cell growth. As an advantage of the inducible system, all double transgenic cells could be generated without fearing a fast effect of an active knock-down. Two experiments were set up in parallel and an shRNA targeting Renilla was chosen as a control system to monitor side-effects of the system. The best sequence candidate, KD 1, from the qRT-PCR data shown in 5.2.2 was applied for the knock-down of MLL/AF4. Different concentrations of tamoxifen were tested in parallel varying from 40 nM to 120 nM (data not shown). A concentration of 60 nM was chosen for cell line experiments showing an efficient and reliable flipping that was visualized

by expression of the inducible colour eGFP after three days (79.08 % for the Renilla knock-down assay and 74.86 % for the MLL/AF4 knock-down assay) (**Figure 28**). The maximum of the flipping was reached three days after tamoxifen treatment. More in detail, the control assay showed a strong flipping of almost 80 % at day 3, which stayed stable over 35 days until the experiment was stopped (**Figure 28A**). This proved that none of the constructs had toxic side-effects and that the eGFP expression itself did not harm the cells. In contrast, the experiment for the proof of gene function of MLL/AF4 showed a strong reduction of the eGFP expressing cells within the 35 days. Induced cells with an active expression of the shRNA targeting MLL/AF4 decreased over time to 17.71 % at day 35 (**Figure 28B**). Moreover and as described before, cells were double positive for mtagBFP and eGFP expression in the first days due to the rather long half life time of mtagBFP (Subach et al., 2011). After approximately 5 days, a part of the cells shifted in the gating and was subsequently located in the upper left gate only expressing eGFP. Similar results were seen applying sequence KD 2 for the knock-down of MLL/AF4 (data not shown).

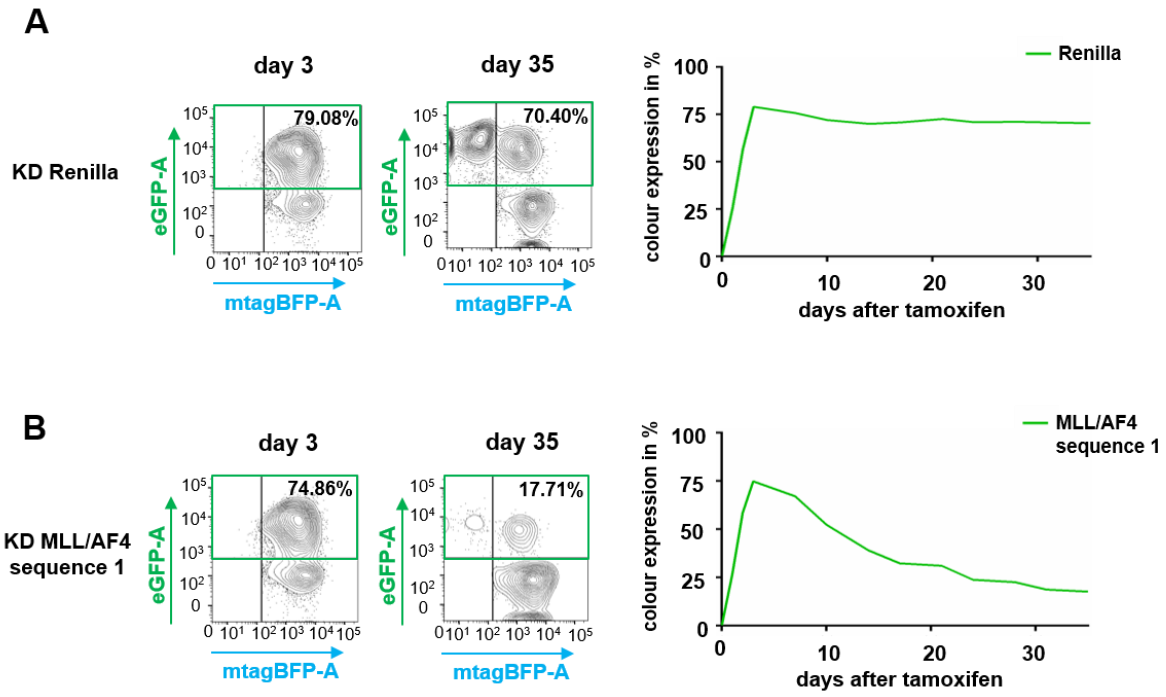

Figure 28: SEM cell line cells with an induced MLL/AF4 knock-down decrease over time
An inducible experiment was performed to compare the growth behavior of cells with MLL/AF4 knock-down in comparison to control cells with a knock-down targeting Renilla. **A:** In the control assay, cells reached a flipping of 79.08 % at day 3 visualized by eGFP expression. Cells with eGFP expression stayed stable over 35 days. **B:** In the MLL/AF4 knock-down assay, 74.86 % of the cells were induced at day 3 and expressed eGFP. Over time, this cell population diminished to 17.71 % at day 35.

Consistent with the *in vivo* data of the constitutive competitive system, the inducible assay confirmed the important role of MLL/AF4 for leukemia cell growth in SEM cell line cells *in vitro*.

Thus, the inducible system enabled us to analyze the importance of a specific gene for tumor cell growth. As the knock-down was activated upon tamoxifen application at a certain time point, the system mimics the clinical situation, where mutated leukemia cells are already present at a certain stage and treatment occurs at defined time points during tumor growth progression. We could show that MLL/AF4 is essential for growth of MLL/AF4 positive ALL cell line cells *in vitro*.

5.3.2 An inducible competitive knock-down system

The final aim was to perform the experiments in PDX ALL cells *in vivo*. Nevertheless and as major limitation, a direct comparison of the control experiment and the MLL/AF4 knock-down assay is challenging. Especially for *in vivo* experiments, separate mice would be required for control Renilla and MLL/AF4 knock-down experiments. PDX cells might engraft differently and several handling steps of the mice could influence the flipping system. One risk factor was given by the tamoxifen treatment, which is dependent on the weight of the mice. Equal GEPDX cell engraftment and constant tamoxifen application are highly postulated to compare the results within one experiment.

The competitive system represented a clear advantage by injecting control cells and cells with the MLL/AF4 knock-down into the same animal in the non-inducible approach. Moreover, it showed an easy and reliable experimental analysis. Therefore, we were now aiming to establish an inducible competitive knock-down system to combine both advantages of the inducible and the competitive system in one approach. Our idea was to inject mice with two different and distinguishable cell populations, each of them containing a different tamoxifen inducible knock-down system. While all cells contained the identical amount of $CreER^{T2}$, one subpopulation would enable inducible expression of a control shRNA monitored by two fluorochromes, whereas the second population would allow inducible expression of the verum shRNA monitored by two different fluorochromes. Both subpopulations would be injected into a single animal enabling to follow up all subpopulations within the same animal.

Towards this aim, a second FLIP construct was required to distinguish control cells and cells with a knock-down of the gene of interest (GOI). Therefore, two additional fluorochromes were required and the two colours, near-infra-red fluorescent protein (iRFP) and T-Sapphire, were chosen. The colour combination was selected and established in collaboration with Dr. Kristoffer Riecken (Mohme et al., 2017). In total, four lasers were needed to measure the five fluorochromes, mCherry, iRFP, mtagBFP, T-Sapphire, and eGFP, in parallel. Detailed filter settings for each laser are listed in **Table 12**. Two of the fluorochromes, mtagBFP and T-Sapphire, were excited by the same violet laser and showed an overlapping emission spectrum (**Figure 29A**). EGFP, which was excited by the blue laser, showed a very strong emission spectrum and was additionally very close to mtagBFP and T-Sapphire (**Figure 29B**). Therefore, a compensation had to be set up to clearly distinguish these three fluorochromes. The other two remaining fluorochromes, mCherry (excited by the yellow/green laser) and iRFP (excited by the red laser) showed clearly separated emission spectra (**Figure 29C + D**).

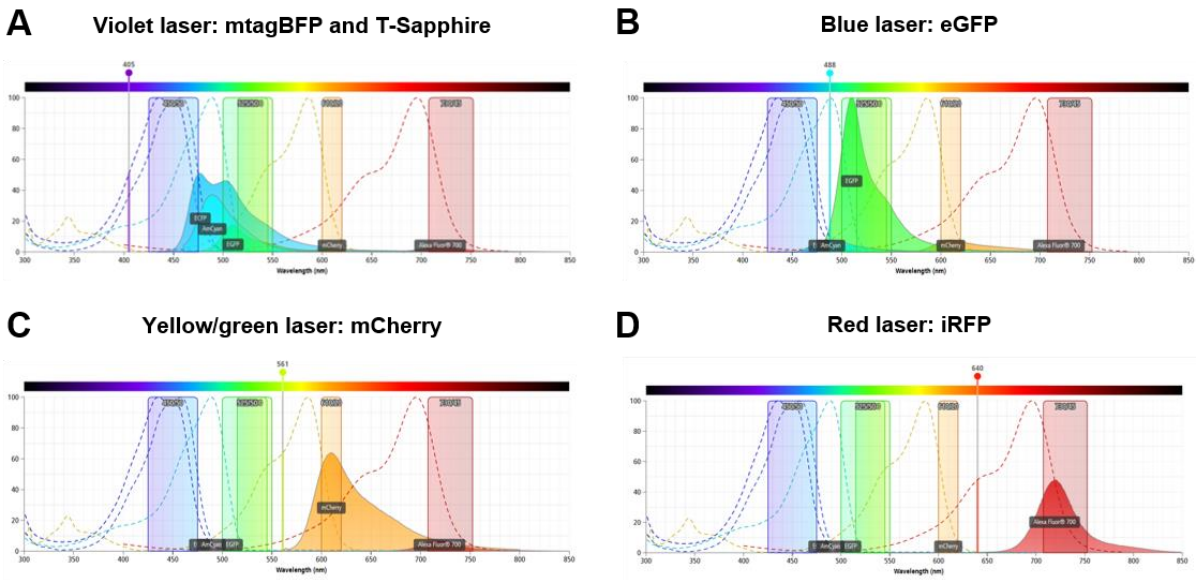

Figure 29: Fluorescence spectrum of the five fluorochromes
A: A violet laser with an excitation wavelength of 405 nm was applied to measure mtagBFP and T-Sapphire. As both fluorochromes emission spectra showed an overlapping, a compensation was required. **B:** A blue laser with an excitation wavelength of 488 nm was applied to measure eGFP. As the emission spectrum of eGFP was overlapping with T-Sapphire and mtagBFP, a compensation was needed. **C:** A yellow/green laser with an excitation wavelength of 561 nm was used to monitor mCherry. **D:** A red laser with an excitation wavelength of 640 nm was applied to monitor iRFP. Adapted from https://www.bdbiosciences.com.

My supervisor Dr. Michela Carlet and I decided to select T-Sapphire as the second inducible colour in parallel to eGFP. Both were derived from the same organism *Aequorea Victoria* and we were aiming to have two very similar fluorochromes to visualize the flipping mechanism. The new construct was cloned exactly in the same way as the first mtagBFP/eGFP FLIP construct of the inducible system, which was described before (**Figure 26**). IRFP was replacing mtagBFP and was applied as a constitutive marker to enrich positively transduced cells and to monitor the cells by flow cytometry. T-Sapphire was introduced in inverse direction coupled to the miR30 cassette (**Figure 30A**). In the following, the new construct was applied for control cells after the shRNA targeting Renilla had been inserted into the miR30 background.

Altogether, three constructs were used to perform inducible competitive experiments, the CreER^{T2}-mCherry construct, the mtagBFP/eGFP FLIP construct and the iRFP/T-Sapphire FLIP construct (**Figure 30B**). Cells were transduced in two consecutive rounds as described before. First, all cells were transduced with the CreER^{T2}-mCherry construct and enriched by FACS. This guaranteed an equal expression level of the Cre recombinase in all cells. In a next step, cells were divided into three groups. Control cells were transduced with the iRFP/T-Sapphire FLIP construct containing an shRNA targeting Renilla in the miR30 cassette. Other CreER^{T2}-mCherry positive cells were transduced with the mtagBFP/eGFP FLIP construct containing an shRNA targeting Renilla. Finally, a third group of cells was transduced with the mtagBFP/eGFP FLIP construct containing an shRNA targeting MLL/AF4. This enabled experiments with two different sets of cell mixtures: In control experiments, both FLIP constructs, mtagBFP/eGFP and iRFP/T-Sapphire, contained an shRNA targeting Renilla. To test the role of MLL/AF4, the iRFP/T-Sapphire construct contained an shRNA targeting Renilla, whereas the mtagBFP/eGFP construct contained an shRNA targeting MLL/AF4.

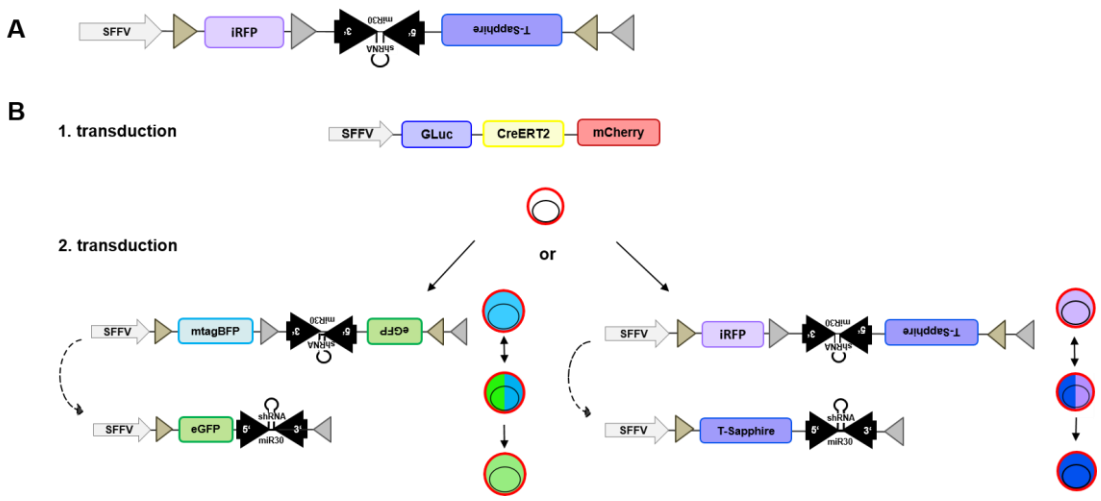

Figure 30: Schematic representation of the inducible competitive five colour system.
A: The FLIP construct constitutively expressed iRFP under an SFFV promoter. The fluorochrome T-Sapphire coupled to the miR30 cassette was inserted in inverse direction and was expressed upon tamoxifen treatment. **B:** Cells were first transduced with the CreER^{T2}-mCherry construct. Next, cells were divided into two groups and transduced either with the mtagBFP/eGFP FLIP construct or with the iRFP/T-Sapphire FLIP construct. SFFV, spleen focus-forming virus; mtagBFP, monomeric tag blue fluorescent protein; eGFP, enhanced green fluorescent protein; iRFP, near-infra-red fluorescent protein; shRNA, short-hairpin RNA.

To test the efficiency of the new iRFP/T-Sapphire FLIP construct, double transgenic cells were treated with tamoxifen and fluorochrome expression was analyzed by flow cytometry. Cells were gated in a similar way as described for the mtagBFP/eGFP FLIP construct (**Figure 27**). In a first step, cell debris and dead cells were excluded. The viable cells were then gated on mCherry expression to select cells with CreER^{T2} expression. Finally, the two markers of the FLIP cassette were visualized gating iRFP against T-Sapphire. Without tamoxifen application, cells only expressed the constitutive marker iRFP. Upon tamoxifen treatment, the inducible fluorochrome T-Sapphire was expressed (**Figure 31**).

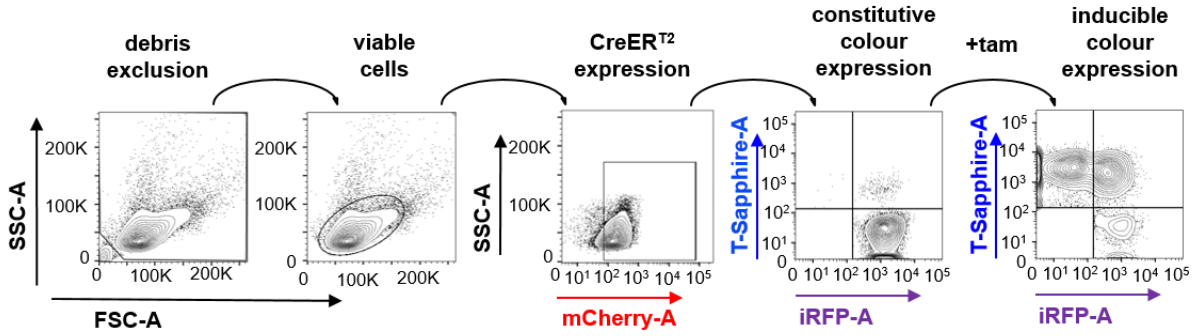

Figure 31: Gating strategy of double transgenic cells with the iRFP/T-Sapphire FLIP cassette
Cells were first gated by forward scatter against side scatter (FSC/SSC). After exclusion of the debris, living cells were selected and gated on mCherry positive cells to monitor cells with CreER^{T2} expression. Next, the FLIP construct was gated using iRFP versus T-Sapphire. Cells constitutively expressed iRFP and showed T-Sapphire expression upon tamoxifen treatment.

All three lentiviral constructs, the CreER^{T2}-mCherry construct, the mtagBFP/eGFP FLIP construct, and the iRFP/T-Sapphire FLIP construct, were finally used to produce lentiviruses and were first applied for transduction of SEM cell line cells. Lentiviral transduction of SEM ALL cell line cells was highly efficient and production of highly transgenic cells without sorting was feasible.

Double transgenic cell line cells were generated by two rounds of FACS to perform inducible competitive experiments *in vitro* and were easily amplified and available for several experiments. Double transgenic cells were successfully established for SEM cell lines. Additionally, one control cell line, NALM-6, was added to perform control experiments in a cell line without MLL/AF4 rearrangement.

In summary, lentiviral constructs for an inducible competitive knock-down system with five fluorochromes were designed and successfully applied to cell line cells.

5.3.3 Silencing of MLL/AF4 altered proliferation of SEM cells *in vitro*

To test the inducible competitive five colour system in SEM cell line cells *in vitro*, the two different cell populations containing either an shRNA targeting Renilla (control population) in the iRFP/T-Sapphire construct or an shRNA targeting MLL/AF4 (knock-down of the GOI) in the mtagBFP/eGFP construct were mixed 1:1 (4.3.8). Additionally, a control experiment with shRNA targeting Renilla in both FLIP constructs was set up to control for eventual toxicity. Without treatment, the competitive mixture expressed three fluorochromes, mCherry, mtagBFP and iRFP (**Figure 32A**). The system was induced by tamoxifen administration (4.3.6). 60nM tamoxifen were applied to the cells, as described before, and competing cell populations were monitored for 30 days in culture. Five fluorochromes, mCherry, iRFP, mtagBFP, T-Sapphire, and eGFP, were expressed in parallel upon tamoxifen treatment and a compensation was applied for the detection by flow cytometry. The flipping rates and the behavior of the two inducible colours, eGFP and T-Sapphire, were highly similar. Fluorochrome expression was analyzed by flow cytometry every day for the first 3 days followed by a measurement twice per week. Cells showed an efficient and reliable flipping and reached the maximum of the inducible fluorochrome expression after three days (41.08 % for eGFP and 44.28 % for T-Sapphire, respectively) (**Figure 32B**). The two distinguishable cell populations of the mixture were followed over time by the different FLIP constructs monitoring mtagBFP against eGFP and iRFP against T-Sapphire. To

investigate the effect of the knock-down, the two induced cell populations were visualized over time in a “single competitive” approach (**Figure 32C**). Shortly after the cells started to express the inducible colour, the constitutively expressed colour decreased. The ratio of the mixed cell populations was followed up by flow cytometry and analyzed by monitoring two fluorochrome expression levels against each other over time. This was performed for the two constitutive colours, mtagBFP and iRFP, as well as for the two inducible colours, eGFP and T-Sapphire, over time in a “double competitive” approach (**Figure 32D**). All depicted dot plots were pre-gated on living cells using forward scatter versus side scatter (FSC/SSC) and on mCherry^{+} to select CreER^{T2} expression, as described before.

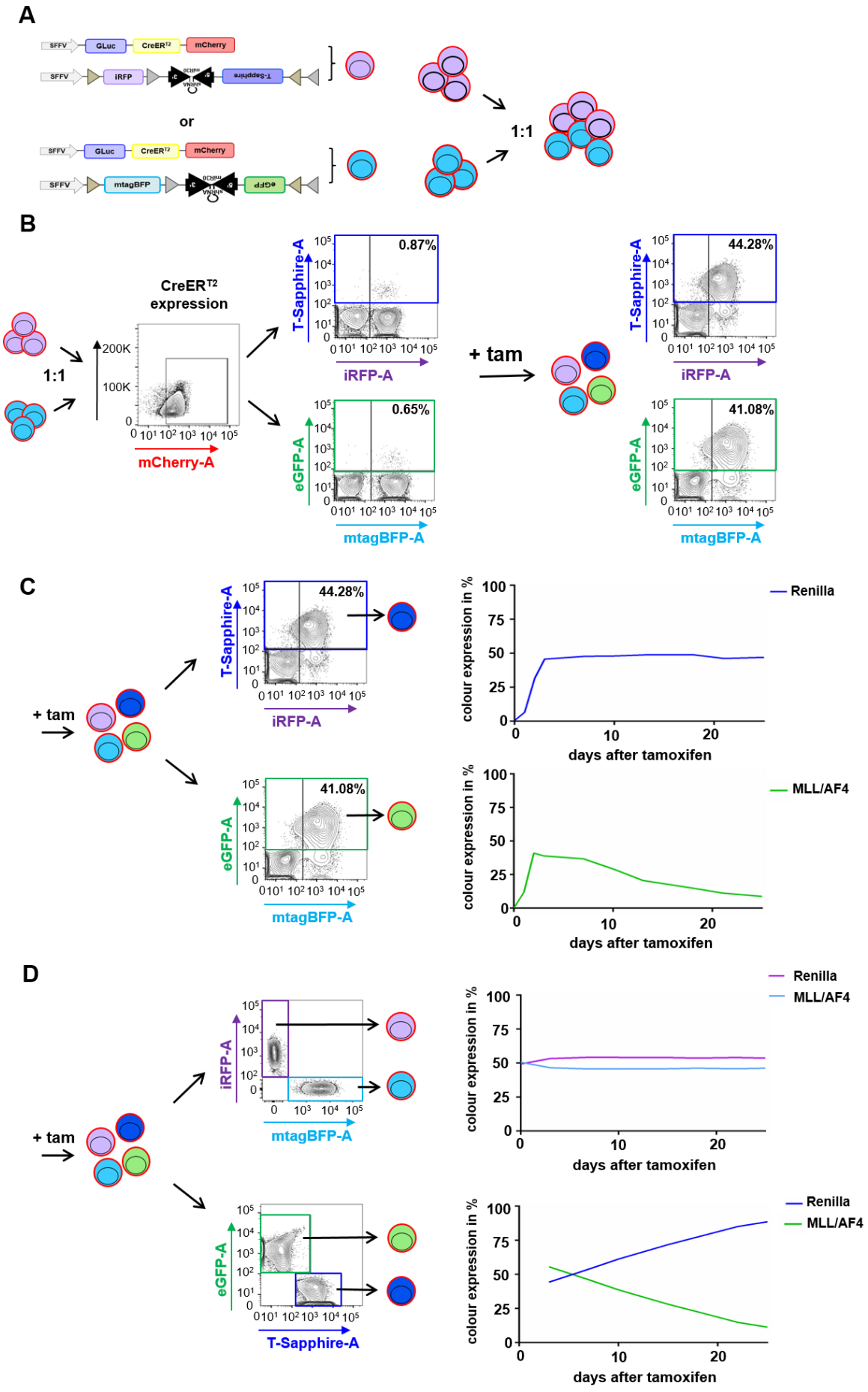
A
SFFV
GLuc
CreER^{T2}
mCherry
SFFV
iRFP
T-Sapphire
or
SFFV
GLuc
CreER^{T2}
mCherry
SFFV
mtagBFP
eGFP
1:1
B
CreER^{T2} expression
1:1
200K
100K
0
mCherry-A
T-Sapphire-A
0.87%
iRFP-A
eGFP-A
0.65%
mtagBFP-A
+ tam
T-Sapphire-A
44.28%
iRFP-A
eGFP-A
41.08%
mtagBFP-A
C
+ tam
T-Sapphire-A
44.28%
iRFP-A
eGFP-A
41.08%
mtagBFP-A
colour expression in %
days after tamoxifen
Renilla
MLL/AF4
D
+ tam
iRFP-A
mtagBFP-A
eGFP-A
T-Sapphire-A
colour expression in %
days after tamoxifen
Renilla
MLL/AF4

Figure 32: An inducible competitive knock-down system in SEM cells *in vitro*
A: Without treatment, competing cell populations expressed three fluorochromes, mCherry, iRFP, and mtagBFP. **B**: An inducible competitive knock-down system was set up mixing cells with a control knock-down targeting Renilla 1:1 with cells containing a knock-down of MLL/AF4. Knock-down was activated by addition of tamoxifen visualized by T-Sapphire or eGFP fluorochrome expression. **C:** The two different cell populations of the mixture were analyzed in a single competitive approach according to the fluorochromes of each FLIP construct, iRFP against T-Sapphire or mtagBFP against eGFP. Each induced cell population, T-Sapphire$^+$ cells or eGFP$^+$ cells were monitored over time to visualize the knock-down effect. **D**: The two mixed cell populations were analyzed in a double competitive approach monitoring the two constitutive colours mtagBFP against iRFP and the two inducible colours T-Sapphire against eGFP over time. All depicted dot plots were pre-gated on living cells using forward scatter versus side scatter and on mCherry$^+$ for CreER^{T2} expression. Tam, tamoxifen.

In the following, we checked several control points to ensure a reliable and specific readout of the system.

First, we controlled for an unspecific expression of the two inducible colours, eGFP and T-Sapphire, without tamoxifen application. Leakiness of the system might occur upon spontaneous CreER^{T2} activity. One risk factor for leakiness could be an overloading of the system with the Cre recombinase. Therefore, the CreER^{T2}-mCherry construct was titrated in cell line cells in order to obtain comparable transduction efficiencies as in PDX cells. Before enrichment of the cells by FACS, transduction efficiency was checked by flow cytometry. Thus, this ensured single integrations of the vector in the recipient genome. According to described mathematical modeling, transduction rates of below 10 % are highly associated with single integrations (Charrier et al., 2011; Christodoulou et al., 2016; Cooper et al., 2011).

Leakiness was checked at the beginning of the experiment and showed an average level of 0.45 % ± 0.14 % (**Figure 33A**). Moreover, control experiments were set up without treatment application in parallel to tamoxifen induced assays. The unspecific fluorochrome expression of the two inducible colours, eGFP and T-Sapphire, was monitored at each time point over time. Leakiness was clearly under 1 % at all stages of the experiment for both inducible colours (**Figure 33B**). Therefore, expression of the inducible colours, eGFP and T-Sapphire, was a specific reaction only occurring upon tamoxifen application.

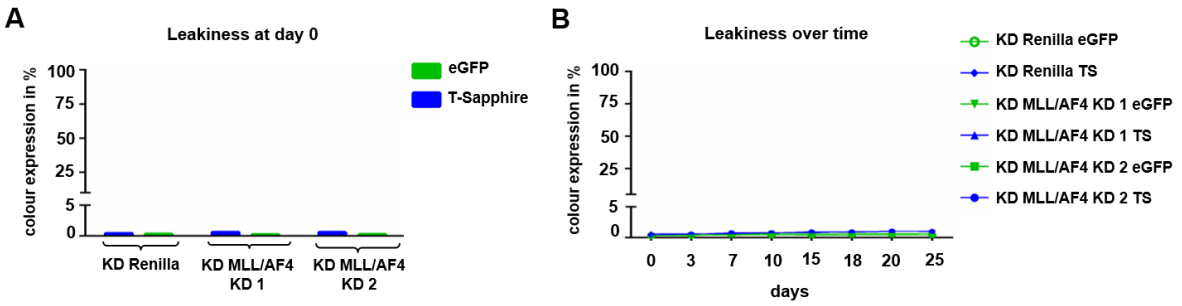

Figure 33: No leakiness was detected in the inducible competitive system
A: Unspecific expression of the two inducible colours, eGFP and T-Sapphire, was checked at the beginning of the experiment and was clearly below 1 %. **B:** Leakiness was monitored in an experiment without tamoxifen application and stayed stable over time. KD, knock-down; eGFP, enhanced green fluorescent protein; TS, T-Sapphire.

The inducible competitive knock-down system was based on the expression of the Cre recombinase. Therefore, stable CreER^{T2} expression was monitored by expression of the fluorochrome mCherry at all stages of the experiment. Direct coupling of the CreER^{T2} expression to the fluorochrome mCherry allowed an easy monitoring by flow cytometry. As described before, similar transduction rates of the CreER^{T2}-mCherry construct were present in cell line cells and in PDX cells by titrating the construct in cell line cells. As PDX cells were difficult to transduce, they showed low transduction rates of ~ 1 %, which was described before. For both, cell line cells and PDX cells, a low expression of the CreER^{T2} recombinase was present to avoid CreER^{T2} toxicity in the cells.

In the SEM cell line experiment, a transduction efficiency of under 10 % was chosen and cells were subsequently sorted and transduced for the FLIP construct (**Figure 34A**). During the experimental time course, the stability of the CreER^{T2} expression was monitored by mCherry, which was inserted in the gating strategy as shown before (**Figure 31**). Tamoxifen was given at day 0 and control experiments (ctrl) were monitored without tamoxifen treatment. No changes in the Cre recombinase expression level were detected during the experiments and the average value was 96.6 % ± 1.7 %, even after addition of tamoxifen. Here, no difference was seen in the different second FLIP constructs containing an shRNA targeting Renilla or an shRNA targeting MLL/AF4. Moreover, the mCherry fluorochrome was equally expressed independently of tamoxifen application (**Figure 34B**). Thus, we concluded that a stable and reliable CreER^{T2} expression level was present in all transgenic cells and at all time points.

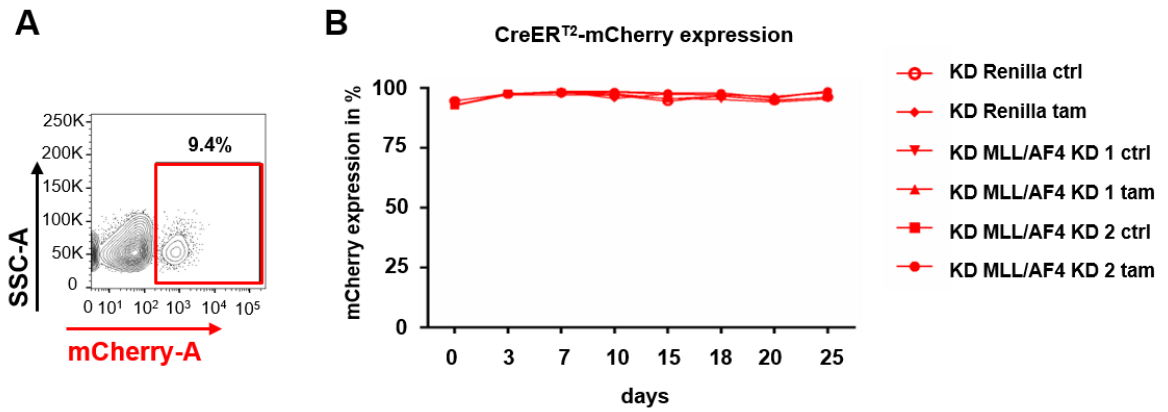

Figure 34: Single integrated CreER^{T2} showed a stable expression level over time
A: The lentiviral vector with the gene for CreER^{T2}-mCherry expression was titrated to achieve a transduction rate under 10 %, which correlated with single integrations in the recipient genome. **B:** The expression level of the CreER^{T2}, which was monitored by the mCherry fluorochrome applying flow cytometry, showed equal rates of 96.6 % ± 1.7 % during the experimental time course. Highly similar values were observed in the tamoxifen treated experiment, where tamoxifen was applied at day 0, and in the control assay without tamoxifen treatment (ctrl). ctrl, control; tam, tamoxifen.

Next, the specific apoptosis rate was analyzed to validate the influence of the tamoxifen treatment and thereby monitoring the effect of nuclear localized Cre on cell viability. Therefore, cells were gated on viable cells as described by forward scatter against side scatter (**Figure 31**). Dead cells were monitored as the absolute apoptosis of the experiment. The absolute apoptosis rate at day 0 for cell line cells before tamoxifen treatment showed an average of 4.93 % ± 0.21 %. Cells, which were treated with tamoxifen, were affected in viability and the absolute apoptosis rate was increased to 20.7 % ± 0.41 % at day 3 and showed a maximum of 25.43 % ± 0.87 % at day 7. Control cells without tamoxifen application still showed an absolute apoptosis rate of 4.17 % ± 0.09 % at day 3, which stayed similar during the experimental timeline. (**Figure 35A**). In a next step, the difference between two apoptosis rates from one measurement time point to the following one was taken into account. The specific apoptosis rate showed a toxicity of tamoxifen with a maximum at day 7 after tamoxifen treatment (**Figure 35B**). The application of tamoxifen led to CreER^{T2} activation followed by a toxicity of the Cre recombinase, which has already been described in literature (Loonstra et al., 2001).

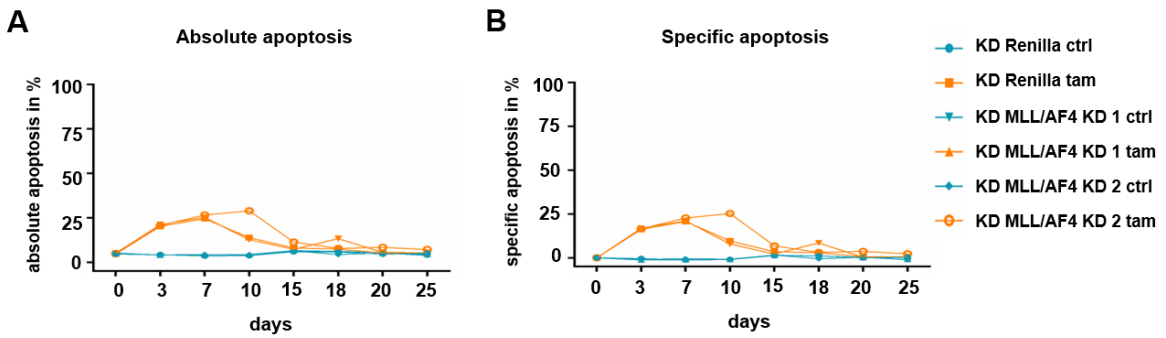

Figure 35: Apoptosis rate in the inducible competitive knock-down system
A: Absolute apoptosis rates were monitored during the experimental time course. Tamoxifen was given at day 0. Apoptosis rates increased upon tamoxifen treatment and showed a maximum at day 7 with an average of 25.43 % ± 0.87 %. Without tamoxifen treatment, cells showed a constant absolute apoptosis rate of 4 % – 5 %. **B:** The specific apoptosis, which compared the absolute apoptosis from one time point to the next one, was calculated. Again, the effect of the tamoxifen treatment was visible, which led to Cre toxicity in the cells. Ctrl, control; tam, tamoxifen.

The FLIP construct itself should not affect the cell growth without activation. Therefore, the maintenance of the colour distribution of mixed cells was monitored without inducing the Cre recombinase upon tamoxifen applying the double competitive analysis. Two colours were constitutively expressed by the FLIP cassette, mtagBFP and iRFP, as described before. Without tamoxifen application, none of the two competing cell populations should have a growth advantage, as no shRNA is expressed to target the GOI. Experiments were performed without tamoxifen application and monitored in parallel to tamoxifen treated assays, as already described. No changes in the distribution of the two competing cell populations were detected during the experimental time line. In an experiment with an shRNAs targeting Renilla in each of the two different FLIP cassettes, mtagBFP and iRFP expression stayed stable over 25 days and showed no effect on colour expression (**Figure 36A**). The same result was seen in an experiment with an shRNA targeting MLL/AF4 in the mtagBFP/eGFP FLIP cassette (**Figure 36B**).

In the tamoxifen treated assay, the ratio of both non-induced cell populations characterized by a single expression of the constitutive colours should stay stable as well. The distribution of the two competing cell populations monitored by mtagBFP or iRFP should not be affected by a decrease of induced cells. No change was seen for the expression level of mtagBFP and iRFP in both experimental set ups with either two shRNAs targeting Renilla or an shRNA targeting MLL/AF4 in the mtagBFP/eGFP FLIP cassette (**Figure 36C + D**).

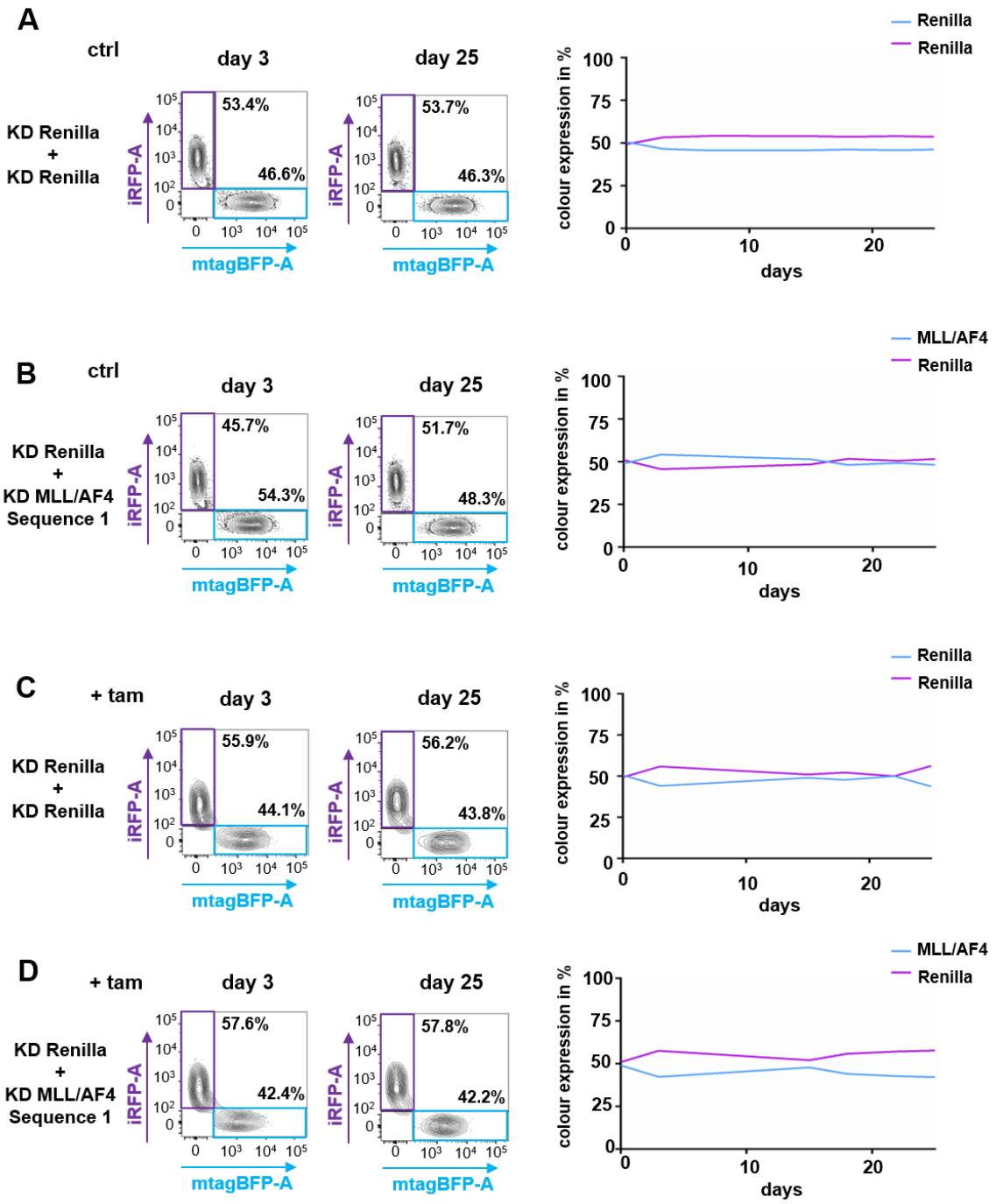

Figure 36: Constitutive colours show equal expression levels in the competing cell populations
A + B: Control experiments were performed without tamoxifen treatment using either two shRNAs Renilla in both FLIP constructs or an shRNA targeting MLL/AF4 in the mtagBFP/eGFP FLIP cassette. Colour distribution of the two constitutive fluorochromes, mtagBFP and iRFP, stayed constant over the experimental time course. **C + D:** The ratio of cell populations, which were single positive for the constitutive colour, iRFP or mtagBFP, stayed equal after tamoxifen treatment in the inducible competitive system. No difference was observed in the expression of iRFP against mtagBFP in the control experiment with two shRNAs against Renilla and in the experiment with shRNA targeting MLL/AF4 in the mtagBFP/eGFP FLIP cassette. KD, knock-down; ctrl, control; tam, tamoxifen.

Finally, cell populations containing the activated shRNA were analyzed with the double competitive approach, which were visualized by expression of the two inducible

colours, T-Sapphire or eGFP. The maximum of the flipping efficiency was achieved at day 3 after tamoxifen treatment and hence, taken as starting point to monitor the two induced cell populations with activated shRNA expression. Looking at both populations separately in a single competitive approach, both $eGFP^+$ and $T\text{-}Sapphire^+$ cells achieved an equal level of induced cells at day 3. Directly comparing the knock-down positive subfractions of both cell populations in a double competitive approach, no decrease of the $eGFP^+$ population was detected in the control experiment with an shRNA targeting Renilla in both constructs. As expected, the mixture of the two competing cell populations stayed stable over time (**Figure 37A**).In contrast, $eGFP^+$ cells, which expressed shRNA targeting MLL/AF4, showed a significant growth disadvantage over time, decreasing from 60.8 % at day 3 to 11.4 % at day 25 for the knock-down sequence KD 1 (**Figure 37B**). A similar effect was monitored in the experiment with the second knock-down sequence KD 2 and eGFP expressing cells decreased from 60.9 % at day 3 to 13.3 % at day 25 (**Figure 37C**). These data strongly contributes to the suggestion that the fusion protein MLL/AF4 is essential for tumor cell survival.

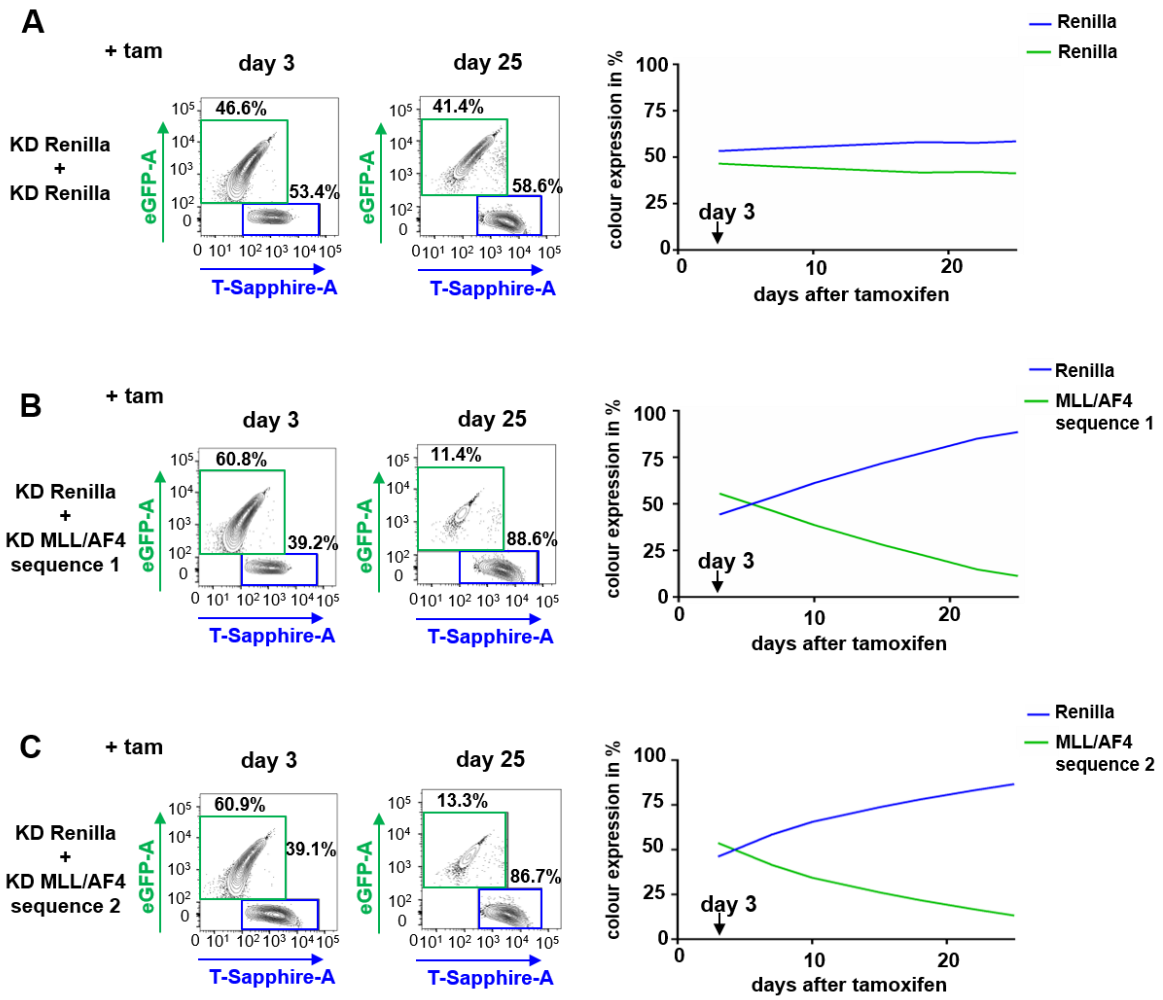

Figure 37: The MLL/AF4 knock-down induced a growth disadvantage in SEM cell lines *in vitro*
A: A knock-down targeting Renilla was used in both constructs to control the system. Tamoxifen was given at day 0. Both fluorochromes, eGFP and T-Sapphire, were expressed equally upon tamoxifen induction and expression level stayed highly similar over time. **B + C:** Knock-down of MLL/AF4 visualized by eGFP expression lead to a growth disadvantage over time. Experiment was performed with two different MLL/AF4 knock-down sequences, sequence KD 1 and KD 2. KD, knock-down.

With this assay, I successfully established an inducible competitive knock-down system in SEM cell line cells *in vitro* and could show that a knock-down of MLL/AF4 induced a major growth disadvantage in SEM cells *in vitro*.

The same experiment was performed in NALM-6 cell line cells, which do not have the chromosomal rearrangement of MLL/AF4. In the control experiment with shRNA targeting Renilla in both competing cell populations, colour distribution of eGFP and T-Sapphire stayed highly similar during the time course of the double competitive approach (**Figure 38A**). In a parallel experiment, an shRNA targeting the GOI MLL/AF4 was inserted in the miR30 cassette. Therefore, the most potent shRNA sequence candidate, KD 1, was used. No off-target effect was visible by an shRNA expression against MLL/AF4 in non-rearranged NALM-6 cells and colour distribution of eGFP and

T-Sapphire expression stayed very similar during the time course of the double competitive experiment (**Figure 38B**).

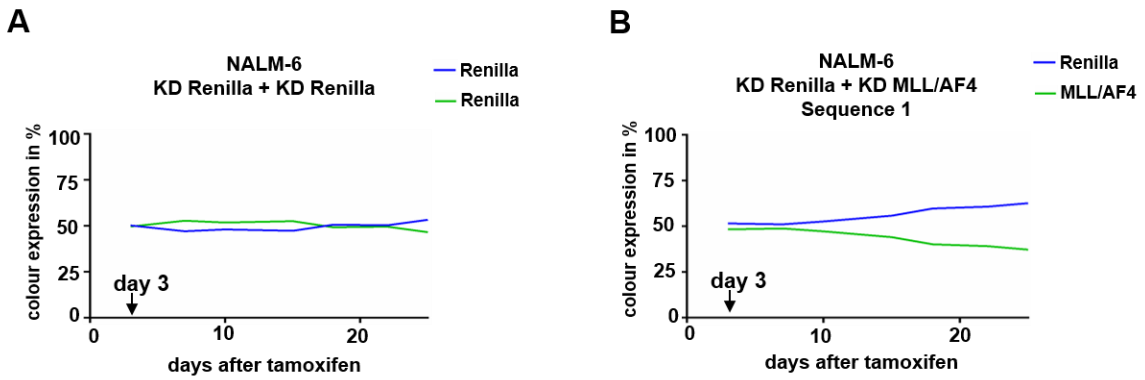

Figure 38: NALM-6 cells were not affected by a knock-down targeting MLL/AF4
A: In the control experiment, both cell populations expressed an shRNA targeting Renilla. Tamoxifen was given at day 0. The colour distribution of the two inducible fluorochromes, eGFP and T-Sapphire, stayed highly similar during the double competitive experiment. **B:** An shRNA targeting MLL/AF4 was expressed in the eGFP positive cell population and an shRNA targeting Renilla in the T-Sapphire positive cells. The colour distribution stayed very similar during the time course. KD, knock-down.

Taken together, an inducible competitive knock-down system with five fluorochromes was successfully established to investigate the importance of the fusion gene MLL/AF4 for cell survival. Applying the system to SEM cell line cells *in vitro*, a strong growth disadvantage of cells with the MLL/AF4 knock-down was observed. These data are consistent with the PDX *in vivo* data performed in the constitutive competitive system showing a strong growth disadvantage for leukemia cells upon MLL/AF4 knock-down. In a next step, we were aiming to test the inducible competitive system *in vivo* in PDX cells growing in mice.

5.3.4 Silencing of MLL/AF4 using an inducible competitive knock-down system in PDX cells *in vivo*

To perform inducible competitive assays *in vivo*, double transgenic PDX cells were generated for the five colour system identically as in SEM cells. This required repetitive passaging through mice, lentiviral transduction and enrichment by flow cytometry. Due to low lentiviral transduction rates of MLL-rearranged ALL samples, two rounds of amplifying cells in mice followed by sorting were necessary to achieve > 90 % positive transgenic cells. Depending on the passaging time of the individual PDX samples listed in **Table 27**, several months were required for generating GEPDX cells (**Figure 39**).

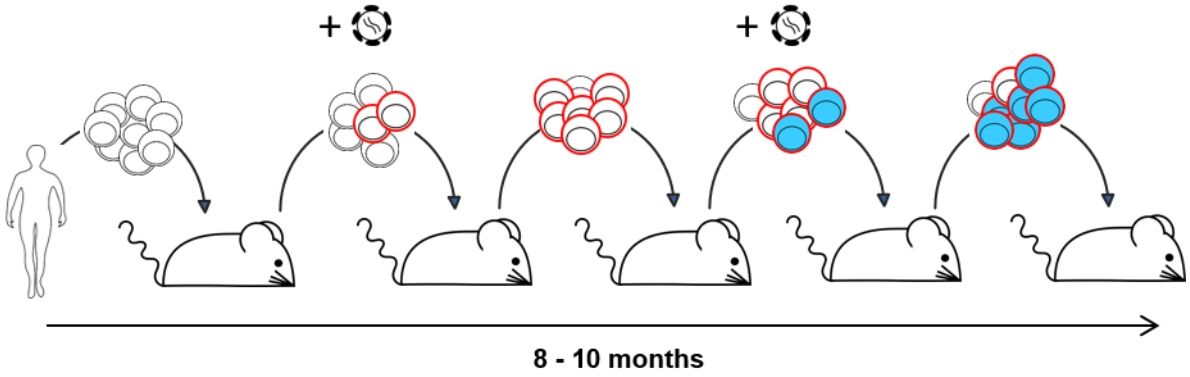

Figure 39: Generation of transgenic PDX cells for an inducible competitive system *in vivo*
Due to low transduction efficiencies, two passages of mice were required for highly enriched transgenic PDX cells (> 90 %). PDX cells were first transduced with the CreER^{T2}–mCherry construct and second with the shRNA expressing construct, shown here for the mtagBFP/eGFP FLIP construct. Depending on the PDX sample, several months were required to generate GEPDX cells.

Transgenic PDX cells did not show leakiness, which is in accordance to data from cell line cells. The schematic representation of the inducible competitive five colour assay in PDX cells *in vivo* is depicted in **Figure 40**.

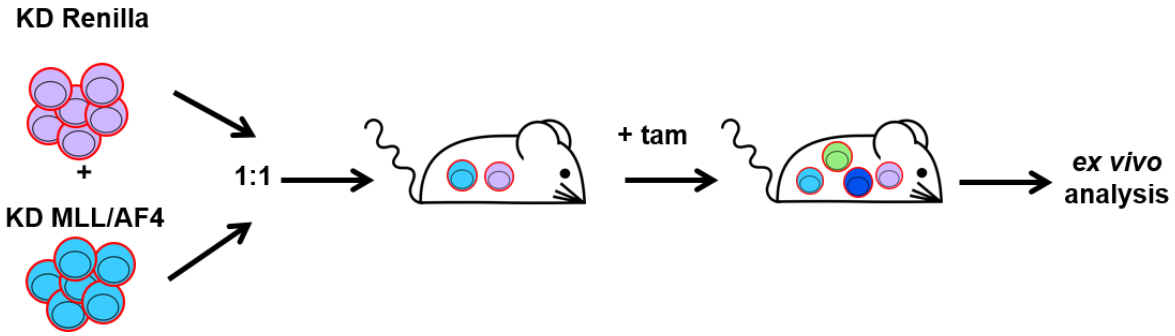

Figure 40: Schematic representation of the competitive inducible assay in PDX cells *in vivo*
Control cells with a knock-down targeting Renilla (KD Renilla) were mixed in a 1:1 ratio with cells containing a knock-down targeting MLL/AF4 (KD MLL/AF4). Cells were engrafted in immunodeficient NSG mice and treated with tamoxifen to induce CreER^{T2} activity. Leukemia cells were re-isolated at certain time points or at full-blown leukemia and analyzed *ex vivo*. KD, knock-down, tam, tamoxifen.

Double transgenic PDX cells of the fastest growing sample, ALL-707, were freshly isolated from mice and mixed in a 1:1 ratio. Mice were injected with competitive cell populations at a total of 300,000 cells per mouse. Correct colour distribution of the initial mixture was confirmed by flow cytometry before injection. As in cell line cells, two experiments were set up in parallel to control for toxicity. Either control cells with a construct to knock-down Renilla were mixed with cells containing shRNA against MLL/AF4 or both cell populations contained constructs with shRNA targeting Renilla, as previously described. Mice were treated with tamoxifen to induce the flipping *in vivo*

(4.2.7). We aimed for an early tamoxifen application in order to have a long period between induction of MLL/AF4 knock-down and analysis of the phenotype *ex vivo*. Therefore, tamoxifen was given at day 7 and control mice received corn oil without tamoxifen (**Figure 41A**). According to data of my colleague Sarah Ebinger, homing of PDX cells takes place within the first 48 h in the bone marrow and tamoxifen treatment at day 7 should not disturb this process (Ebinger et al., 2016). Positive engraftment and leukemia cell growth was monitored by *in vivo* bioluminescent imaging, enabled by GLuc expression in the cells (GLuc: 10^7 bioluminescence photons/second). As soon as a positive imaging signal was detected at day 8 after tamoxifen, control mice without tamoxifen treatment were sacrificed and analyzed to detect colour distribution of the engrafted cell populations with the double competitive analysis. Expression of the two constitutive markers, mtagBFP and iRFP, was measured by flow cytometry *ex vivo*. All mice, which were analyzed at this time point, showed an equal colour distribution of the two constitutive fluorochromes, which was highly similar to the injected cell mixture. This meant that the injected competing cell populations engrafted equally in the immunodeficient mice.

The last time point for cell analysis was taken 30 days after tamoxifen treatment, as mice showed signs of leukemia disease monitored by blood measurement. Again, colour distribution of the competing cell populations was analyzed by flow cytometry. In the corn oil control experiment with shRNA targeting Renilla in both FLIP cassettes or with shRNA targeting MLL/AF4 in the mtagBFP/eGFP FLIP cassette, the two constitutive markers mtagBFP and iRFP showed very similar expression rates, which had already been observed at day 8. (**Figure 41B + C**).

These data confirmed the cell line data of the internal controls and showed that the constitutive colour expression was stable over time.

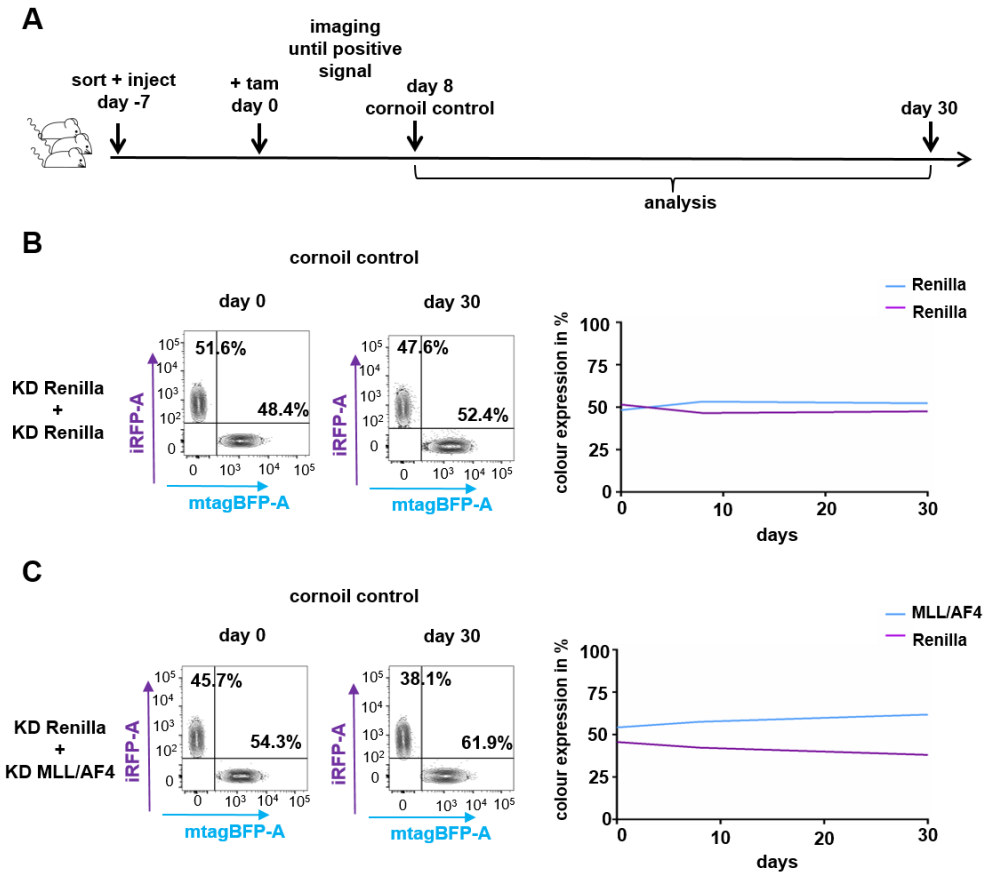

Figure 41: An inducible competitive knock-down system in PDX cells *in vivo*
A: Schematic representation of the experimental time line. ALL-707 PDX cells were sorted, mixed 1:1 and injected into mice. Tamoxifen was given 7 days after PDX cell injection. Tumor growth was monitored by bioluminescent *in vivo* imaging and once the signal was positive, corn oil treated control mice were taken down for analysis. All other mice were taken down at day 30. **B**: PDX cells were injected in a 1:1 ratio. In the double competitive assay containing an shRNA targeting Renilla in both constructs, the distribution of the two constitutive colours, mtagBFP and iRFP, stayed highly similar over 30 days in corn oil treated mice. **C**: In a parallel experiment, an shRNA targeting MLL/AF4 was applied in the mtagBFP/eGFP construct. Again, the distribution of the two constitutive fluorochromes, mtagBFP and iRFP, stayed constant over 30 days in corn oil treated mice. KD, knock-down; tam, tamoxifen.

As in cell line cells, leakiness was under 1 % for both constructs (0.04 % for eGFP and 0.14 % for T-Sapphire, respectively) and is exemplary shown in **Figure 42A** for two mice at day 30, which had been treated with corn oil. In the tamoxifen treated mice, both constructs of the two different cell populations showed similar flipping rates of around 15 % for eGFP and for T-Sapphire (**Figure 42B**). The flipping rate itself was rather low compared to cell line cells, which achieved over 40 % flipping in the inducible competitive system.

To analyze the mixture with the double competitive approach, the ratio of the constitutive colours, mtagBFP and iRFP, was checked for all tamoxifen treated mice. Similar results were monitored as for corn oil treated mice and no changes were detected in the distribution of the two non-induced cell populations (**Figure 42C**). This

means that the constitutive fluorochrome expression was not influenced by tamoxifen application or by the activated knock-down of MLL/AF4.

No difference was observed in the colour distribution of the inducible colours, eGFP and T-Sapphire, between control cells and PDX cells with MLL/AF4 knock-down after 30 days. In the control experiment, in which both shRNA targeted Renilla, the ratio of cells expressing T-Sapphire to eGFP was 44.93 % ± 3.23 % to 55.07 % ± 3.23 %. Applying an shRNA targeting MLL/AF4 in the eGFP expressing cells, the ratio was 41.13 % ± 0.33 % T-Sapphire expression to 58.87 % ± 0.33 % eGFP expression (**Figure 42D**).

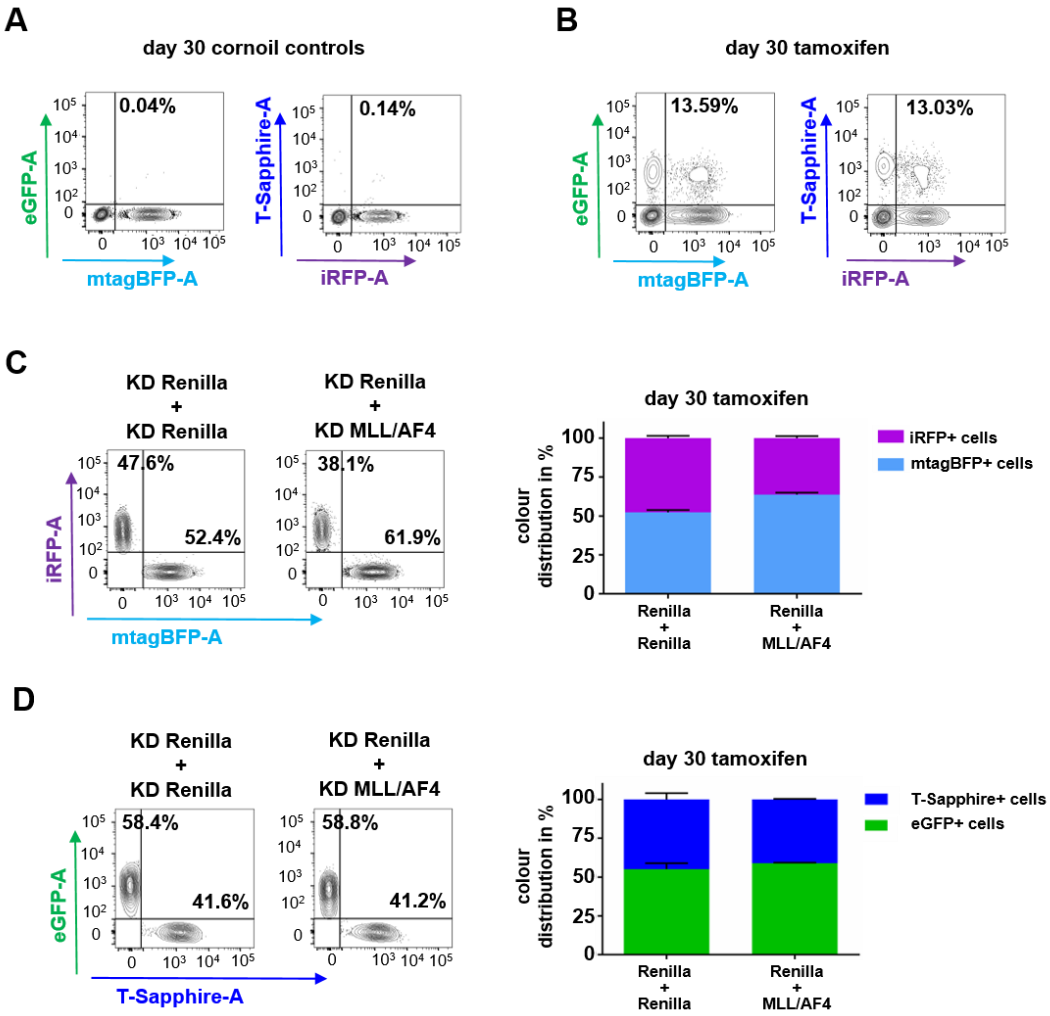

Figure 42: The MLL/AF4 knock-down in PDX cells *in vivo* did not affect the cell distribution
A: Leakiness was under 1 % for both inducible fluorochromes without tamoxifen application. **B:** A flipping rate of ~ 15% was observed for eGFP and for T-Sapphire. **C:** Constitutive colour expression of mtagBFP and iRFP was not changed upon tamoxifen treatment and showed similar results as for corn oil treated mice. Data is shown representatively in a dot plot and summarized for all mice in a diagram. Each column represents the mean of three individual mice. **D**: Competitive flipping efficiency showed no decrease of PDX cells upon MLL/AF4 knock-down *in vivo* at day 30. Data is shown representatively in a dot plot and summarized for all mice in a diagram. Each column represents the mean of three individual mice. KD, knock-down.

Thus, while SEM ALL cells showed a clear phenotype upon loss of MLL/AF4, no effect could be detected in the analyzed PDX samples. One reason might be the low transduction rate of PDX cells in comparison to SEM cells. In PDX cells, both constructs were inserted in the genome with single integrations (Charrier et al., 2011; Christodoulou et al., 2016; Cooper et al., 2011). Single expression of shRNA targeting MLL/AF4 might not be sufficient to induce a strong knock-down inducing leukemia cell death. In contrast, SEM cell line cells were transduced with the FLIP construct with an average efficiency of ~ 30 %. Additionally, flipping rates were rather low (15 %) compared to cell line data. Higher transduction rates might be able to compensate this issue and lead to an increase of both flipping rate and knock-down efficiency. Therefore, further technical optimization is required to study the role of MLL/AF4 in PDX cells.

Nevertheless, we were able to establish an inducible competitive knock-down system with five fluorochromes, which can be used for further knock-down approaches to investigate the importance of novel genes for cellular survival.

Taken together, these data reveal an important role of MLL/AF4 for survival and growth of leukemia cells. Silencing of the fusion transcript led to a growth disadvantage in SEM cells *in vitro* as well as in PDX cells *in vivo* applying the constitutive competitive system. Further studies are required to increase the transduction efficiency of MLL-rearranged PDX ALL samples and to successfully apply the inducible five colour system for MLL/AF4 PDX ALL cells.

In total, the data of this work reveals MLL/AF4 as a promising candidate for developing novel cancer therapy with this tumor specific target in leukemia cells. Functional delivery systems for successful application *in vivo* are highly required to apply the silencing with high efficiency to the target cells in patients.

6. Discussion

Acute leukemia patients with chromosomal rearrangements often show an aggressive disease progression with bad prognosis and poor survival. Important and frequent chromosomal translocations are for example MLL-rearranged subtypes such as t(4;11) MLL/AF4 (Dimartino and Cleary, 1999; Ottmann and Pfeifer, 2009; Schoch et al., 2003; Taki et al., 1996). Novel therapeutic approaches are highly demanded requiring to investigate the disease biology more in detail.

Patient material can be amplified infinitively in the individualized xenograft mouse model in severely immunodeficient mice. Although several PDX ALL mouse models exist for pediatric samples, engraftment of adult ALL samples causes more difficulties (Jones et al., 2017; Townsend et al., 2016; Woiterski et al., 2013). Therefore, in this study we optimized engraftment of primary adult ALL samples in the individual xenograft mouse model achieving high reliability and frequency.

The fusion t(4;11) MLL/AF4 is a characteristic sequence only present in acute leukemia cells and hence, its importance as a cancer specific target was validated in cell line cells *in vitro* and in PDX cells *in vivo* in this study. To analyze the function of the chromosomal translocation MLL/AF4, an inducible competitive knock-down system was established. This system serves as a valuable tool for testing potential new targets and their importance for cancer therapy.

6.1 Reliable engraftment of primary adult ALL cells

Cell lines do not represent a suitable model to study acute leukemia in patients as they have additional alterations caused by the immortalization process or intensive passaging in culture (Gillet et al., 2011; Petitjean et al., 2007). Moreover, they are putatively monoclonal, which is not representative for the complexity of acute leukemia in patients. Besides, for several mutations found in leukemia patients, no established cell lines are available at all. Therefore, our lab is working with an established individualized PDX mouse model enabling to study characteristics of the heterogenic disease in detail. This allows us to investigate the behavior of acute leukemia patient cells of ALL or AML *in vivo* in the correct microenvironment.

In contrast to primary pediatric ALL samples, engraftment and amplification of adult patient cells was reported to be challenging (Notta et al., 2011; Patel et al., 2014). Patel

and colleagues suggested pretreatment of the mice by total body irradiation, which induces an unspecific inflammation in the bone marrow. Even applying this method, they achieved low engraftment rates for primary adult ALL cells. In contrast to published data, our results show highly reliable and frequent engraftment rates for primary adult ALL samples without pretreatment of the mice. Successful engraftment rates might depend on the sample quality. Cell viability might easily be affected by long transport journeys of fresh patient samples before final freezing. Therefore, total body irradiation of mice could compensate for low cell viability and achieve higher engraftment rates in mice. All samples in our study were characterized by chromosomal rearrangements, which might facilitate the primary engraftment due to aggressive growth. Nevertheless, Patel and colleagues worked with similar subtypes and used identical immunodeficient mice in their study. Moreover and in accordance with the literature, we showed that fresh samples have better engraftment conditions resulting in higher engraftment rates of primary samples. The time required for the first passage until full-blown leukemia was faster without prior freezing/thawing procedure as well. This indicates the importance of high cell quality when samples arrive at the research lab and suggests to work with optimized protocols for cell freezing/thawing processes (Bonnet, 2008).

In summary, we achieved very high engraftment rates for primary adult ALL samples, which are comparable to those described for primary pediatric ALL samples (Morisot et al., 2010; Woiterski et al., 2013).

6.2 Genetic engineering of PDX samples with chromosomal translocations

Successful engraftment of primary acute leukemia cells enables amplification of patient cells and their further application to study the molecular biology of the disease or for preclinical therapy trials (Ebinger et al., 2016; Jones et al., 2017). Genetic engineering of PDX cells using lentiviral transduction represents a valuable technique.

Here, I used a third generation lentiviral vector system for genetic engineering of PDX cells and cell lines as described in literature (Dull et al., 1998; Naldini et al., 1996; Zufferey et al., 1999). In contrast to retroviruses, lentiviral transduction allows infection of both dividing and non-dividing cells. This is important for genetic engineering of PDX cells, as they do not proliferate *in vitro*. Genetic engineering enables, for example,

expression of a luciferase in PDX cells to monitor tumor growth applying bioluminescence *in vivo* imaging (Jones et al., 2017; Terziyska et al., 2012; Vick et al., 2015). Lentiviral vectors integrate into the genome of PDX cells, which raises the assumption of altering PDX cell characteristics. In former studies of our group, no influence of lentiviral transduction has been observed yet, which would have led to an altered behavior of PDX cells (Ebinger et al., 2016; Terziyska et al., 2012; Vick et al., 2015).

Here, I successfully established genetically engineered PDX cells from primary adult ALL samples, which we subsequently called GEPDX cells. Samples with chromosomal rearrangement were a challenging subgroup for lentiviral transduction showing very low transduction rates. Improving transduction efficiency of lentiviral vectors is broadly discussed in literature, as several groups describe difficulties with genetic engineering of primary and PDX cells (Chono et al., 2011; Denning et al., 2013; Ricks et al., 2008). Advanced methods suggest to use transduction enhancers that reduce strong electrostatic repulsion between cell and virus. Centrifugation of target cells during transduction is another technique to lower negative charges and increase transduction rates. (Lin et al., 2012; O'Doherty et al., 2000). In this project, I tested different transduction enhancers, polybrene and lentiBOOST, but no increase of the transduction rate was detected. As high transduction efficiencies of PDX cells are an important issue for subsequent experiments, our lab is still working on improving the transduction rates of several challenging samples.

High transduction rates for certain subgroups like adult AML samples or pediatric non-rearranged acute leukemia PDX cells could be easily achieved. In contrast, rearranged adult and pediatric ALL samples showed very low transduction levels. Nevertheless, transgenic cell enrichment by FACS enabled establishing GEPDX cell populations allowing subsequent studies.

6.3 MLL/AF4 rearrangements as a potential target in acute leukemia treatment

After successful engraftment and genetic engineering of adult ALL PDX samples in parallel to pediatric samples, I focused on analyzing the importance of fusion proteins for leukemia cell survival. The major target was MLL/AF4, which is described to be an

oncogenic driver and to induce an aggressive form of the hematologic disease (Behm et al., 1996; Hilden et al., 2006).

Only few fusion partners are found highly frequently fused to MLL in acute leukemia, most importantly AF4 in ALL and AF9 in AML (Krivtsov and Armstrong, 2007; Meyer et al., 2013a). Additionally, the breakpoint region of the fusion mRNA transcripts showed identical sequences for large groups of patients (Felix et al., 1998; Langer et al., 2003; Meyer et al., 2013b). This could enable a novel therapeutic approach targeting the breakpoint sequence on mRNA level, which is highly tumor cell specific without affecting healthy cells.

In this study, I used MLL/AF4 as a potential therapeutic target to analyze its oncogenic function for cell survival and its role in tumor development. We already had a constitutive competitive knock-down system established in the lab and hence, I applied this system to investigate the knock-down of MLL/AF4 in PDX cells *in vivo* growing in mice. In this experimental setup, control cells and the knock-down population were in the same approach and enabled to have a highly sensitive readout.

The knock-down was performed by introducing an shRNA into a miR30 backbone as described by Fellmann and colleagues (Fellmann et al., 2013; Fellmann et al., 2011). As the miR30 cassette integrates directly into the genome of the target cell, it provides shRNA expression by a polymerase II leading to efficient processing of the shRNA combined with low cellular toxicity (Cullen, 2004, 2005; Lee et al., 2002).

I found two potent shRNA sequences that reduced the mRNA expression level of MLL/AF4 to 25.49 % for KD 1 and to 43.79 % for KD 2. A reduction of 75 % does not represent a strong knock-down as described for other genes in literature, which achieved a knock-down efficiency of 80 % - 90 % (Lee et al., 2014; Singh et al., 2008). For the knock-down of MLL/AF4, no better knock-down sequence was possible as the sequence design of the 22 nucleotide sense strand was restricted to the fusion breakpoint and had to contain both parts, the MLL and the AF4 region. Nevertheless, sequence candidate KD 1 showed a good knock-down effect on mRNA level and was used for further experiments in PDX cells *in vivo*.

I observed a strong growth disadvantage of PDX ALL cells *in vivo* in mice upon the knock-down of MLL/AF4 with the constitutive competitive system. I showed this for three MLL/AF4-rearranged adult PDX samples, ALL-706, ALL-707, and ALL-763. Although injecting control cells and cells with MLL/AF4 knock-down in a 1:1 ratio, I could not monitor cells containing the knock-down of MLL/AF4 at the day of re-analysis

anymore. As low transduction rates led to low construct-positive cell numbers, which had to be enriched in time-consuming sorting, low cell numbers were injected into mice. Consequently, the time until mice developed full-blown leukemia was increased up to 80 days instead of the periods known for the passaging time of each sample. Already at early stages and as soon as a positive imaging signal was detected, cell analysis showed a clear knock-down effect, thus only mtagBFP positive control cells could be re-isolated from the murine bone marrow.

Generally, the cell viability decreased during long sorting processes, as PDX cells were sorted at room temperature and kept in sorting buffer not containing the optimal ingredients as patient medium. Therefore and due to low transduction rates, no mouse could be injected with high cell numbers (10 Mio) and taken down after few days to control for equal distribution of both cell populations.

Nevertheless, fluorochromes had been tested previously in our lab injecting only mtagBFP or eGFP labelled cells in a 1:1 ratio to control for colour toxicity (data unpublished). No influence on growth behavior or engraftment was detected by expression of the two different fluorochromes.

MLL rearrangements in acute leukemia are known to be aggressive driver mutations, which require very few additional alterations to develop the hematopoietic disease (Metzeler et al., 2016). Therefore, it is a highly interesting target, as oncogenic potential of the cells could be reversed at an early stage. In this project, I identified a very efficient sequence for silencing MLL/AF4. This could be used as a new treatment option for leukemia patients with the same sequence of MLL/AF4. Therefore, efficient and reliable delivery systems are highly required to transport the shRNA directly to the target cells. Two application forms are possible as described before. Either genetically engineering the altered cells *ex vivo* and re-transplanting them into the patient or applying a vehicle system to transport the RNA particles to the target cells of the patient (He et al., 2014; Jyotsana et al., 2017). Specific delivery systems are needed that avoid the first-pass effect of the liver and that reach only the desired cell type. Many groups are working on establishing promising transport systems consisting for example of polyethylenimine or polycaprolactone. More in detail, polyetylenimine is a cationic polymer, which enables the complexation of unmodified siRNA molecules and functions as a delivery system. Adding specific peptide ligands onto the surface of the vesicle capsule, tumor cells are recognized by a ligand receptor mechanism (Aigner, 2006; Cao et al., 2010; Wang et al., 2010).

Recently, Jyotsana and colleagues developed a novel form of lipid nanoparticles to encapsulate siRNA within a microfluidics based device. They described successful encapsulation of over 90 % siRNA and showed high delivery efficiency in cell lines *in vitro* and *in vivo* and in a patient ALL model *in vivo*. The applied siRNA was directed against a fusion transcript, TCF3-PBX1, which is the most frequent rearrangement in B-ALL. The authors claim that Apolipoprotein E and the low-density lipoprotein receptor on the surface of leukemia cells are associating with the nanoparticles and therefore responsible for the uptake of the encapsulated siRNA (Jyotsana et al., 2017). This data represents a highly efficient and promising approach in personalized therapy of leukemia. Until today, no surface ligand has been found, which is only expressed on leukemia cells. In line with our data, fusion genes represent an ideal target, as they are leukemia cell specific.
Besides, off-target effects of persisting shRNA need to be investigated in more detail before RNA interference can be applied in treatment of acute leukemia patients. Several groups described toxic side-effects of siRNA and proposed various chemical modifications to stabilize and specify siRNA delivery. (Fedorov et al., 2006; Jackson and Linsley, 2010; Selvam et al., 2017).

Taken together, targeting the fusion breakpoint MLL/AF4 with a constitutive competitive knock-down approach showed a strong growth disadvantage in PDX cells *in vivo* growing in mice. Two sequence candidates were successfully validated and the knock-down phenotype was achieved in three PDX ALL cells, ALL-706, ALL-707, and ALL-763, *in vivo* growing in mice. To apply the knock-down strategy as a treatment into clinical application, novel and improved delivery systems are highly required to bring the knock-down sequence with high efficiency and reliability to the leukemia target cells.

6.4 Establishing an inducible competitive knock-down system for target validation

Since the knock-down was supposed to be lethal, we were next aiming to apply an inducible knock-down system in order to be able to induce the knock-down of target genes at a specific time point. Moreover, we wanted to molecularly mimic the clinical situation in patients as closely as possible. When leukemia is diagnosed in patients, they already have a certain stage of the disease manifested in their body. In contrast

to cells with the constitutive competitive system, which contain the knock-down of MLL/AF4 from the time point of injection into the mice, an inducible system allows to initiate the knock-down at defined time points of leukemia burden in mice. Hence, this mimics the clinical situation and enables therapeutic intervention at an advanced stage of the disease.

An inducible system with three fluorochromes had already been established in the lab. The clear disadvantage of this non-competitive system was that control Renilla and MLL/AF4 knock-down experiments would need to be performed in separate mice *in vivo*. Thereby, the direct comparison of the two assays and the readout would be very challenging and do not allow easy conclusions of an *in vivo* experiment.

Therefore, we established an inducible competitive knock-down system with five fluorochromes combining the already existing two systems, the constitutive competitive approach and the inducible approach, in this project. The competitive form is highly useful to monitor control cells and knock-down population within the same approach and to have a highly sensitive readout. It allows injection of two different cell populations, control Renilla and knock-down MLL/AF4, into the same animal in *in vivo* experiments and hence both cell groups are proceeded and treated in exactly the same way. A system with several fluorochromes in parallel had been described in literature by Mohme and colleagues and was considered for establishing our colour combination (Mohme et al., 2017). Two more fluorochromes, iRFP and T-Sapphire, were added to the three colours of the inducible system, mCherry, mtagBFP, and eGFP. As the emission spectra showed an overlap of the three colours mtagBFP, T-Sapphire, and eGFP, a compensation was set up to clearly distinguish all fluorochromes.

The inducibility of the system is based on the expression of a CreER^{T2} recombinase, an efficient approach to catalyze site-specific DNA recombination (Feil et al., 2009; Indra et al., 1999; Ventura et al., 2004). We applied a technique, which had already been described by Oberdoerffer and colleagues, containing two differently mutated loxP sites to obtain two enzymatic CreER^{T2} steps (Oberdoerffer et al., 2003). The differently mutated loxP sites were inserted in a FLIP cassette containing the reporter genes and the miR30 cassette for shRNA expression as described by Stern and colleagues (Stern et al., 2008). This enabled us to work with a stable system irreversibly expressing the shRNA coupled to a marker upon tamoxifen treatment. Furthermore, we established a system with five fluorochromes as reporter genes to facilitate cell enrichment by FACS and to directly monitor knock-down induction upon

tamoxifen treatment. Having a constitutive and an inducible marker in the vector ensured to monitor all steps of the reaction and was highly useful for sorting of specific cell populations.

To exclude cell toxicity caused by one of the fluorochromes, by off-target CreER^{T2} activity or by overloading of the natural siRNA pathway with exogenous shRNA expression, control experiments without MLL/AF4 targeted shRNA were performed. In the literature, it was shown that especially eGFP may lead to undesirable side-effects on cell physiology. Baens and colleagues reported that eGFP expression inhibits polyubiquitination leading to an enhanced stability of the tumor suppressor protein p53 (Baens et al., 2006). In contrast, I did not observe any effects in our system and monitored equal behavior of the different fluorochromes in all control experiments.

Moreover, I frequently monitored unspecific expression of the inducible colours, eGFP and T-Sapphire, which would indicate a leakiness of the system. No leakiness was found in this system neither in cell line cells nor in PDX cells and expression levels of both inducible colours stayed far below 1 % without tamoxifen treatment.

In addition, I controlled for constant levels of CreER^{T2} expression throughout the experiment. The presence of the CreER^{T2} enzyme at any time is an important requirement to prove the functionality of the system. As the Cre Recombinase expression level was directly correlating with the expression of mCherry, the enzyme stability was conveniently monitored by flow cytometry.

To avoid off-target CreER^{T2} activity, which might cause toxicity in the cells, the construct containing CreER^{T2} was inserted with single integrations in the genome due to transduction rates under 10 %. A single integration in contrast to multiple integrations enables the lowest expression level of a gene inserted in the genome of the target cell (Charrier et al., 2011; Christodoulou et al., 2016; Cooper et al., 2011). As PDX cells were difficult to transduce, transduction rates were far below 10 % and ensured single integrations of the CreER^{T2} construct. Therefore, the first virus was titrated onto cell line cells to simulate the approach in PDX cells. In literature, several groups describe a Cre toxicity due to its non-specific endonuclease activity. Loonstra and colleagues claim a careful titration of the Cre Recombinase, as the toxicity is dependent on the level of active Cre (Loonstra et al., 2001). In our system, we detected the CreER^{T2} toxicity upon tamoxifen activation correlating with an increase in absolute apoptosis of over 20 % at day 7. Afterwards, cell apoptosis decreased again and levels were similar as found for non-treated control cells (~ 5 %).

With this system, I successfully showed a strong growth reduction upon MLL/AF4 knock-down in SEM cell line cells *in vitro*. This proved the efficiency of the inducible competitive system as well as the importance of MLL/AF4 for survival and growth of the leukemia cells. Moreover, I observed highly similar expression of the two inducible colours, eGFP and T-Sapphire. Both inducible colours, eGFP and T-Sapphire, originally come from the same donor organism *Aequorea victoria* and sequences are very similar (Day and Davidson, 2009; Snapp, 2009). Therefore, we had hypothesized that both inducible fluorochromes should have a highly similar expression kinetic and show equal flipping kinetics in the target cells.

By applying the system to PDX cells *in vivo*, I could not observe a clear phenotype after inducible knock-down of MLL/AF4, as seen in SEM cell line cells. I found an equal distribution of the two competing cell populations expressing the constitutive fluorochromes, mtagBFP and iRFP, without treatment. The system was induced by tamoxifen administration and both inducible colours, eGFP and T-Sapphire, were expressed at similar rates. Flipping rates were rather low and showed values around 13 %, which might be one reason for not leading to an effect on the growth behavior upon MLL/AF4 knock-down. Nevertheless, the percentage would have been enough to observe the effect of MLL/AF4 silencing. Unfortunately, this was not present, as eGFP positive cells expressing the shRNA against the translocation didn’t die and behaved exactly like the induced control cells. Altogether, no effect of the MLL/AF4 knock-down was observed in the inducible competitive system that showed equal ratios of control cells and cells with knock-down.

The data of the inducible competitive system applied to PDX cells was in contrast to the clear phenotype achieved with the constitutive competitive system in PDX cells. One reason could be that the knock-down of the constitutive competitive system in PDX cells was already present at the time point of cell injection, which might have led to a strong influence on the homing and the growth behavior already at the very beginning. In the inducible competitive system, cells were able to home before the knock-down of MLL/AF4 was induced by tamoxifen application at day 7 post cell injection. Ideally, a control mouse would need to be taken down in the constitutive competitive system at an early time point to observe the PDX cell distribution in the beginning of the experiment. This was not possible, as the cell numbers enriched by FACS restricted the number of injected PDX cells in mice.

In contrast to the inducible competitive system in PDX cells, cell line cells achieved flipping rates of over 40 % in the inducible competitive analysis, which might be an explanation for the strong phenotype visible upon MLL/AF4 knock-down in cell line cells. Another reason for the non-functionality in PDX cells might be the low transduction efficiency, which was under 1 %, leading to single integrations in the genome of the target cells. Single integrations of the FLIP construct might not be enough to successfully silence existing mRNA in the cells and to fully knock-down the MLL/AF4 protein. In cell line cells, the transduction efficiency of the FLIP construct was higher showing rates between 30 % - 50 %. An additional experiment to mimic the situation in PDX cells would be a low transduction rate leading to single integrations for both constructs in cell line cells. However, it remains unclear why the construct shows a better flipping efficiency in cell line cells than in PDX cells, where ~ 37 % off the cells remained non-induced expressing only the constitutive colour. High flipping rates in combination with higher expression of the shRNA could lead to a strong phenotype of the MLL/AF4 knock-down. Therefore, improving the lentiviral transduction efficiency is a promising approach to increase integration sites leading to a higher shRNA expression. Novel protocols for lentiviral transduction are required applying for example different media or new transduction enhancers to increase the transduction efficiency.

Another approach to increase the expression level of the shRNA is to concatamerize the shRNA expression system. Several miR30 cassettes could be cloned one after another and thereby increase the expression rate of the shRNAs even though single integrations of the vector are present in the genome (Grimm and Kay, 2007; Sharbati-Tehrani et al., 2008).

Besides, the presence of AF4/MLL could function as an oncogenic driver and compensate the knock-down of MLL/AF4 in the leukemia cells. As it remains unclear in literature, which of the two fusion proteins is the oncogenic driver, both might contribute to the initiation and maintenance of leukemia (Bursen et al., 2010; Krivtsov et al., 2008; Montes et al., 2011). However, this does not explain why leukemia cells show a strong growth disadvantage in PDX cells upon MLL/AF4 knock-down using a constitutive competitive system.

Nevertheless, the established inducible competitive system represents a novel technique and a highly valuable tool for target validation. It allows monitoring control cells and knock-down population in the same approach and directly visualizes changes

in the ratio of the competing cell populations *in vitro* and *in vivo* by fluorochrome expression, which has not been described in the literature yet.

6.5 Conclusion and Outlook

Taken together, we were able to show reliable and frequent engraftment rates for primary adult rearranged ALL samples *in vivo* in mice. Additional genetic engineering by lentiviral transduction allowed us to generate GEPDX mouse models, which are highly useful to study the leukemia disease in greater detail.
Moreover, we established an inducible competitive knock-down system combining novel techniques of miR30 based shRNA expression with differently mutated loxP sites for site-specific CreER^{T2} dependent recombination. This method enabled target validation in PDX cells *in vivo* in a cellular background, where the heterogeneity of acute leukemia and the influences of the microenvironment are present.
Silencing MLL/AF4, a potent target for tumor specific therapy, with the developed inducible competitive system, I observed a strong growth disadvantage of leukemia cells upon knock-down in cell line cells *in vitro* supporting the importance of the fusion protein for tumor cells. Additionally, I managed to perform competitive experiments in PDX cells *in vivo* applying a constitutive competitive approach, where I could prove the important role of the MLL/AF4 translocation in ALL.

In summary, MLL/AF4 provides a promising target for novel therapeutic approaches being highly tumor specific and hence avoiding side-effects in patients. It is important to improve RNA interference delivery systems to be able to apply individual shRNA therapy to acute leukemia patients.

7. Supplementary

Table 28: Engraftment of primary adult rearranged ALL samples.

	Number of engrafted samples	**In %**
all	13/15	86.68
fresh only	5/5	100
frozen only	8/10	80
t(9;22) all	8/10	80
t(9;22) fresh only	3/3	100
t(9;22) frozen only	5/7	71.43
t(4;11) all	5/5	100
t(4;11) fresh only	2/2	100
t(4;11) frozen only	3/3	100

Engraftment data of all samples.

Table 29: Inserts used in lentiviral constructs and their origin.

Insert/nucleic acid	**Donor organism**
dsRED (Discosoma species red fluorescent protein)	Discosoma species
eGFP (enhanced green fluorescent protein)	Aequorea victoria
iRFP (near infrared fluorescent protein)	Rhodopseudomonas palustris
mCherry	Discosoma species
mtagBFP (monomeric tag blue fluorescent protein)	Entacmaea quadricolor
T-Sapphire	Aequorea victoria
eFFly (enhanced firefly luciferase)	Photinus pyralis
GLuc (Gaussia luciferase)	Gaussia princeps
Cre (Cre recombinase)	Bakteriophage P1
ER^{T2} (estrogen receptor T2)	Homo sapiens
LoxP sites	Bakteriophage P1
miR30	Homo sapiens
EF1α (elongation factor 1 alpha)	Homo sapiens
SFFV (spleen focus-forming virus)	Spleen focus-forming virus

Table 30: Clinical data of pediatric ALL and adult AML patients and sample characteristics.

UPN	Subtype	Age (years)	Gender	Disease stage	Sample type	Major cytogenetic group
ALL-199	pediatric	8	f	relapse	BM	trisomy 21
ALL-265	pediatric	5	f	relapse	BM	trisomy 21
ALL-346	pediatric	1	f	relapse	unknown	normal
ALL-706	pediatric	5	f	diagnosis	BM	t(4;11)
ALL-707	pediatric	2	m	diagnosis	PB	t(4;11)
ALL-762	pediatric	1	f	diagnosis	PB	t(4;11)
ALL-763	pediatric	17	f	diagnosis	BM	t(4;11)
ALL-703	pediatric	1	f	diagnosis	BM	t(9;11)
ALL-704	pediatric	1	f	diagnosis	BM	t(9;11)
ALL-705	pediatric	1	f	diagnosis	BM	t(9;11)
AML-388	adult	57	m	diagnosis	BM	t(6;11)
AML-669	adult	49	f	relapse	PB	t(9;11)
AML-393	adult	47	f	relapse	BM	t(10;11)

The presence of chromosomal rearrangements was confirmed by both FISH and PCR analysis in most samples. Non-rearranged samples were used as controls for experiments. ALL, acute lymphoblastic leukemia; AML, acute myeloid leukemia; BM, bone marrow; PB, peripheral blood; UPN, unique patient number; f, female; m, male.

8. List of abbreviations

α-MEM	minimum essential medium α
α-TG	α-Thioglycerol
ABD	actin-binding domain
ABL	abelson murine leukemia viral oncogene homolog
AF4	ALL1 fused gene from chromosome 4
AF5q31	ALL1 fused gene from 5q31
AF6	ALL1 fused gene from chromosome 6
AF9	ALL1 fused gene from chromosome 9
AFF	AF4/FMR2 family member
ALF	AF4/LAF4/FMR2
ALL	acute lymphoblastic leukemia
AML	acute myeloid leukemia
amp	ampicillin
ASH2L	absent, small or homeotic 2 like
ATP	adenosine triphosphate
BCR	breakpoint cluster region
BD	bromodomain
BLI	bioluminescent imaging
BM	bone marrow
BSA	bovine serum albumin
°C	degree celsius
CBP	CREB binding protein
CD	cluster of differentiation
cDNA	complementary DNA
CFP	cyan fluorescent protein
cGy	ZentiGray
Cl^-	chloride
CMF-PBS	calcium and magnesium free PBS
CML	chronic myeloid leukemia
CMV	cytomegalovirus
Cre	cyclization recombination
CREB	cAMP response element-binding protein
$CreER^{T2}$	Cre recombinase estrogen receptor T2
DBD	DNA-binding domain
ddH_2O	double distilled water

DMEM	Dulbecco’s modified eagle medium
DMSO	dimethyl sulfoxide
DNA	desoxyribonucleic acid
DNMT3A	DNA methyl transferase 3A
DOT1L	disruptor of telomeric silencing 1-like
dsRED	Discosoma species red fluorescent protein
E.coli	Escherichia coli
EDTA	Ethylenediaminetetraacetic acid
EF1α	elongation factor 1 alpha
eFFly	enhanced Firefly
eGFP	enhanced green fluorescent protein
ELL	Eleven-Nineteen Lysine-rich Leukemia
ENL	eleven-nineteen leukemia
EPS15	Epidermal growth factor receptor substrate 15
EZH2	enhancer of zeste homolog 2
FACS	fluorescence-activated cell sorting
FCM	flow cytometry
FCS	fetal calf serum
floxed	flanked by loxP sites
FMR2	fragile X mental retardation 2
for	forward
FSC	forward scatter
g	gram
g	gravity
GEMM	genetically engineered mouse models
GEPDX	genetically engineered patient derived xenograft
GLuc	Gaussia luciferase
GOI	gene of interest
GRB2	growth factor receptor-bound protein 2
Gy	Gray
H	histone
H_2O	water
HAT	histone acetyltransferase
HBG	HEPES buffered glucose
HDAC	histone deacetylases
HEPES	4-(2-hydroxyethyl)-1-piperazineethanesulfonic acid
HF	high fidelity

Hsp	heat shock protein
HSPC	hematopoietic stem progenitor cells
I	isoleucin
IDH2	isocitrate dehydrogenase 2
IgG	immunoglobulin G
IL2Rγ	interleukin 2 receptor gamma
IMEM	Iscove's Modified Dulbecco's Medium
iRFP	near-infra-red fluorescent protein
ITS	insulin-transferrin-selenium
L	liter
LAF4	lymphoid nuclear protein related to AF4
LEDGF	lens epithelium derived growth factor
LIC	leukemia initiating cells
LoxP	locus of crossing [x-ing]-over of bacteriophage P1
LSD1	lysine specific demethylase 1
K	lysine
K^+	potassium
kDa	kilodalton
KMT2A	histone-lysine N-methyltransferase 2A
LB	Luria Broth
LTR	long terminal repeats
M	molar
MACS	magnetic-activated cell sorting
MBD	methyl-CpG-binding domain
MCDK	mouse cell depletion kit
Menin	multiple endocrine neoplasia
mg	milligram
Mg^{2+}	magnesium
MGP	matrix γ-carboxyglutamate protein
min	minute
miRNA	microRNA
ml	milliliter
MLL	mixed lineage leukemia
MLLT3	myeloid/lymphoid or mixed-lineage leukemia translocated to chromosome 3
mM	millimolar
Mn^{2+}	manganese

MOF	males absent on the first
MOPS	3-(N-morpholino)propanesulfonic acid
mRNA	messenger RNA
Mrp/plf3	mitogen regulated protein/proliferin 3
mtagBFP	monomeric tag blue fluorescent protein
Na^+	sodium
NEAA	non essential amino acids
NES	nuclear exporting signal
ng	nanogram
NLS	nuclear localization signal
nM	nanomolar
NOD	Non-obese diabetic
NSG	NOD scid gamma
p	protein
P-TEFb	positive transcription elongation factor b
P2A	porcine teschovirus-1 2A
PB	peripheral blood
PBE	phosphate buffered saline with EDTA
PBS	phosphate buffered saline
PCR	polymerase chain reaction
PDX	patient derived xenograft
Pen/Strep	penicillin/streptomycin
PERP	p53 apoptosis effector related to Pmp22
pH	potentia Hydrogenii
PH	pleckstrin homology
PHD	plant homeodomain
PM	patient medium
pMol	picomol
PO_4^{3-}	phosphate
Pol II	RNA polymerase II
Pri-miRNA	primary micro RNA
qRT-PCR	quantitative real-time PCR
RAC-GAP	Ras-related C3 botulinum toxin substrate guanosine triphosphatase-activating protein
RB	retinoblastoma
RBBP5	retinoblastoma-binding protein 5
rev	reverse

rev	regulator of expression of virion proteins
RISC	RNA-induced silencing complex
RNA	ribonucleic acid
RNAi	RNA interference
RNase	ribonuclease
rpm	rounds per minute
RPMI	Roswell Park Memorial Institute
RRE	Rev Response Elements
RT	room temperature
S	second
scid	severe combined immune deficiency
SEC	super elongation complex
SET	[Su(var)3-9, Enhancer-of-zeste and Trithorax]
SFFV	spleen focus-forming virus
shRNA	short-hairpin RNA
SIAH	seven in absentia homologues
siRNA	small-interfering RNA
SSC	side scatter
T	threonin
T2A	thoseaasigna virus 2A
TAE	tris-acetate-EDTA
Taspase1	threonine aspartase1
TET1	ten-eleven translocation 1
TKI	tyrosine kinase inhibitors
TP53	tumor suppressor 53
TRX	trithorax
TUM	Technische Universität München
µl	microliter
µM	micromolar
VSMA	vascular smooth muscle α–actin
VSV-G	vesicular stomatitis virus G
WHO	World Health Organization
wt	wild type
w/v	weight per volume
YEATS	YNK7, ENL, AF9 and TFIIF small subunit

9. List of figures

10. List of tables

11. References

Abukhdeir, A.M., Vitolo, M.I., Argani, P., De Marzo, A.M., Karakas, B., Konishi, H., Gustin, J.P., Lauring, J., Garay, J.P., Pendleton, C.*, et al.* (2008). Tamoxifen-stimulated growth of breast cancer due to p21 loss. Proceedings of the National Academy of Sciences of the United States of America *105*, 288-293.

Agliano, A., Martin-Padura, I., Mancuso, P., Marighetti, P., Rabascio, C., Pruneri, G., Shultz, L.D., and Bertolini, F. (2008). Human acute leukemia cells injected in NOD/LtSz-scid/IL-2Rgamma null mice generate a faster and more efficient disease compared to other NOD/scid-related strains. International journal of cancer *123*, 2222-2227.

Aigner, A. (2006). Delivery systems for the direct application of siRNAs to induce RNA interference (RNAi) in vivo. Journal of biomedicine & biotechnology *2006*, 71659.

Amin, H.M., Yang, Y., Shen, Y., Estey, E.H., Giles, F.J., Pierce, S.A., Kantarjian, H.M., O'Brien, S.M., Jilani, I., and Albitar, M. (2005). Having a higher blast percentage in circulation than bone marrow: clinical implications in myelodysplastic syndrome and acute lymphoid and myeloid leukemias. Leukemia *19*, 1567-1572.

Andre, M.C., Erbacher, A., Gille, C., Schmauke, V., Goecke, B., Hohberger, A., Mang, P., Wilhelm, A., Mueller, I., Herr, W.*, et al.* (2010). Long-term human CD34+ stem cell-engrafted nonobese diabetic/SCID/IL-2R gamma(null) mice show impaired CD8+ T cell maintenance and a functional arrest of immature NK cells. Journal of immunology (Baltimore, Md : 1950) *185*, 2710-2720.

Anglin, J.L., and Song, Y. (2013). A medicinal chemistry perspective for targeting histone H3 lysine-79 methyltransferase DOT1L. Journal of medicinal chemistry *56*, 8972-8983.

Arber, D.A., Orazi, A., Hasserjian, R., Thiele, J., Borowitz, M.J., Le Beau, M.M., Bloomfield, C.D., Cazzola, M., and Vardiman, J.W. (2016). The 2016 revision to the World Health Organization classification of myeloid neoplasms and acute leukemia. Blood *127*, 2391-2405.

Attardi, L.D., Reczek, E.E., Cosmas, C., Demicco, E.G., McCurrach, M.E., Lowe, S.W., and Jacks, T. (2000). PERP, an apoptosis-associated target of p53, is a novel member of the PMP-22/gas3 family. Genes & development *14*, 704-718.

Baens, M., Noels, H., Broeckx, V., Hagens, S., Fevery, S., Billiau, A.D., Vankelecom, H., and Marynen, P. (2006). The dark side of EGFP: defective polyubiquitination. PloS one *1*, e54.

Baersch, G., Mollers, T., Hotte, A., Dockhorn-Dworniczak, B., Rube, C., Ritter, J., Jurgens, H., and Vormoor, J. (1997). Good engraftment of B-cell precursor ALL in NOD-SCID mice. Klinische Padiatrie *209*, 178-185.

Baker, A., Gregory, G.P., Verbrugge, I., Kats, L., Hilton, J.J., Vidacs, E., Lee, E.M., Lock, R.B., Zuber, J., Shortt, J.*, et al.* (2016). The CDK9 Inhibitor Dinaciclib Exerts Potent Apoptotic and Antitumor Effects in Preclinical Models of MLL-Rearranged Acute Myeloid Leukemia. Cancer research *76*, 1158-1169.

Ballabio, E., and Milne, T.A. (2012). Molecular and Epigenetic Mechanisms of MLL in Human Leukemogenesis. Cancers *4*, 904-944.

Barrett, D.M., Seif, A.E., Carpenito, C., Teachey, D.T., Fish, J.D., June, C.H., Grupp, S.A., and Reid, G.S. (2011). Noninvasive bioluminescent imaging of primary patient acute lymphoblastic leukemia: a strategy for preclinical modeling. Blood *118*, e112-117.

Barth, B.M., Keasey, N.R., Wang, X., Shanmugavelandy, S.S., Rampal, R., Hricik, T., Cabot, M.C., Kester, M., Wang, H.G., Shultz, L.D.*, et al.* (2014). Engraftment of Human Primary Acute Myeloid Leukemia Defined by Integrated Genetic Profiling in NOD/SCID/IL2rgammanull Mice

for Preclinical Ceramide-Based Therapeutic Evaluation. Journal of leukemia (Los Angeles, Calif) *2*.

Bassan, R., and Hoelzer, D. (2011). Modern therapy of acute lymphoblastic leukemia. Journal of clinical oncology : official journal of the American Society of Clinical Oncology *29*, 532-543.

Baylin, S.B., and Jones, P.A. (2011). A decade of exploring the cancer epigenome - biological and translational implications. Nature reviews Cancer *11*, 726-734.

Behm, F.G., Raimondi, S.C., Frestedt, J.L., Liu, Q., Crist, W.M., Downing, J.R., Rivera, G.K., Kersey, J.H., and Pui, C.H. (1996). Rearrangement of the MLL gene confers a poor prognosis in childhood acute lymphoblastic leukemia, regardless of presenting age. Blood *87*, 2870-2877.

Benedikt, A., Baltruschat, S., Scholz, B., Bursen, A., Arrey, T.N., Meyer, B., Varagnolo, L., Muller, A.M., Karas, M., Dingermann, T.*, et al.* (2011). The leukemogenic AF4-MLL fusion protein causes P-TEFb kinase activation and altered epigenetic signatures. Leukemia *25*, 135-144.

Bensaid, M., Melko, M., Bechara, E.G., Davidovic, L., Berretta, A., Catania, M.V., Gecz, J., Lalli, E., and Bardoni, B. (2009). FRAXE-associated mental retardation protein (FMR2) is an RNA-binding protein with high affinity for G-quartet RNA forming structure. Nucleic acids research *37*, 1269-1279.

Bitoun, E., and Davies, K.E. (2005). The robotic mouse: unravelling the function of AF4 in the cerebellum. Cerebellum (London, England) *4*, 250-260.

Bitoun, E., Oliver, P.L., and Davies, K.E. (2007). The mixed-lineage leukemia fusion partner AF4 stimulates RNA polymerase II transcriptional elongation and mediates coordinated chromatin remodeling. Human molecular genetics *16*, 92-106.

Bjorkholm, M., Derolf, A.R., Hultcrantz, M., Kristinsson, S.Y., Ekstrand, C., Goldin, L.R., Andreasson, B., Birgegard, G., Linder, O., Malm, C.*, et al.* (2011). Treatment-related risk factors for transformation to acute myeloid leukemia and myelodysplastic syndromes in myeloproliferative neoplasms. Journal of clinical oncology : official journal of the American Society of Clinical Oncology *29*, 2410-2415.

Bomken, S., Buechler, L., Rehe, K., Ponthan, F., Elder, A., Blair, H., Bacon, C.M., Vormoor, J., and Heidenreich, O. (2013). Lentiviral marking of patient-derived acute lymphoblastic leukaemic cells allows in vivo tracking of disease progression. Leukemia *27*, 718-721.

Bonnet, D. (2008). In vivo evaluation of leukemic stem cells through the xenotransplantation model. Current protocols in stem cell biology *Chapter 3*, Unit 3.2.

Borkhardt, A., and Heidenreich, O. (2004). RNA interference as a potential tool in the treatment of leukaemia. Expert opinion on biological therapy *4*, 1921-1929.

Bousquet, M., Zhuang, G., Meng, C., Ying, W., Cheruku, P.S., Shie, A.T., Wang, S., Ge, G., Wong, P., Wang, G.*, et al.* (2013). miR-150 blocks MLL-AF9-associated leukemia through oncogene repression. Molecular cancer research : MCR *11*, 912-922.

Broeker, P.L., Super, H.G., Thirman, M.J., Pomykala, H., Yonebayashi, Y., Tanabe, S., Zeleznik-Le, N., and Rowley, J.D. (1996). Distribution of 11q23 breakpoints within the MLL breakpoint cluster region in de novo acute leukemia and in treatment-related acute myeloid leukemia: correlation with scaffold attachment regions and topoisomerase II consensus binding sites. Blood *87*, 1912-1922.

Brummelkamp, T.R., Bernards, R., and Agami, R. (2002). A system for stable expression of short interfering RNAs in mammalian cells. Science (New York, NY) *296*, 550-553.

Burke, M.J., and Bhatla, T. (2014). Epigenetic modifications in pediatric acute lymphoblastic leukemia. Frontiers in pediatrics *2*, 42.

Bursen, A., Moritz, S., Gaussmann, A., Moritz, S., Dingermann, T., and Marschalek, R. (2004). Interaction of AF4 wild-type and AF4.MLL fusion protein with SIAH proteins: indication for t(4;11) pathobiology? Oncogene *23*, 6237-6249.

Bursen, A., Schwabe, K., Ruster, B., Henschler, R., Ruthardt, M., Dingermann, T., and Marschalek, R. (2010). The AF4.MLL fusion protein is capable of inducing ALL in mice without requirement of MLL.AF4. Blood *115*, 3570-3579.

Byrne, M., Wray, J., Reinert, B., Wu, Y., Nickoloff, J., Lee, S.H., Hromas, R., and Williamson, E. (2014). Mechanisms of oncogenic chromosomal translocations. Annals of the New York Academy of Sciences *1310*, 89-97.

Cao, H., Jiang, X., Chai, C., and Chew, S.Y. (2010). RNA interference by nanofiber-based siRNA delivery system. Journal of controlled release : official journal of the Controlled Release Society *144*, 203-212.

Castro Alves, C., Terziyska, N., Grunert, M., Gundisch, S., Graubner, U., Quintanilla-Martinez, L., and Jeremias, I. (2012). Leukemia-initiating cells of patient-derived acute lymphoblastic leukemia xenografts are sensitive toward TRAIL. Blood *119*, 4224-4227.

Chang, K., Marran, K., Valentine, A., and Hannon, G.J. (2013). Creating an miR30-based shRNA vector. Cold Spring Harbor protocols *2013*, 631-635.

Charrier, S., Ferrand, M., Zerbato, M., Precigout, G., Viornery, A., Bucher-Laurent, S., Benkhelifa-Ziyyat, S., Merten, O.W., Perea, J., and Galy, A. (2011). Quantification of lentiviral vector copy numbers in individual hematopoietic colony-forming cells shows vector dose-dependent effects on the frequency and level of transduction. Gene therapy *18*, 479-487.

Chaturvedi, A., Araujo Cruz, M.M., Jyotsana, N., Sharma, A., Yun, H., Gorlich, K., Wichmann, M., Schwarzer, A., Preller, M., Thol, F.*, et al.* (2013). Mutant IDH1 promotes leukemogenesis in vivo and can be specifically targeted in human AML. Blood *122*, 2877-2887.

Chen, C.S., Hilden, J.M., Frestedt, J., Domer, P.H., Moore, R., Korsmeyer, S.J., and Kersey, J.H. (1993). The chromosome 4q21 gene (AF-4/FEL) is widely expressed in normal tissues and shows breakpoint diversity in t(4;11)(q21;q23) acute leukemia. Blood *82*, 1080-1085.

Chen, W., Li, Q., Hudson, W.A., Kumar, A., Kirchhof, N., and Kersey, J.H. (2006). A murine Mll-AF4 knock-in model results in lymphoid and myeloid deregulation and hematologic malignancy. Blood *108*, 669-677.

Chen, Y., Jie, W., Yan, W., Zhou, K., and Xiao, Y. (2012). Lysine-specific histone demethylase 1 (LSD1): A potential molecular target for tumor therapy. Critical reviews in eukaryotic gene expression *22*, 53-59.

Chono, H., Goto, Y., Yamakawa, S., Tanaka, S., Tosaka, Y., Nukaya, I., and Mineno, J. (2011). Optimization of lentiviral vector transduction into peripheral blood mononuclear cells in combination with the fibronectin fragment CH-296 stimulation. Journal of biochemistry *149*, 285-292.

Christman, J.K. (2002). 5-Azacytidine and 5-aza-2'-deoxycytidine as inhibitors of DNA methylation: mechanistic studies and their implications for cancer therapy. Oncogene *21*, 5483-5495.

Christodoulou, I., Patsali, P., Stephanou, C., Antoniou, M., Kleanthous, M., and Lederer, C.W. (2016). Measurement of lentiviral vector titre and copy number by cross-species duplex quantitative PCR. Gene therapy *23*, 113-118.

Cogan, J.G., Subramanian, S.V., Polikandriotis, J.A., Kelm, R.J., Jr., and Strauch, A.R. (2002). Vascular smooth muscle alpha-actin gene transcription during myofibroblast differentiation requires Sp1/3 protein binding proximal to the MCAT enhancer. The Journal of biological chemistry *277*, 36433-36442.

Cooper, A.R., Patel, S., Senadheera, S., Plath, K., Kohn, D.B., and Hollis, R.P. (2011). Highly efficient large-scale lentiviral vector concentration by tandem tangential flow filtration. Journal of virological methods *177*, 1-9.

Cruickshank, M.N., Ford, J., Cheung, L.C., Heng, J., Singh, S., Wells, J., Failes, T.W., Arndt, G.M., Smithers, N., Prinjha, R.K.*, et al.* (2017). Systematic chemical and molecular profiling of MLL-rearranged infant acute lymphoblastic leukemia reveals efficacy of romidepsin. Leukemia *31*, 40-50.

Cullen, B.R. (2004). Transcription and processing of human microRNA precursors. Molecular cell *16*, 861-865.

Cullen, B.R. (2005). RNAi the natural way. Nature genetics *37*, 1163-1165.

Davis, H.E., Morgan, J.R., and Yarmush, M.L. (2002). Polybrene increases retrovirus gene transfer efficiency by enhancing receptor-independent virus adsorption on target cell membranes. Biophysical chemistry *97*, 159-172.

Davis, H.E., Rosinski, M., Morgan, J.R., and Yarmush, M.L. (2004). Charged polymers modulate retrovirus transduction via membrane charge neutralization and virus aggregation. Biophysical journal *86*, 1234-1242.

Dawson, M.A., Kouzarides, T., and Huntly, B.J. (2012). Targeting epigenetic readers in cancer. The New England journal of medicine *367*, 647-657.

Day, R.N., and Davidson, M.W. (2009). The fluorescent protein palette: tools for cellular imaging. Chemical Society reviews *38*, 2887-2921.

De Braekeleer, M., Morel, F., Le Bris, M.J., Herry, A., and Douet-Guilbert, N. (2005). The MLL gene and translocations involving chromosomal band 11q23 in acute leukemia. Anticancer research *25*, 1931-1944.

Denning, W., Das, S., Guo, S., Xu, J., Kappes, J.C., and Hel, Z. (2013). Optimization of the transductional efficiency of lentiviral vectors: effect of sera and polycations. Molecular biotechnology *53*, 308-314.

Dickins, R.A., Hemann, M.T., Zilfou, J.T., Simpson, D.R., Ibarra, I., Hannon, G.J., and Lowe, S.W. (2005). Probing tumor phenotypes using stable and regulated synthetic microRNA precursors. Nature genetics *37*, 1289-1295.

Dimartino, J.F., and Cleary, M.L. (1999). Mll rearrangements in haematological malignancies: lessons from clinical and biological studies. British journal of haematology *106*, 614-626.

Dohner, K., Paschka, P., and Dohner, H. (2015). [Acute myeloid leukemia]. Der Internist *56*, 354-363.

Dou, Y., Milne, T.A., Tackett, A.J., Smith, E.R., Fukuda, A., Wysocka, J., Allis, C.D., Chait, B.T., Hess, J.L., and Roeder, R.G. (2005). Physical association and coordinate function of the H3 K4 methyltransferase MLL1 and the H4 K16 acetyltransferase MOF. Cell *121*, 873-885.

Du, Q., Luu, P.L., Stirzaker, C., and Clark, S.J. (2015). Methyl-CpG-binding domain proteins: readers of the epigenome. Epigenomics *7*, 1051-1073.

Dull, T., Zufferey, R., Kelly, M., Mandel, R.J., Nguyen, M., Trono, D., and Naldini, L. (1998). A third-generation lentivirus vector with a conditional packaging system. Journal of virology *72*, 8463-8471.

Ebinger, S., Ozdemir, E.Z., Ziegenhain, C., Tiedt, S., Castro Alves, C., Grunert, M., Dworzak, M., Lutz, C., Turati, V.A., Enver, T.*, et al.* (2016). Characterization of Rare, Dormant, and Therapy-Resistant Cells in Acute Lymphoblastic Leukemia. Cancer cell *30*, 849-862.

Elbashir, S.M., Harborth, J., Lendeckel, W., Yalcin, A., Weber, K., and Tuschl, T. (2001). Duplexes of 21-nucleotide RNAs mediate RNA interference in cultured mammalian cells. Nature *411*, 494-498.

Esparza, S.D., and Sakamoto, K.M. (2005). Topics in pediatric leukemia--acute lymphoblastic leukemia. MedGenMed : Medscape general medicine *7*, 23.

Estey, E.H. (2014). Acute myeloid leukemia: 2014 update on risk-stratification and management. American journal of hematology *89*, 1063-1081.

Fedorov, Y., Anderson, E.M., Birmingham, A., Reynolds, A., Karpilow, J., Robinson, K., Leake, D., Marshall, W.S., and Khvorova, A. (2006). Off-target effects by siRNA can induce toxic phenotype. RNA (New York, NY) *12*, 1188-1196.

Feil, R., Wagner, J., Metzger, D., and Chambon, P. (1997). Regulation of Cre recombinase activity by mutated estrogen receptor ligand-binding domains. Biochemical and biophysical research communications *237*, 752-757.

Feil, S., Valtcheva, N., and Feil, R. (2009). Inducible Cre mice. Methods in molecular biology (Clifton, NJ) *530*, 343-363.

Felix, C.A., Hosler, M.R., Slater, D.J., Parker, R.I., Masterson, M., Whitlock, J.A., Rebbeck, T.R., Nowell, P.C., and Lange, B.J. (1998). MLL genomic breakpoint distribution within the breakpoint cluster region in de novo leukemia in children. Journal of pediatric hematology/oncology *20*, 299-308.

Fellmann, C., Hoffmann, T., Sridhar, V., Hopfgartner, B., Muhar, M., Roth, M., Lai, D.Y., Barbosa, I.A., Kwon, J.S., Guan, Y.*, et al.* (2013). An optimized microRNA backbone for effective single-copy RNAi. Cell reports *5*, 1704-1713.

Fellmann, C., Zuber, J., McJunkin, K., Chang, K., Malone, C.D., Dickins, R.A., Xu, Q., Hengartner, M.O., Elledge, S.J., Hannon, G.J.*, et al.* (2011). Functional identification of optimized RNAi triggers using a massively parallel sensor assay. Molecular cell *41*, 733-746.

Feng, Z., Yao, Y., Zhou, C., Chen, F., Wu, F., Wei, L., Liu, W., Dong, S., Redell, M., Mo, Q.*, et al.* (2016). Pharmacological inhibition of LSD1 for the treatment of MLL-rearranged leukemia. Journal of hematology & oncology *9*, 24.

Fire, A., Xu, S., Montgomery, M.K., Kostas, S.A., Driver, S.E., and Mello, C.C. (1998). Potent and specific genetic interference by double-stranded RNA in Caenorhabditis elegans. Nature *391*, 806-811.

Fisher, B., Costantino, J.P., Wickerham, D.L., Redmond, C.K., Kavanah, M., Cronin, W.M., Vogel, V., Robidoux, A., Dimitrov, N., Atkins, J.*, et al.* (1998). Tamoxifen for prevention of breast cancer: report of the National Surgical Adjuvant Breast and Bowel Project P-1 Study. Journal of the National Cancer Institute *90*, 1371-1388.

Fiskus, W., Sharma, S., Shah, B., Portier, B.P., Devaraj, S.G., Liu, K., Iyer, S.P., Bearss, D., and Bhalla, K.N. (2014). Highly effective combination of LSD1 (KDM1A) antagonist and pan-histone deacetylase inhibitor against human AML cells. Leukemia *28*, 2155-2164.

Forneris, F., Binda, C., Dall'Aglio, A., Fraaije, M.W., Battaglioli, E., and Mattevi, A. (2006). A highly specific mechanism of histone H3-K4 recognition by histone demethylase LSD1. The Journal of biological chemistry *281*, 35289-35295.

Frohling, S., and Dohner, H. (2008). Chromosomal abnormalities in cancer. The New England journal of medicine *359*, 722-734.

Gallipoli, P., Giotopoulos, G., and Huntly, B.J. (2015). Epigenetic regulators as promising therapeutic targets in acute myeloid leukemia. Therapeutic advances in hematology *6*, 103-119.

Garcia-Alai, M.M., Allen, M.D., Joerger, A.C., and Bycroft, M. (2010). The structure of the FYR domain of transforming growth factor beta regulator 1. Protein science : a publication of the Protein Society *19*, 1432-1438.

Gaussmann, A., Wenger, T., Eberle, I., Bursen, A., Bracharz, S., Herr, I., Dingermann, T., and Marschalek, R. (2007). Combined effects of the two reciprocal t(4;11) fusion proteins MLL.AF4 and AF4.MLL confer resistance to apoptosis, cell cycling capacity and growth transformation. Oncogene *26*, 3352-3363.

Gillet, J.P., Calcagno, A.M., Varma, S., Marino, M., Green, L.J., Vora, M.I., Patel, C., Orina, J.N., Eliseeva, T.A., Singal, V.*, et al.* (2011). Redefining the relevance of established cancer cell lines to the study of mechanisms of clinical anti-cancer drug resistance. Proceedings of the National Academy of Sciences of the United States of America *108*, 18708-18713.

Gilliland, D.G., and Griffin, J.D. (2002). Role of FLT3 in leukemia. Current opinion in hematology *9*, 274-281.

Gopalakrishnapillai, A., Kolb, E.A., Dhanan, P., Bojja, A.S., Mason, R.W., Corao, D., and Barwe, S.P. (2016). Generation of Pediatric Leukemia Xenograft Models in NSG-B2m Mice: Comparison with NOD/SCID Mice. Frontiers in oncology *6*, 162.

Greaves, M.F., and Wiemels, J. (2003). Origins of chromosome translocations in childhood leukaemia. Nature reviews Cancer *3*, 639-649.

Grembecka, J., He, S., Shi, A., Purohit, T., Muntean, A.G., Sorenson, R.J., Showalter, H.D., Murai, M.J., Belcher, A.M., Hartley, T.*, et al.* (2012). Menin-MLL inhibitors reverse oncogenic activity of MLL fusion proteins in leukemia. Nature chemical biology *8*, 277-284.

Grimm, D., and Kay, M.A. (2007). Combinatorial RNAi: a winning strategy for the race against evolving targets? Molecular therapy : the journal of the American Society of Gene Therapy *15*, 878-888.

Haberland, J., and Wolf, U. (2015). Trendanalysen zur Inzidenz und Mortalität an Krebs in Deutschland seit 1970 - Trends of cancer related incidence and mortality in Germany since 1970 (Epidemiologie und Gesundheitsberichterstattung).

Hans, S., Kaslin, J., Freudenreich, D., and Brand, M. (2009). Temporally-controlled site-specific recombination in zebrafish. PloS one *4*, e4640.

Hansen, J.C. (2012). Human mitotic chromosome structure: what happened to the 30-nm fibre? The EMBO journal *31*, 1621-1623.

Harris, W.J., Huang, X., Lynch, J.T., Spencer, G.J., Hitchin, J.R., Li, Y., Ciceri, F., Blaser, J.G., Greystoke, B.F., Jordan, A.M.*, et al.* (2012). The histone demethylase KDM1A sustains the oncogenic potential of MLL-AF9 leukemia stem cells. Cancer cell *21*, 473-487.

Hauer, J., Borkhardt, A., Sanchez-Garcia, I., and Cobaleda, C. (2014). Genetically engineered mouse models of human B-cell precursor leukemias. Cell cycle (Georgetown, Tex) *13*, 2836-2846.

He, S., Malik, B., Borkin, D., Miao, H., Shukla, S., Kempinska, K., Purohit, T., Wang, J., Chen, L., Parkin, B.*, et al.* (2016). Menin-MLL inhibitors block oncogenic transformation by MLL-fusion proteins in a fusion partner-independent manner. Leukemia *30*, 508-513.

He, W., Bennett, M.J., Luistro, L., Carvajal, D., Nevins, T., Smith, M., Tyagi, G., Cai, J., Wei, X., Lin, T.A.*, et al.* (2014). Discovery of siRNA lipid nanoparticles to transfect suspension leukemia cells and provide in vivo delivery capability. Molecular therapy : the journal of the American Society of Gene Therapy *22*, 359-370.

Heckl, B.C., Carlet, M., Vick, B., Roolf, C., Alsadeq, A., Grunert, M., Liu, W.H., Liebl, A., Hiddemann, W., Marschalek, R.*, et al.* (2018). Frequent and reliable engraftment of certain adult primary acute lymphoblastic leukemias in mice. Leukemia & lymphoma, 1-4.

Herrmann, H., Blatt, K., Shi, J., Gleixner, K.V., Cerny-Reiterer, S., Mullauer, L., Vakoc, C.R., Sperr, W.R., Horny, H.P., Bradner, J.E.*, et al.* (2012). Small-molecule inhibition of BRD4 as a new potent approach to eliminate leukemic stem- and progenitor cells in acute myeloid leukemia AML. Oncotarget *3*, 1588-1599.

Hilden, J.M., Dinndorf, P.A., Meerbaum, S.O., Sather, H., Villaluna, D., Heerema, N.A., McGlennen, R., Smith, F.O., Woods, W.G., Salzer, W.L.*, et al.* (2006). Analysis of prognostic factors of acute lymphoblastic leukemia in infants: report on CCG 1953 from the Children's Oncology Group. Blood *108*, 441-451.

Hsieh, J.J., Cheng, E.H., and Korsmeyer, S.J. (2003a). Taspase1: a threonine aspartase required for cleavage of MLL and proper HOX gene expression. Cell *115*, 293-303.

Hsieh, J.J., Ernst, P., Erdjument-Bromage, H., Tempst, P., and Korsmeyer, S.J. (2003b). Proteolytic cleavage of MLL generates a complex of N- and C-terminal fragments that confers protein stability and subnuclear localization. Molecular and cellular biology *23*, 186-194.

Hutter, G., Nickenig, C., Garritsen, H., Hellenkamp, F., Hoerning, A., Hiddemann, W., and Dreyling, M. (2004). Use of polymorphisms in the noncoding region of the human mitochondrial genome to identify potential contamination of human leukemia-lymphoma cell lines. The hematology journal : the official journal of the European Haematology Association *5*, 61-68.

Inaba, H., Greaves, M., and Mullighan, C.G. (2013). Acute lymphoblastic leukaemia. Lancet (London, England) *381*, 1943-1955.

Indra, A.K., Warot, X., Brocard, J., Bornert, J.M., Xiao, J.H., Chambon, P., and Metzger, D. (1999). Temporally-controlled site-specific mutagenesis in the basal layer of the epidermis: comparison of the recombinase activity of the tamoxifen-inducible Cre-ER(T) and Cre-ER(T2) recombinases. Nucleic acids research *27*, 4324-4327.

Isaacs, A.M., Oliver, P.L., Jones, E.L., Jeans, A., Potter, A., Hovik, B.H., Nolan, P.M., Vizor, L., Glenister, P., Simon, A.K.*, et al.* (2003). A mutation in Af4 is predicted to cause cerebellar ataxia and cataracts in the robotic mouse. The Journal of neuroscience : the official journal of the Society for Neuroscience *23*, 1631-1637.

Isnard, P., Core, N., Naquet, P., and Djabali, M. (2000). Altered lymphoid development in mice deficient for the mAF4 proto-oncogene. Blood *96*, 705-710.

Ito, M., Hiramatsu, H., Kobayashi, K., Suzue, K., Kawahata, M., Hioki, K., Ueyama, Y., Koyanagi, Y., Sugamura, K., Tsuji, K.*, et al.* (2002). NOD/SCID/gamma(c)(null) mouse: an excellent recipient mouse model for engraftment of human cells. Blood *100*, 3175-3182.

Jackson, A.L., and Linsley, P.S. (2010). Recognizing and avoiding siRNA off-target effects for target identification and therapeutic application. Nature reviews Drug discovery *9*, 57-67.

Jacoby, E., Chien, C.D., and Fry, T.J. (2014). Murine models of acute leukemia: important tools in current pediatric leukemia research. Frontiers in oncology *4*, 95.

Jones, L., Richmond, J., Evans, K., Carol, H., Jing, D., Kurmasheva, R.T., Billups, C.A., Houghton, P.J., Smith, M.A., and Lock, R.B. (2017). Bioluminescence Imaging Enhances Analysis of Drug Responses in a Patient-Derived Xenograft Model of Pediatric ALL. Clinical cancer research : an official journal of the American Association for Cancer Research *23*, 3744-3755.

Jyotsana, N., Sharma, A., Chaturvedi, A., Scherr, M., Kuchenbauer, F., Sajti, L., Barchanski, A., Lindner, R., Noyan, F., Suhs, K.W.*, et al.* (2017). RNA interference efficiently targets human leukemia driven by a fusion oncogene in vivo. Leukemia.

Kalender Atak, Z., De Keersmaecker, K., Gianfelici, V., Geerdens, E., Vandepoel, R., Pauwels, D., Porcu, M., Lahortiga, I., Brys, V., Dirks, W.G.*, et al.* (2012). High accuracy mutation detection in leukemia on a selected panel of cancer genes. PloS one *7*, e38463.

Kamel-Reid, S., Letarte, M., Sirard, C., Doedens, M., Grunberger, T., Fulop, G., Freedman, M.H., Phillips, R.A., and Dick, J.E. (1989). A model of human acute lymphoblastic leukemia in immune-deficient SCID mice. Science (New York, NY) *246*, 1597-1600.

Krivtsov, A.V., and Armstrong, S.A. (2007). MLL translocations, histone modifications and leukaemia stem-cell development. Nature reviews Cancer *7*, 823-833.

Krivtsov, A.V., Feng, Z., Lemieux, M.E., Faber, J., Vempati, S., Sinha, A.U., Xia, X., Jesneck, J., Bracken, A.P., Silverman, L.B.*, et al.* (2008). H3K79 methylation profiles define murine and human MLL-AF4 leukemias. Cancer cell *14*, 355-368.

Krug, U., Gale, R.P., Berdel, W.E., Muller-Tidow, C., Stelljes, M., Metzeler, K., Sauerland, M.C., Hiddemann, W., and Buchner, T. (2017). Therapy of older persons with acute myeloid leukaemia. Leukemia research *60*, 1-10.

Langer, T., Metzler, M., Reinhardt, D., Viehmann, S., Borkhardt, A., Reichel, M., Stanulla, M., Schrappe, M., Creutzig, U., Ritter, J.*, et al.* (2003). Analysis of t(9;11) chromosomal breakpoint sequences in childhood acute leukemia: almost identical MLL breakpoints in therapy-related AML after treatment without etoposides. Genes, chromosomes & cancer *36*, 393-401.

Lee, Y., Jeon, K., Lee, J.T., Kim, S., and Kim, V.N. (2002). MicroRNA maturation: stepwise processing and subcellular localization. The EMBO journal *21*, 4663-4670.

Lee, Y.J., Won, T.J., Hyung, K.E., Lee, M.J., Moon, Y.H., Lee, I.H., Go, B.S., and Hwang, K.W. (2014). Bcl-2 knockdown accelerates T cell receptor-triggered activation-induced cell death in jurkat T cells. The Korean journal of physiology & pharmacology : official journal of the Korean Physiological Society and the Korean Society of Pharmacology *18*, 73-78.

Ley, T.J., Ding, L., Walter, M.J., McLellan, M.D., Lamprecht, T., Larson, D.E., Kandoth, C., Payton, J.E., Baty, J., Welch, J.*, et al.* (2010). DNMT3A mutations in acute myeloid leukemia. The New England journal of medicine *363*, 2424-2433.

Ley, T.J., Miller, C., Ding, L., Raphael, B.J., Mungall, A.J., Robertson, A., Hoadley, K., Triche, T.J., Jr., Laird, P.W., Baty, J.D.*, et al.* (2013). Genomic and epigenomic landscapes of adult de novo acute myeloid leukemia. The New England journal of medicine *368*, 2059-2074.

Li, S., Mason, C.E., and Melnick, A. (2016). Genetic and epigenetic heterogeneity in acute myeloid leukemia. Current opinion in genetics & development *36*, 100-106.

Lin, C., Smith, E.R., Takahashi, H., Lai, K.C., Martin-Brown, S., Florens, L., Washburn, M.P., Conaway, J.W., Conaway, R.C., and Shilatifard, A. (2010). AFF4, a component of the ELL/P-TEFb elongation complex and a shared subunit of MLL chimeras, can link transcription elongation to leukemia. Molecular cell *37*, 429-437.

Lin, P., Lin, Y., Lennon, D.P., Correa, D., Schluchter, M., and Caplan, A.I. (2012). Efficient lentiviral transduction of human mesenchymal stem cells that preserves proliferation and differentiation capabilities. Stem cells translational medicine *1*, 886-897.

Lock, R.B., Liem, N., Farnsworth, M.L., Milross, C.G., Xue, C., Tajbakhsh, M., Haber, M., Norris, M.D., Marshall, G.M., and Rice, A.M. (2002). The nonobese diabetic/severe combined immunodeficient (NOD/SCID) mouse model of childhood acute lymphoblastic leukemia reveals intrinsic differences in biologic characteristics at diagnosis and relapse. Blood *99*, 4100-4108.

Loonstra, A., Vooijs, M., Beverloo, H.B., Allak, B.A., van Drunen, E., Kanaar, R., Berns, A., and Jonkers, J. (2001). Growth inhibition and DNA damage induced by Cre recombinase in mammalian cells. Proceedings of the National Academy of Sciences of the United States of America *98*, 9209-9214.

Luo, Z., Lin, C., Guest, E., Garrett, A.S., Mohaghegh, N., Swanson, S., Marshall, S., Florens, L., Washburn, M.P., and Shilatifard, A. (2012). The super elongation complex family of RNA

polymerase II elongation factors: gene target specificity and transcriptional output. Molecular and cellular biology *32*, 2608-2617.

Malfuson, J.V., Etienne, A., Turlure, P., de Revel, T., Thomas, X., Contentin, N., Terre, C., Rigaudeau, S., Bordessoule, D., Vey, N.*, et al.* (2008). Risk factors and decision criteria for intensive chemotherapy in older patients with acute myeloid leukemia. Haematologica *93*, 1806-1813.

Marschalek, R. (2016). Systematic Classification of Mixed-Lineage Leukemia Fusion Partners Predicts Additional Cancer Pathways. Annals of laboratory medicine *36*, 85-100.

Marschalek, R., Nilson, I., Lochner, K., Greim, R., Siegler, G., Greil, J., Beck, J.D., and Fey, G.H. (1997). The structure of the human ALL-1/MLL/HRX gene. Leukemia & lymphoma *27*, 417-428.

Matt, T. (2002). Transcriptional control of the inflammatory response: a role for the CREB-binding protein (CBP). Acta medica Austriaca *29*, 77-79.

McMahon, K.A., Hiew, S.Y., Hadjur, S., Veiga-Fernandes, H., Menzel, U., Price, A.J., Kioussis, D., Williams, O., and Brady, H.J. (2007). Mll has a critical role in fetal and adult hematopoietic stem cell self-renewal. Cell stem cell *1*, 338-345.

Melko, M., Douguet, D., Bensaid, M., Zongaro, S., Verheggen, C., Gecz, J., and Bardoni, B. (2011). Functional characterization of the AFF (AF4/FMR2) family of RNA-binding proteins: insights into the molecular pathology of FRAXE intellectual disability. Human molecular genetics *20*, 1873-1885.

Metzeler, K.H., Herold, T., Rothenberg-Thurley, M., Amler, S., Sauerland, M.C., Gorlich, D., Schneider, S., Konstandin, N.P., Dufour, A., Braundl, K.*, et al.* (2016). Spectrum and prognostic relevance of driver gene mutations in acute myeloid leukemia. Blood *128*, 686-698.

Meyer, C., Hofmann, J., Burmeister, T., Groger, D., Park, T.S., Emerenciano, M., Pombo de Oliveira, M., Renneville, A., Villarese, P., Macintyre, E.*, et al.* (2013a). The MLL recombinome of acute leukemias in 2013. Leukemia *27*, 2165-2176.

Meyer, C., Popov, A., Plekhanova, O., Kustanovich, A., Volochnik, A., Riger, T., Demina, A., Druy, A., Fleischman, E., Sokova, O.*, et al.* (2013b). MLL genomic DNA Breakpoints In Infant Acute Leukemia. Blood *122*, 1350-1350.

Mohme, M., Maire, C.L., Riecken, K., Zapf, S., Aranyossy, T., Westphal, M., Lamszus, K., and Fehse, B. (2017). Optical Barcoding for Single-Clone Tracking to Study Tumor Heterogeneity. Molecular therapy : the journal of the American Society of Gene Therapy *25*, 621-633.

Montes, R., Ayllon, V., Gutierrez-Aranda, I., Prat, I., Hernandez-Lamas, M.C., Ponce, L., Bresolin, S., Te Kronnie, G., Greaves, M., Bueno, C.*, et al.* (2011). Enforced expression of MLL-AF4 fusion in cord blood CD34+ cells enhances the hematopoietic repopulating cell function and clonogenic potential but is not sufficient to initiate leukemia. Blood *117*, 4746-4758.

Morisot, S., Wayne, A.S., Bohana-Kashtan, O., Kaplan, I.M., Gocke, C.D., Hildreth, R., Stetler-Stevenson, M., Walker, R.L., Davis, S., Meltzer, P.S.*, et al.* (2010). High frequencies of leukemia stem cells in poor-outcome childhood precursor-B acute lymphoblastic leukemias. Leukemia *24*, 1859-1866.

Nakamura, T., Mori, T., Tada, S., Krajewski, W., Rozovskaia, T., Wassell, R., Dubois, G., Mazo, A., Croce, C.M., and Canaani, E. (2002). ALL-1 is a histone methyltransferase that assembles a supercomplex of proteins involved in transcriptional regulation. Molecular cell *10*, 1119-1128.

Naldini, L., Blomer, U., Gallay, P., Ory, D., Mulligan, R., Gage, F.H., Verma, I.M., and Trono, D. (1996). In vivo gene delivery and stable transduction of nondividing cells by a lentiviral vector. Science (New York, NY) *272*, 263-267.

Nambiar, M., Kari, V., and Raghavan, S.C. (2008). Chromosomal translocations in cancer. Biochimica et biophysica acta *1786*, 139-152.

Nennecke, A., Wienecke, A., and Kraywinkel, K. (2014). Inzidenz und Überleben bei Leukämien in Deutschland nach aktuellen standardisierten Kategorien. Bundesgesundheitsblatt - Gesundheitsforschung - Gesundheitsschutz *57*, 93-102.

Nilson, I., Lochner, K., Siegler, G., Greil, J., Beck, J.D., Fey, G.H., and Marschalek, R. (1996). Exon/intron structure of the human ALL-1 (MLL) gene involved in translocations to chromosomal region 11q23 and acute leukaemias. British journal of haematology *93*, 966-972.

Nilson, I., Reichel, M., Ennas, M.G., Greim, R., Knorr, C., Siegler, G., Greil, J., Fey, G.H., and Marschalek, R. (1997). Exon/intron structure of the human AF-4 gene, a member of the AF-4/LAF-4/FMR-2 gene family coding for a nuclear protein with structural alterations in acute leukaemia. British journal of haematology *98*, 157-169.

Notta, F., Mullighan, C.G., Wang, J.C., Poeppl, A., Doulatov, S., Phillips, L.A., Ma, J., Minden, M.D., Downing, J.R., and Dick, J.E. (2011). Evolution of human BCR-ABL1 lymphoblastic leukaemia-initiating cells. Nature *469*, 362-367.

O'Doherty, U., Swiggard, W.J., and Malim, M.H. (2000). Human immunodeficiency virus type 1 spinoculation enhances infection through virus binding. Journal of virology *74*, 10074-10080.

Oberdoerffer, P., Otipoby, K.L., Maruyama, M., and Rajewsky, K. (2003). Unidirectional Cre-mediated genetic inversion in mice using the mutant loxP pair lox66/lox71. Nucleic acids research *31*, e140.

Ogryzko, V.V., Schiltz, R.L., Russanova, V., Howard, B.H., and Nakatani, Y. (1996). The transcriptional coactivators p300 and CBP are histone acetyltransferases. Cell *87*, 953-959.

Oliver, P.L., Bitoun, E., Clark, J., Jones, E.L., and Davies, K.E. (2004). Mediation of Af4 protein function in the cerebellum by Siah proteins. Proceedings of the National Academy of Sciences of the United States of America *101*, 14901-14906.

Osborne, C.K., Zhao, H., and Fuqua, S.A. (2000). Selective estrogen receptor modulators: structure, function, and clinical use. Journal of clinical oncology : official journal of the American Society of Clinical Oncology *18*, 3172-3186.

Ottmann, O.G., and Pfeifer, H. (2009). Management of Philadelphia chromosome-positive acute lymphoblastic leukemia (Ph+ ALL). Hematology American Society of Hematology Education Program, 371-381.

Paczulla, A.M., Dirnhofer, S., Konantz, M., Medinger, M., Salih, H.R., Rothfelder, K., Tsakiris, D.A., Passweg, J.R., Lundberg, P., and Lengerke, C. (2017). Long-term observation reveals high-frequency engraftment of human acute myeloid leukemia in immunodeficient mice. Haematologica *102*, 854-864.

Paddison, P.J., Caudy, A.A., Bernstein, E., Hannon, G.J., and Conklin, D.S. (2002). Short hairpin RNAs (shRNAs) induce sequence-specific silencing in mammalian cells. Genes & development *16*, 948-958.

Patel, B., Dey, A., Castleton, A.Z., Schwab, C., Samuel, E., Sivakumaran, J., Beaton, B., Zareian, N., Zhang, C.Y., Rai, L.*, et al.* (2014). Mouse xenograft modeling of human adult acute lymphoblastic leukemia provides mechanistic insights into adult LIC biology. Blood *124*, 96-105.

Peirs, S., Van der Meulen, J., Van de Walle, I., Taghon, T., Speleman, F., Poppe, B., and Van Vlierberghe, P. (2015). Epigenetics in T-cell acute lymphoblastic leukemia. Immunological reviews *263*, 50-67.

Petitjean, A., Mathe, E., Kato, S., Ishioka, C., Tavtigian, S.V., Hainaut, P., and Olivier, M. (2007). Impact of mutant p53 functional properties on TP53 mutation patterns and tumor

phenotype: lessons from recent developments in the IARC TP53 database. Human mutation *28*, 622-629.

Picaud, S., Fedorov, O., Thanasopoulou, A., Leonards, K., Jones, K., Meier, J., Olzscha, H., Monteiro, O., Martin, S., Philpott, M.*, et al.* (2015). Generation of a Selective Small Molecule Inhibitor of the CBP/p300 Bromodomain for Leukemia Therapy. Cancer research *75*, 5106-5119.

Plass, C., Pfister, S.M., Lindroth, A.M., Bogatyrova, O., Claus, R., and Lichter, P. (2013). Mutations in regulators of the epigenome and their connections to global chromatin patterns in cancer. Nature reviews Genetics *14*, 765-780.

Pui, C.H., Carroll, W.L., Meshinchi, S., and Arceci, R.J. (2011). Biology, risk stratification, and therapy of pediatric acute leukemias: an update. Journal of clinical oncology : official journal of the American Society of Clinical Oncology *29*, 551-565.

Pui, C.H., and Evans, W.E. (2006). Treatment of acute lymphoblastic leukemia. The New England journal of medicine *354*, 166-178.

Pui, C.H., Mullighan, C.G., Evans, W.E., and Relling, M.V. (2012). Pediatric acute lymphoblastic leukemia: where are we going and how do we get there? Blood *120*, 1165-1174.

Pui, C.H., Robison, L.L., and Look, A.T. (2008). Acute lymphoblastic leukaemia. Lancet (London, England) *371*, 1030-1043.

Rabinovich, B.A., Ye, Y., Etto, T., Chen, J.Q., Levitsky, H.I., Overwijk, W.W., Cooper, L.J., Gelovani, J., and Hwu, P. (2008). Visualizing fewer than 10 mouse T cells with an enhanced firefly luciferase in immunocompetent mouse models of cancer. Proceedings of the National Academy of Sciences of the United States of America *105*, 14342-14346.

Redon, R., Ishikawa, S., Fitch, K.R., Feuk, L., Perry, G.H., Andrews, T.D., Fiegler, H., Shapero, M.H., Carson, A.R., Chen, W.*, et al.* (2006). Global variation in copy number in the human genome. Nature *444*, 444-454.

Ricks, D.M., Kutner, R., Zhang, X.Y., Welsh, D.A., and Reiser, J. (2008). Optimized lentiviral transduction of mouse bone marrow-derived mesenchymal stem cells. Stem cells and development *17*, 441-450.

Rohle, D., Popovici-Muller, J., Palaskas, N., Turcan, S., Grommes, C., Campos, C., Tsoi, J., Clark, O., Oldrini, B., Komisopoulou, E.*, et al.* (2013). An inhibitor of mutant IDH1 delays growth and promotes differentiation of glioma cells. Science (New York, NY) *340*, 626-630.

Rossler, T., and Marschalek, R. (2013). An alternative splice process renders the MLL protein either into a transcriptional activator or repressor. Die Pharmazie *68*, 601-607.

Roth, S.Y., Denu, J.M., and Allis, C.D. (2001). Histone acetyltransferases. Annual review of biochemistry *70*, 81-120.

Rothbart, S.B., and Strahl, B.D. (2014). Interpreting the language of histone and DNA modifications. Biochimica et biophysica acta *1839*, 627-643.

Schenk, T., Chen, W.C., Gollner, S., Howell, L., Jin, L., Hebestreit, K., Klein, H.U., Popescu, A.C., Burnett, A., Mills, K.*, et al.* (2012). Inhibition of the LSD1 (KDM1A) demethylase reactivates the all-trans-retinoic acid differentiation pathway in acute myeloid leukemia. Nature medicine *18*, 605-611.

Schoch, C., Schnittger, S., Klaus, M., Kern, W., Hiddemann, W., and Haferlach, T. (2003). AML with 11q23/MLL abnormalities as defined by the WHO classification: incidence, partner chromosomes, FAB subtype, age distribution, and prognostic impact in an unselected series of 1897 cytogenetically analyzed AML cases. Blood *102*, 2395-2402.

Schraets, D., Lehmann, T., Dingermann, T., and Marschalek, R. (2003). MLL-mediated transcriptional gene regulation investigated by gene expression profiling. Oncogene *22*, 3655-3668.

Selvam, C., Mutisya, D., Prakash, S., Ranganna, K., and Thilagavathi, R. (2017). Therapeutic potential of chemically modified siRNA: Recent trends. Chemical biology & drug design *90*, 665-678.

Seto, E., and Yoshida, M. (2014). Erasers of histone acetylation: the histone deacetylase enzymes. Cold Spring Harbor perspectives in biology *6*, a018713.

Shahbazian, M.D., and Grunstein, M. (2007). Functions of site-specific histone acetylation and deacetylation. Annual review of biochemistry *76*, 75-100.

Shankar, D.B., Cheng, J.C., Kinjo, K., Federman, N., Moore, T.B., Gill, A., Rao, N.P., Landaw, E.M., and Sakamoto, K.M. (2005). The role of CREB as a proto-oncogene in hematopoiesis and in acute myeloid leukemia. Cancer cell *7*, 351-362.

Sharbati-Tehrani, S., Kutz-Lohroff, B., Scholven, J., and Einspanier, R. (2008). Concatameric cloning of porcine microRNA molecules after assembly PCR. Biochemical and biophysical research communications *375*, 484-489.

Shi, Y., Lan, F., Matson, C., Mulligan, P., Whetstine, J.R., Cole, P.A., Casero, R.A., and Shi, Y. (2004). Histone demethylation mediated by the nuclear amine oxidase homolog LSD1. Cell *119*, 941-953.

Shultz, L.D., Lyons, B.L., Burzenski, L.M., Gott, B., Chen, X., Chaleff, S., Kotb, M., Gillies, S.D., King, M., Mangada, J.*, et al.* (2005). Human lymphoid and myeloid cell development in NOD/LtSz-scid IL2R gamma null mice engrafted with mobilized human hemopoietic stem cells. Journal of immunology (Baltimore, Md : 1950) *174*, 6477-6489.

Shultz, L.D., Schweitzer, P.A., Christianson, S.W., Gott, B., Schweitzer, I.B., Tennent, B., McKenna, S., Mobraaten, L., Rajan, T.V., Greiner, D.L.*, et al.* (1995). Multiple defects in innate and adaptive immunologic function in NOD/LtSz-scid mice. Journal of immunology (Baltimore, Md : 1950) *154*, 180-191.

Siegel, R.L., Miller, K.D., and Jemal, A. (2016). Cancer statistics, 2016. CA: a cancer journal for clinicians *66*, 7-30.

Siegel, R.W., Jain, R., and Bradbury, A. (2001). Using an in vivo phagemid system to identify non-compatible loxP sequences. FEBS letters *505*, 467-473.

Silva, J.M., Li, M.Z., Chang, K., Ge, W., Golding, M.C., Rickles, R.J., Siolas, D., Hu, G., Paddison, P.J., Schlabach, M.R.*, et al.* (2005). Second-generation shRNA libraries covering the mouse and human genomes. Nature genetics *37*, 1281-1288.

Singh, A., Boldin-Adamsky, S., Thimmulappa, R.K., Rath, S.K., Ashush, H., Coulter, J., Blackford, A., Goodman, S.N., Bunz, F., Watson, W.H.*, et al.* (2008). RNAi-mediated silencing of nuclear factor erythroid-2-related factor 2 gene expression in non-small cell lung cancer inhibits tumor growth and increases efficacy of chemotherapy. Cancer research *68*, 7975-7984.

Slany, R.K. (2009). The molecular biology of mixed lineage leukemia. Haematologica *94*, 984-993.

Snapp, E.L. (2009). Fluorescent proteins: a cell biologist's user guide. Trends in cell biology *19*, 649-655.

Sprussel, A., Schulte, J.H., Weber, S., Necke, M., Handschke, K., Thor, T., Pajtler, K.W., Schramm, A., Konig, K., Diehl, L.*, et al.* (2012). Lysine-specific demethylase 1 restricts hematopoietic progenitor proliferation and is essential for terminal differentiation. Leukemia *26*, 2039-2051.

Stern, P., Astrof, S., Erkeland, S.J., Schustak, J., Sharp, P.A., and Hynes, R.O. (2008). A system for Cre-regulated RNA interference in vivo. Proceedings of the National Academy of Sciences of the United States of America *105*, 13895-13900.

Sterner, D.E., and Berger, S.L. (2000). Acetylation of histones and transcription-related factors. Microbiology and molecular biology reviews : MMBR *64*, 435-459.

Stewart, C.F. (2009). Treating children with acute lymphoblastic leukemia and Down syndrome: pharmacokinetics provides insight into vincristine therapy. Pediatric blood & cancer *52*, 1-2.

Subach, O.M., Cranfill, P.J., Davidson, M.W., and Verkhusha, V.V. (2011). An enhanced monomeric blue fluorescent protein with the high chemical stability of the chromophore. PloS one *6*, e28674.

Taki, T., Ida, K., Bessho, F., Hanada, R., Kikuchi, A., Yamamoto, K., Sako, M., Tsuchida, M., Seto, M., Ueda, R.*, et al.* (1996). Frequency and clinical significance of the MLL gene rearrangements in infant acute leukemia. Leukemia *10*, 1303-1307.

Taverna, S.D., Li, H., Ruthenburg, A.J., Allis, C.D., and Patel, D.J. (2007). How chromatin-binding modules interpret histone modifications: lessons from professional pocket pickers. Nature structural & molecular biology *14*, 1025-1040.

Terziyska, N., Castro Alves, C., Groiss, V., Schneider, K., Farkasova, K., Ogris, M., Wagner, E., Ehrhardt, H., Brentjens, R.J., zur Stadt, U.*, et al.* (2012). In vivo imaging enables high resolution preclinical trials on patients' leukemia cells growing in mice. PloS one *7*, e52798.

Thol, F., Damm, F., Ludeking, A., Winschel, C., Wagner, K., Morgan, M., Yun, H., Gohring, G., Schlegelberger, B., Hoelzer, D.*, et al.* (2011). Incidence and prognostic influence of DNMT3A mutations in acute myeloid leukemia. Journal of clinical oncology : official journal of the American Society of Clinical Oncology *29*, 2889-2896.

Thomas, M., Gessner, A., Vornlocher, H.P., Hadwiger, P., Greil, J., and Heidenreich, O. (2005). Targeting MLL-AF4 with short interfering RNAs inhibits clonogenicity and engraftment of t(4;11)-positive human leukemic cells. Blood *106*, 3559-3566.

Tiemann, K., and Rossi, J.J. (2009). RNAi-based therapeutics-current status, challenges and prospects. EMBO molecular medicine *1*, 142-151.

Townsend, E.C., Murakami, M.A., Christodoulou, A., Christie, A.L., Koster, J., DeSouza, T.A., Morgan, E.A., Kallgren, S.P., Liu, H., Wu, S.C.*, et al.* (2016). The Public Repository of Xenografts Enables Discovery and Randomized Phase II-like Trials in Mice. Cancer cell *29*, 574-586.

Urano, A., Endoh, M., Wada, T., Morikawa, Y., Itoh, M., Kataoka, Y., Taki, T., Akazawa, H., Nakajima, H., Komuro, I.*, et al.* (2005). Infertility with defective spermiogenesis in mice lacking AF5q31, the target of chromosomal translocation in human infant leukemia. Molecular and cellular biology *25*, 6834-6845.

Van der Meulen, J., Van Roy, N., Van Vlierberghe, P., and Speleman, F. (2014). The epigenetic landscape of T-cell acute lymphoblastic leukemia. The international journal of biochemistry & cell biology *53*, 547-557.

Van Vlierberghe, P., Ambesi-Impiombato, A., Perez-Garcia, A., Haydu, J.E., Rigo, I., Hadler, M., Tosello, V., Della Gatta, G., Paietta, E., Racevskis, J.*, et al.* (2011). ETV6 mutations in early immature human T cell leukemias. The Journal of experimental medicine *208*, 2571-2579.

Ventura, A., Meissner, A., Dillon, C.P., McManus, M., Sharp, P.A., Van Parijs, L., Jaenisch, R., and Jacks, T. (2004). Cre-lox-regulated conditional RNA interference from transgenes. Proceedings of the National Academy of Sciences of the United States of America *101*, 10380-10385.

Vick, B., Rothenberg, M., Sandhofer, N., Carlet, M., Finkenzeller, C., Krupka, C., Grunert, M., Trumpp, A., Corbacioglu, S., Ebinger, M.*, et al.* (2015). An advanced preclinical mouse model for acute myeloid leukemia using patients' cells of various genetic subgroups and in vivo bioluminescence imaging. PloS one *10*, e0120925.

Walrath, J.C., Hawes, J.J., Van Dyke, T., and Reilly, K.M. (2010). Genetically engineered mouse models in cancer research. Advances in cancer research *106*, 113-164.

Wang, J., Lu, Z., Wientjes, M.G., and Au, J.L. (2010). Delivery of siRNA therapeutics: barriers and carriers. The AAPS journal *12*, 492-503.

Winters, A.C., and Bernt, K.M. (2017). MLL-Rearranged Leukemias-An Update on Science and Clinical Approaches. Frontiers in pediatrics *5*, 4.

Wiznerowicz, M., Szulc, J., and Trono, D. (2006). Tuning silence: conditional systems for RNA interference. Nature methods *3*, 682-688.

Woiterski, J., Ebinger, M., Witte, K.E., Goecke, B., Heininger, V., Philippek, M., Bonin, M., Schrauder, A., Rottgers, S., Herr, W.*, et al.* (2013). Engraftment of low numbers of pediatric acute lymphoid and myeloid leukemias into NOD/SCID/IL2Rcgammanull mice reflects individual leukemogenecity and highly correlates with clinical outcome. International journal of cancer *133*, 1547-1556.

Woods, B.A., and Levine, R.L. (2015). The role of mutations in epigenetic regulators in myeloid malignancies. Immunological reviews *263*, 22-35.

Xia, Z.B., Anderson, M., Diaz, M.O., and Zeleznik-Le, N.J. (2003). MLL repression domain interacts with histone deacetylases, the polycomb group proteins HPC2 and BMI-1, and the corepressor C-terminal-binding protein. Proceedings of the National Academy of Sciences of the United States of America *100*, 8342-8347.

Xu, J., Zhang, W., Yan, X.J., Lin, X.Q., Li, W., Mi, J.Q., Li, J.M., Zhu, J., Chen, Z., and Chen, S.J. (2016). DNMT3A mutation leads to leukemic extramedullary infiltration mediated by TWIST1. Journal of hematology & oncology *9*, 106.

Yang, J.J., Park, T.S., and Wan, T.S. (2017). Recurrent Cytogenetic Abnormalities in Acute Myeloid Leukemia. Methods in molecular biology (Clifton, NJ) *1541*, 223-245.

Yokoyama, A., Kitabayashi, I., Ayton, P.M., Cleary, M.L., and Ohki, M. (2002). Leukemia proto-oncoprotein MLL is proteolytically processed into 2 fragments with opposite transcriptional properties. Blood *100*, 3710-3718.

Yokoyama, A., Lin, M., Naresh, A., Kitabayashi, I., and Cleary, M.L. (2010). A higher-order complex containing AF4 and ENL family proteins with P-TEFb facilitates oncogenic and physiologic MLL-dependent transcription. Cancer cell *17*, 198-212.

Yokoyama, A., Wang, Z., Wysocka, J., Sanyal, M., Aufiero, D.J., Kitabayashi, I., Herr, W., and Cleary, M.L. (2004). Leukemia proto-oncoprotein MLL forms a SET1-like histone methyltransferase complex with menin to regulate Hox gene expression. Molecular and cellular biology *24*, 5639-5649.

Yu, B.D., Hanson, R.D., Hess, J.L., Horning, S.E., and Korsmeyer, S.J. (1998). MLL, a mammalian trithorax-group gene, functions as a transcriptional maintenance factor in morphogenesis. Proceedings of the National Academy of Sciences of the United States of America *95*, 10632-10636.

Yu, B.D., Hess, J.L., Horning, S.E., Brown, G.A., and Korsmeyer, S.J. (1995). Altered Hox expression and segmental identity in Mll-mutant mice. Nature *378*, 505-508.

Zentner, G.E., and Henikoff, S. (2013). Regulation of nucleosome dynamics by histone modifications. Nature structural & molecular biology *20*, 259-266.

Zhang, J., Ding, L., Holmfeldt, L., Wu, G., Heatley, S.L., Payne-Turner, D., Easton, J., Chen, X., Wang, J., Rusch, M.*, et al.* (2012). The genetic basis of early T-cell precursor acute lymphoblastic leukaemia. Nature *481*, 157-163.

Zhang, L., Wang, J., Coetzer, M., Angione, S., Kantor, R., and Tripathi, A. (2015a). One-Step Ligation on RNA Amplification for the Detection of Point Mutations. The Journal of molecular diagnostics : JMD *17*, 679-688.

Zhang, T., Cooper, S., and Brockdorff, N. (2015b). The interplay of histone modifications - writers that read. EMBO reports *16*, 1467-1481.

Zheng, J. (2013). Oncogenic chromosomal translocations and human cancer (review). Oncology reports *30*, 2011-2019.

Zheng, Y.C., Ma, J., Wang, Z., Li, J., Jiang, B., Zhou, W., Shi, X., Wang, X., Zhao, W., and Liu, H.M. (2015). A Systematic Review of Histone Lysine-Specific Demethylase 1 and Its Inhibitors. Medicinal research reviews *35*, 1032-1071.

Zimmermann, C., Yuen, D., Mischitelle, A., Minden, M.D., Brandwein, J.M., Schimmer, A., Gagliese, L., Lo, C., Rydall, A., and Rodin, G. (2013). Symptom burden and supportive care in patients with acute leukemia. Leukemia research *37*, 731-736.

Zou, Y.R., Muller, W., Gu, H., and Rajewsky, K. (1994). Cre-loxP-mediated gene replacement: a mouse strain producing humanized antibodies. Current biology : CB *4*, 1099-1103.

Zufferey, R., Donello, J.E., Trono, D., and Hope, T.J. (1999). Woodchuck hepatitis virus posttranscriptional regulatory element enhances expression of transgenes delivered by retroviral vectors. Journal of virology *73*, 2886-2892.

12. Declaration

Eidesstattliche Erklärung

Heckl, Birgitta Christine

_____

Name, Vorname

Ich erkläre hiermit an Eides statt,
dass ich die vorliegende Dissertation mit dem Thema

“The molecular function of MLL/AF4 for patient derived acute leukemias growing in mice”

selbständig verfasst, mich außer der angegebenen keiner weiteren Hilfsmittel bedient und alle Erkenntnisse, die aus dem Schrifttum ganz oder annähernd übernommen sind, als solche kenntlich gemacht und nach ihrer Herkunft unter Bezeichnung der Fundstelle einzeln nachgewiesen habe.

Ich erkläre des Weiteren, dass die hier vorgelegte Dissertation nicht in gleicher oder in ähnlicher Form bei einer anderen Stelle zur Erlangung eines akademischen Grades eingereicht wurde.

_____ _____

Ort, Datum Unterschrift Doktorand

13. Acknowledgment

Zuerst möchte ich mich bei **Prof. Dr. Irmela Jeremias** bedanken für die interessante Themenstellung, die Betreuung und die fachlichen Diskussionen, die maßgeblich zum Gelingen dieser Arbeit beigetragen haben.

Besonders bedanke ich mich bei **Prof. Dr. Marc Schmidt-Supprian** für die tolle Betreuung meiner Doktorarbeit, für die Unterstützung und für die wissenschaftlichen Gespräche, von denen ich in vielfältiger Weise profitieren konnte.

Mein großer Dank gilt den Mitgliedern meines Thesis Advisory Committees, **Prof. Dr. Marc Schmidt-Supprian**, **Prof. Dr. Arnd Kieser** und **Prof. Dr. Irmela Jeremias**, für die wertvollen wissenschaftlichen Diskussionen und die guten Ideen in den Committee Meetings.

Vielen Dank an alle Mitglieder der Arbeitsgruppe **AG Apoptose** für die freundliche Einführung und die Zusammenarbeit. Danke an unsere TAs für die praktische Hilfe und für die Aufarbeitung zahlreicher Mäuse. Danke an meine Kolleginnen **Dr. Michela Carlet** und **Kerstin Völse** für das Korrekturlesen dieser Arbeit.
Mein aufrichtiger Dank gilt **Dr. Binje Vick** für ihre motivierende und warmherzige Unterstützung in all den Jahren.
Danke an alle **Mitarbeiter der Tierhaltung** für die Versorgung der vielen Mäuse.

Darüber hinaus möchte ich mich bei all meinen Freunden für die ausdauernde Unterstützung in den letzten Jahren bedanken. Mein ehrlicher Dank geht an **Dr. Martina Grandl** und **Dr. Stephanie Heinzlmeir** für ihre großartige Hilfsbereitschaft und wertvolle Motivation.
Außerdem danke ich all meinen Volleyballern aus der Halle und vom Beachplatz für die tolle Ablenkung, zahlreiche gemeinsame Trainingseinheiten und das sportliche Auspowern.

Schließlich bedanke ich mich von Herzen bei meiner tollen Familie, meinen drei Brüdern **Martin**, **Christian und Sebastian**, und vor allem bei **meinen Eltern**, für die grenzenlose Unterstützung, die unermüdliche Motivation und ihr Vertrauen. Vielen Dank dafür, dass ihr immer für mich da seid!

14. List of publications

14.1 Publications

Birgitta Christine Heckl*, Michela Carlet*, Binje Vick, Catrin Roolf, Ameera Alsadeq, Michaela Grunert, Wen-Hsin Liu, Andrea Liebl, Wolfgang Hiddemann, Rolf Marschalek, Denis Martin Schewe, Karsten Spiekermann, Christian Junghanss, Irmela Jeremias:

"**Frequent and reliable engraftment of certain adult primary acute lymphoblastic leukemias in mice**"

Leuk Lymphoma 2018 Sept 20:1-4.

14.2 Conferences

06/2017 **22nd European Hematology Association (EHA) congress** in Madrid, Spain; abstract: „Adult primary acute leukemia samples with chromosomal translocations grow well in immunodeficient mice, but are difficult to transduce with lentiviruses"

06/2017 **XXX. Annual Meeting of the Kind-Philipp-Stiftung** for pediatric hematology and oncology in Wilsede, Germany; oral presentation: „Genetic characteristics determine lentiviral transduction rates in patient derived ALL cells"

02/2017 **Acute Leukemias XVI** biology and treatment strategies in München, Germany; poster: „Primary adult acute lymphoblastic leukemia cells reliably engraft and grow in immunodeficient mice"

02/2015 **Acute Leukemias XV** biology and treatment strategies in München, Germany

09/2014 **8th international Heinrich F.C. Behr Symposium** (German Cancer Research Center (DKFZ) in Heidelberg, Germany

02/2014 **3rd Advancing in IPF Research (AIR) Symposium** in Düsseldorf, Germany; poster: "Quantitative assessment of lung cell populations during injury and fibrosis"

01/2014 **Deutsches Zentrum für Lungenforschung (DZL) meeting** in Heidelberg, Germany; poster: "Quantitative assessment of lung cell populations during injury and fibrosis"

10/2013 **Munich Lung conference** in Munich, Germany

09/2013 **INSERM Summer Retreat** in Tours, France; poster "Role of macrophages in pulmonary fibrosis"

14.3 Awards

02/2014 2nd poster prize at the 3rd Advancing in IPF Research (AIR) Symposium Düsseldorf, Germany